AN ABSTRACT OF THE THESIS OF

Lihua Zhang for the degree of Doctor of Philosophy in Geology presented on March 22, 2000.

Title: Stable Isotope Investigation of a Hydrothermal Alteration System: Butte Porphyry Copper Deposit

Abstract approved: _____
John H. Dilles

Typical porphyry-type Cu-Mo mineralization predates and underlies the well-known Main Stage polymetallic veins of the Butte district, Montana. This thesis presents the first systematic study of the isotopic characteristics of the pre-Main Stage K-silicate and sericitic wallrock alteration related to the porphyry Cu-Mo stage.

Oxygen and hydrogen isotopic compositions were obtained from hydrous and other silicate minerals of sixty-two samples from the unaltered host rock and ores: four Butte Quartz Monzonite; seven samples from K-silicate alteration; twenty samples of K-silicate alteration affected by late argillic alteration; and twenty-seven samples of gray-sericite alteration. These data support current porphyry Cu-Mo models that the associated hydrothermal fluids that produced pre-Main Stage K-silicate and gray sericite were dominantly magmatic in origin. Butte differs from other porphyry Cu-Mo districts because the widespread Main Stage or younger argillic alteration dominated by meteoric water (δD = -100 to -120‰) has partly to totally reset the hydrogen isotopic compositions of hornblende (δD = -45 to -126‰) and biotite (δD = -61 to -135‰) in the fresh Butte Quartz Monzonite host rock, biotite (δD = -47 to -131‰) of the early high temperature K-silicate alteration assemblages, and locally reset the δD values (-25 to -117‰) of sericite (muscovite) of gray-sericite alteration assemblages. The effect of

argillic alteration on these minerals was to produce D-depleted isotopic composition (δD = -80 to -140‰).

Sulfur isotope analyses have been applied to sulfides and anhydrite from forty-seven samples selected from deep drill cores. These include sulfate-sulfide assemblages in veinlets associated with K-silicate alteration selvages and slightly younger quartz-pyrite veinlets associated with gray-sericite alteration selvages. The K-silicate and gray-sericite sulfide values ($\delta^{34}S$ = +0.4 to +4.7 ‰) presented here are similar to those of Main Stage sulfides reported previously and suggest a conventional "magmatic" value ($\delta^{34}S$ about 2 ‰) for Butte sulfide-sulfur in the hydrothermal fluid. However, the anhydrite from the K-silicate alteration yields a much heavier $\delta^{34}S$ value (+12.9 ‰), therefore, total sulfur ($\delta^{34}S_{\Sigma S}$ ‰) of the early K-silicate assemblage was likely as heavy as 10 per mil, suggesting a possible crustal component to this relatively oxidized system.

Stable Isotope Investigation of a Hydrothermal Alteration System: Butte Porphyry Copper Deposit

By

Lihua Zhang

A THESIS
Submitted to
Oregon State University

in partial fulfillment of the requirements
for the degree of

Doctor of Philosophy

Completed March 22, 2000
Commencement June 2000

Contribution of Authors

Dr. John H. Dilles, Cyrus W. Field, and Dr. Mark H. Reed were involved in the design, analysis, data interpretation, and writing of each manuscript.

ACKNOWLEDGMENTS

Many people have had an impact on my academic career: from school in Jian, China, through the Geological Institute at Chengdu (GIC), China and graduate school at GIC, and finally to graduate school at Oregon State University (OSU).

First I would like to thank my advisors: Drs. Jiyuan Zhou at GIC, and Dr. John Dilles at OSU. They both had a profound effect on me. Particularly, I would like to thank my major professor, Dr. John Dilles, for his support, encouragement, and advice throughout my graduate study at Oregon State university.

I would also like to thank my committee members, Drs. Cyrus W. Field, Roger Nielsen, and Mark H. Reed (from University of Oregon) for their advice during the years and helpful comments and suggestions regarding my thesis. Dr. Field has contributed significantly for writing the sulfur isotope paper, the Chapter III of the thesis.

I thank my former Graduate Representative Council, Dr. Stephen E. Dickenson, for his contribution to my thesis program. Unfortunately, he can not attend my final thesis defense due to his trip out of state. I also thank my current Graduate Representative Council, Dr. Jack A. Barth, who agreed to serve on my committee for my final thesis defense on a short notice.

I thank Robert Houston and Brain Rusk for their contribution to this work. I would also like to thank many graduate students, faculty, and staff in the Department of Geosciences for their friendship and support; I have had a wonderful time being with you all.

Special thanks go to my family members who have been consistently both patient with me and supportive during my twenty-plus-years education.

The work for thesis was supported by the National Science Foundation under contract EAR-9600054. In addition I was supported by the Research Assistantship at the Radiation Center at OSU for more than two years. I would also like to thank Dr. Roman A. Schmitt from Department of Chemistry who has provided me one year Research Assistantship. Finally, I thank Dr. Jack F. Higginbotham from Radiation Center for his encouragement and assistance.

TABLE OF CONTENTS

TABLE OF CONTENTS (Continued)

TABLE OF CONTENTS (Continued)

LIST OF FIGURES

LIST OF FIGURES (Continued)

LIST OF FIGURES (Continued)

LIST OF TABLES

I dedicate this thesis to
my father, Zhang Guizhong
and
my mother, Guo Yumei

Stable Isotope Investigation of a Hydrothermal Alteration System: Butte Porphyry Copper Deposit

1. INTRODUCTION

Typical porphyry-type, fracture-controlled, Cu-Mo mineralization predates and largely underlies the well-known, throughgoing, Main Stage polymetallic veins of Butte. This thesis presents the first systematic study of the oxygen, hydrogen, and sulfur isotopic characteristics of these pre-Main Stage K-silicate and sericitic alterations. The isotopic data obtained allow calculations of isotopic compositions of the causative hydrothermal fluids and of formation temperatures, and, when compared with the existing Main Stage data, could provide bases for assessing the geochemical evolution of hydrothermal fluids from the pre-Main Stage porphyry system (assumed to be associated with magmatic fluids) to the Main Stage vein deposits (associated with meteoric-dominated hydrothermal fluids) for which the Butte district is famous.

Mineralization and Hydrothermal Alteration at Butte - an Overview

Porphyry Cu-Mo ore deposits worldwide were produced by large magmatic-hydrothermal systems fed by granitic porphyry intrusions emplaced usually at depths of 2 to 5 km in the continental crust. It is believed that porphyry-type ore fluids are generated by vapor-saturation during the crystallization of granites and are subsequently focused along fractures, where they ascend, cool, react with wall rocks, and finally mix with shallow crustal fluids, and where hydrothermal wall-rock alteration, vein formation, and ore sulfide precipitation result. Along the path of ascent, the fluids evolve from early, magmatic-dominated fluids to late, meteoric-dominated hydrothermal fluids.

The Butte Mining District of southwest Montana (this thesis study area) resides on a giant fossil magmatic-hydrothermal system which has been a major U.S. producer of hydrothermal Cu-Pb-Zn-Mn-Ag ores for nearly 130 years. Fed by heat and aqueous fluids from an evolving igneous system at depth, the hydrothermal system may have lasted for several millions of years. It is known now that Butte contains both an older or pre-Main Stage porphyry copper style of low-grade, disseminated Cu and Mo ores that were derived from high temperature and high pressure fluids, and a younger or Main Stage, enormous vein system of high-grade copper-zinc-lead-silver sulfides that formed from low temperature and pressure fluids. Erosion, favorable faulting and a century of intensive underground mining followed by the recent open-pit mining and core drilling to ~2 km depth have provided excellent exposures and core samples for scientific study of the entire system. Together with hundreds of kilometers of old underground workings and over 100 km^2 of surface exposures, the Butte district shows an exceptional three-dimensional view of a complex hydrothermal system.

For over a century, therefore, the Butte district has been the location of numerous industry, government, and university investigations directed to hydrothermal ore deposit researches. Most previous studies of the Butte district were focused on the high-grade Main Stage ores, but starting with Meyer (1965), and continuing with Roberts (1975), Brimhall (1972, 1977, 1979, 1980), Page (1979), and Reed (1979), the petrology and fluid inclusions of the high temperature K-silicate alteration and porphyry Cu-Mo mineralization have been studied.

This thesis work takes advantage of these recent deep drill holes, which provide us direct sampling and information on the extent of both the early deep, high-temperature, K-silicate alteration and the recently recognized, little studied, peripheral and slightly younger zones of gray-sericitic alteration. Using stable isotope analyses, this thesis research focuses primarily on testing the hypothesis of the magmatic to meteoric

transition during the hydrothermal fluid evolution in currently accepted porphyry Cu-Mo models.

Stable Isotopic Studies - Chapters of This Thesis

The body of this thesis is comprised of two parts. In Chapter 2, a systematic oxygen and hydrogen isotopic investigation was used to investigate the origin of the pre-Main Stage ore fluids within the Butte district, Montana. Detailed and extensive analyses of oxygen and hydrogen isotopic compositions have been performed systematically on sixty-two samples selected from four distinct intrusion and alteration events: fresh Butte Quartz Monzonite host rock, K-silicate alteration, K-silicate alteration with later argillic alteration overprint, and gray-sericitic alteration.

These samples were carefully chosen from either surface exposures or deep drill holes for the isotopic investigation of the evolution history of porphyry copper mineralization and related alteration sequence at Butte. Among them, four samples of unaltered Butte Quartz Monzonite were selected for determination of isotopic compositions of the host rock. Seven samples of biotite from K-silicate alteration were chosen for investigation of the pre-Main Stage "Early Dark Micaceous" type fluid isotopic compositions. Twenty samples of K-silicate alteration with later argillic superimposed were studied to determine the effect of late argillic fluids on early pre-Main Stage alteration. Twenty-seven samples of gray-sericitic alteration were analyzed for both oxygen and hydrogen isotopic compositions. Within each group, coexisting mineral pairs or triplets were also analyzed to check the state of the isotopic equilibrium during each alteration event.

The primary objective in Chapter 2 is to investigate the origin of the pre-Main Stage ore fluids and thus to quantify the hypothesized magmatic to meteoric transition in ore fluids during the evolution of hydrothermal fluids at Butte. The observations reported in

Chapter 2 provide the first systematic and extensive data set of oxygen and hydrogen isotopic compositions for these pre-Main Stage alterations at Butte.

In Chapter 3, sulfur isotope analyses have been applied to the earlier, deeper, and higher temperature pre-Main Stage type of porphyry Cu-Mo mineralization relative to the well-known Main Stage mineralization. Sulfur-bearing minerals of this early pre-Main Stage hydrothermal event recovered from deep drill core include sulfate-sulfide assemblages in veinlets and slightly younger quartz-pyrite veinlets associated with K-silicate and gray-sericitic (GS) alteration selvages, respectively. Total of forty-seven samples were selected from drill core of several deep drill holes obtained by the Anaconda Company in 1980.

The principal objectives of this investigation were to: (1) determine if the $\delta^{34}S$ composition of early Pre-Main Stage mineralization was similar to that of the later Main Stage event; (2) check for isotopic equilibrium between different sulfur-bearing minerals and derive temperature estimates; and (3) attempt to estimate the isotopic composition of total sulfur ($\delta^{34}S_{\Sigma S}$ ‰) in the Butte hydrothermal system and therefore to gain better insight as to the likely source(s) of this sulfur.

Interpretations of our isotope data have benefited greatly from previous isotopic studies of Main Stage mineralization, from subsequent geologic studies of pre-Main Stage mineralization, and continued improvements in the understanding of isotope fractionation derived from both experiment and theory.

Chapter 2

Oxygen and Hydrogen Isotope Geochemistry of Porphyry Copper Mineralization and Alteration Sequence at Butte, Montana

Lihua Zhang and John H. Dilles

Department of Geosciences, Oregon State University, Corvallis, Oregon 97331-5506

Mark H. Reed

Department of Geological Sciences, University of Oregon, Eugene OR 97403

Cyrus W. Field

Department of Geosciences, Oregon State University, Corvallis, Oregon 97331-5506

In preparation for submission to

Economic Geology

Abstract

Pre-Main Stage porphyry Cu-Mo alteration at Butte, Montana consists of early K-silicate alteration and slightly younger sericitic alteration. Potassium-silicate alteration at Butte is characterized by Early Dark Micaceous veinlets that contain chalcopyrite, pyrite, biotite, K-feldspar, and other silicates that formed at 550°C to 600°C within the Butte Quartz Monzonite (Brimhall, 1977). Previous studies have indicated possible meteoric water in the K-silicate alteration based on low δD values from two biotite samples (Sheppard and Taylor, 1974), which were D-depleted compared to hydrothermal biotite from other porphyry copper deposits. This isotopic depletion was interpreted as due to re-equilibration of early high-temperature Early Dark Micaceous minerals with the younger, low-temperature, meteoric-dominated Main Stage fluids.

To investigate the origin of the pre-Main Stage ore fluids, we have performed systematic analyses of oxygen and hydrogen isotopic compositions on fifty-four samples selected from four groups: fresh Butte Quartz Monzonite (4 samples), K-silicate alteration (7 samples), K-silicate alteration that has been affected by weak to moderate amounts of younger Main Stage argillic alteration (20 samples), and gray-sericitic alteration (27 samples). Major results of this study are tabulated here:

Samples	Mineral	$\delta^{18}O$ mineral (‰)	δD mineral (‰)	$\delta^{18}O$ water (‰)	δD water (‰)	T °C
BQM	Hornblende	+5.2 to +6.0	-149 to -68	+7.4 to +8.2	-126 to -45	700
	Biotite	+4.1 to +5.6	-165 to -88	+6.5 to +8.3	-135 to -61	700
	K-feldspar	+7.5 to +8.4		+7.0 to +7.9		700
	Quartz	+8.6 to +8.9		+7.5 to +7.8		700
K-silicate	Biotite	+4.4 to +5.7	-130 to -77	+6.8 to +8.1	-98 to -47	550
	K-feldspar	+6.4 to +8.9		+5.2 to +7.7		550
	Vein Quartz	+8.9 to +9.6		+7.0 to +7.7		550
K-silicate	Biotite	-2.0 to +6.9	-159 to -115	+0.5 to +9.4	-131 to -84	550
with argillic	K-feldspar	+2.5 to +9.6		+1.5 to +8.6		550
	Kao-rich clay	+0.5 to +7.8	-133 to -118	-8.2 to -2.9	-113 to -98	150
	Mont-rich clay	+7.8	-109	-2.4	-97	150
GS	Sericite	+6.4 to +9.5	-139 to -46	+5.0 to +8.1	-117 to -25	400
	Quartz	+9.1 to +11.8		+4.6 to +7.2		400

We conclude that (1) the light δD values in the mining district suggests that the BQM has partly re-equilibrated with meteoric fluids; (2) the most D-rich fluids associated with K-silicate alteration are similar to felsic magmatic water; (3) the wide range of oxygen isotopic compositions and the D-depletion in the argillically altered K-silicate samples results from isotopic exchange of biotite with the younger, low-temperature, meteoric-dominated Main Stage fluids as initially proposed by Sheppard and Taylor (1974); (4) the range of calculated isotopic compositions of fluids for gray-sericitic alteration are compatible with a mixture of magmatic water found in felsic magmas (Taylor, 1992) with local, exchanged meteoric water. The gray-sericitic fluids range from pure magmatic water (δD ~ -35 ‰, n=4) to <50% magmatic water (δD ~ -93 ‰, n=9).

Introduction

PORPHYRY Cu-Mo ore deposits are the products of the large magmatic-hydrothermal systems driven by granitic porphyry intrusions emplaced at depths of 2 to 5 km in the crust. Compelling field evidence from Yerington, Nevada (Proffett and Dilles, 1984), Ajo, Arizona (Gilluly, 1946; Wadsworth, 1968), and Sierrita Mountains, Arizona (Cooper, 1973) supports the orthomagmatic hypothesis that porphyry-type ore fluids are generated by vapor-saturation during the crystallization of granites and are subsequently focused upward along fractures (Burnham, 1979). The hydrothermal wall-rock alteration, vein formation, and ore sulfide precipitation result when these magmatic aqueous fluids ascend, cool, react with wall rocks, and mix with shallow crustal fluids. A widely accepted hypothesis based on stable isotope data is that the fluids evolve from early, magmatic-dominated fluids to late, meteoric-dominated hydrothermal fluids.

A giant fossil magmatic-hydrothermal system at Butte, Montana, has generated one of the world's largest deposits of copper, molybdenum, zinc, lead, silver, and

manganese (Meyer et al., 1967). Fed by heat and aqueous fluids from an evolving igneous system at depth, the hydrothermal system may have lasted for several millions of years. Erosion, favorable faulting and a century of intensive mining followed by the recent open-pit mining and core drilling to ~2 km depth have provided excellent exposures and core samples for scientific study of the entire system. Together with old underground workings and over 100 km^2 of surface exposures, the Butte district shows an exceptional three-dimensional view of a complex hydrothermal system.

Butte contains both an older or pre-Main Stage porphyry copper style of low-grade, disseminated Cu and Mo ores that were derived from high temperature and high pressure fluids, and a younger or Main Stage, enormous vein system of high-grade copper-zinc-lead-silver sulfides that formed from low temperature and pressure fluids. Early studies in the Butte district were focused on the high-grade Main Stage ores, but starting with Meyer (1965), and continuing with Roberts (1975), Brimhall (1972, 1977, 1979, 1980), Page (1979), and Reed (1979), the petrology and fluid inclusions of the high temperature K-silicate alteration and porphyry Cu-Mo mineralization have been studied. At Butte, the K-silicate alteration is, in part, characterized by "Early Dark Micaceous" vein assemblages, as originally defined by Meyer (1965), and a broad zone of pervasive biotitization of igneous hornblende, accompanied by biotite crackle veinlets and quartz veinlets with biotite-rich selvages (Roberts, 1975).

Sericitic alteration of multiple ages has been recognized in Butte ore deposits, and may have been formed by at least three distinct hydrothermal fluids of possible widely different ages. The gray-sericitic alteration was originally defined as "S" by Meyer et al. (1968) and later was changed to "gray-sericitic alteration" by Reed (1979). This quartz-sericite alteration has an age intermediate between the pre-Main Stage and the Main Stage based on vein cutting relations. Page (1979) conducted a systematic study of the various sericitic alterations by obtaining chemical compositions of hydrothermal

minerals utilizing the techniques of the transmission electron microscope and the electron microprobe.

Previous oxygen and hydrogen isotopic studies of the Boulder batholith and the Butte ore deposits focused mainly on the Main Stage veins and associated alteration (Garlick and Epstein, 1966; Sheppard et al., 1969; and Sheppard and Taylor, 1974). A total of 78 samples have been analyzed. A meteoric hydrothermal origin was suggested by the low and uniform δD values (-140 ±15 ‰) of alteration minerals, the calculated δD values of hydrothermal water (-110±15 ‰) at 300°C, and the large variation in $\delta^{18}O_{water}$ (-12 to +8 ‰) in the Main Stage. This variation of $\delta^{18}O_{water}$ is larger than those observed in most ore deposits directly associated with an igneous host rock.

In earlier studies, two pre-Main Stage biotite samples from the Early Dark Micaceous zone yielded very light δD values of -160 and -170 per mil with $\delta^{18}O$ values of +3 and +5 per mil, respectively. The depleted δD values, when compared to hydrothermal biotite from other porphyry copper deposits, were interpreted by Sheppard and Taylor (1974) as due to possible D/H exchange of biotite with the younger D-depleted Main Stage hydrothermal fluids. This is the only porphyry copper deposit reported with such D-depleted biotite from K-silicate alteration (Hedenquist and Richards, 1998).

This study presents the first systematic examination of the isotopic characteristics of the pre-Main Stage K-silicate and sericitic alterations. It also adds new petrologic information, especially on biotite and sericite compositions. We have investigated the K-silicate alteration samples to determine the extent and origin of D-depleted biotite. We also sought to understand whether or not meteoric water was an important component in the K-silicate alteration fluids or was introduced during a later event, such as the Main Stage. This is the first detailed isotopic study of the gray-sericitic alteration. The isotopic data allow calculations of isotopic compositions of the causative hydrothermal fluids,

and, when compared with the Main Stage data, could provide bases for assessing the evolution of the hydrothermal fluids from the pre-Main Stage porphyry system to the Main Stage vein deposits.

One key factor to this study is the three-dimensional framework of the hydrothermal system that can be sampled on the surface and via 10 drill holes up to 2 km depth in the center of the system. We integrate the isotopic data with geologic and petrologic data derived from drill core summarized in maps and cross-sections. We also present sulfur isotope compositions of the same alterations in a separate paper.

Geologic Setting and Chronological Framework

Regional geology

The ore deposits of Butte District are located at the southern end of the Boulder batholith of western Montana, which is the easternmost of the Late Cretaceous calc-alkaline batholiths of the Cordillera. The batholith is about 122 km long and 50 km wide, and elongated along the north-northeast (Smedes, 1973); it is made up of numerous stocks that were shallowly emplaced into the slightly older Elkhorn Mountains volcanics (Knopf, 1957).

The earliest mafic phases are at the north and south ends of the batholith, as are younger, massive granodiorite intrusions. The Butte Quartz Monzonite is the central intrusion, making up ~ 85 percent of aerial exposures. Biotite breccias and quartz porphyry dikes cut Butte Quartz Monzonite in the Butte area. Younger quartz monzonite in large dike-like plutons intruded south of Butte (Knopf, 1957).

Butte ore deposits are all hosted within Butte Quartz Monzonite (Fig. 1), which is a medium- to coarse-grained rock with a relatively uniform mineralogy of, in decreasing order of abundance, plagioclase, quartz, K-feldspar, biotite, hornblende, magnetite, and

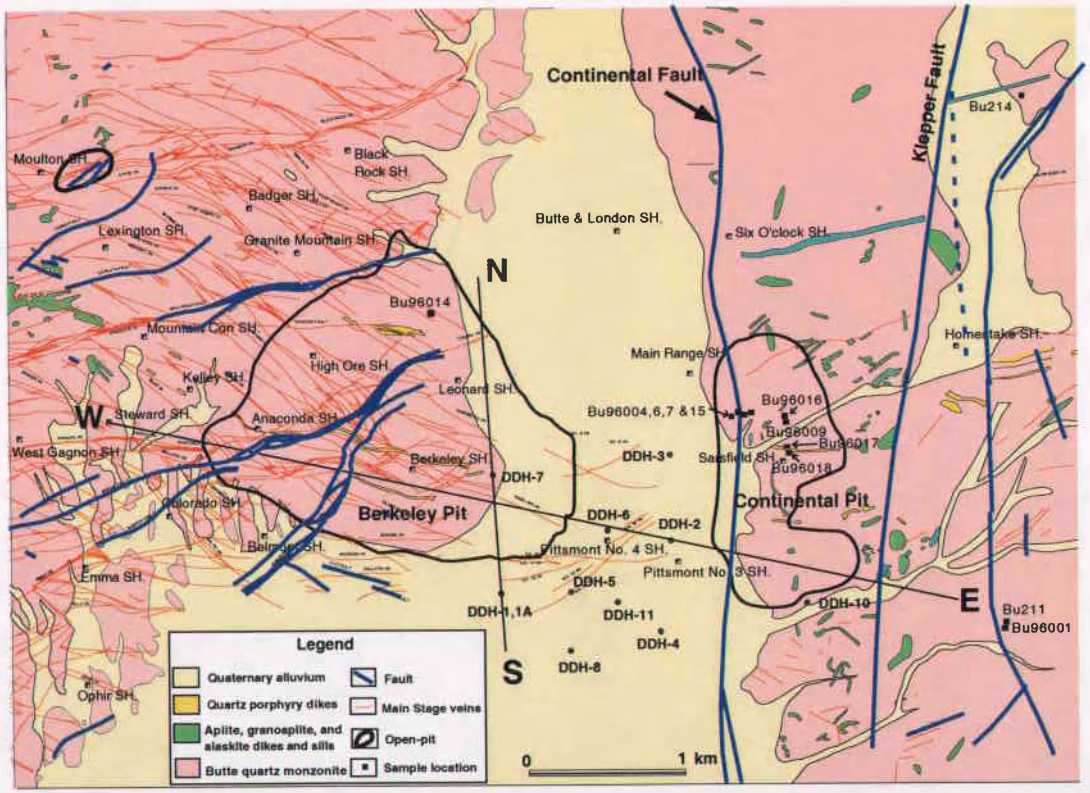

Fig. 1. Generalized geological map of the Butte district after Houston (1999), showing the host rock of Butte Quartz Monzonite, Quartz porphyry dikes related to the pre-Main Stage Cu-Mo mineralization, distribution of the Main Stage veins, and the localities of surface samples used for isotopic study. DDH 1 to DDH 11 indicate location of deep holes drilled by Anaconda 1979-81 used for samples in this study.

sphene, and accessory ilmenite, apatite, and zircon (Roberts, 1975, Appendix I). The uniformity of this host rock makes it possible to track the chemical and mineralogical changes of hydrothermal alteration in exceptional detail. The modern surface of the Butte Quartz Monzonite represents a formation depth of about 7-9 km on the basis of a hornblende geobarometry study (Dilles et al., 1999). Small volumes of aplite, pegmatite, and granoaplite dikes are widespread in the Butte district throughout the Butte Quartz Monzonite and are probably genetically related to it (Fig. 1).

Biotite breccia and quartz porphyry

A small volume of younger, biotite-rich igneous breccia and quartz porphyry dikes were emplaced into the quartz monzonite and aplites and are surrounded by pre-Main Stage porphyry Cu-Mo mineralization (Meyer et al., 1968; Proffett, 1974). The biotite-rich igneous breccias occur both in the western Butte district in deep "Anaconda Dome" area and in the eastern Continental and Pittsmont dome area. These breccias recorded the earliest hydrothermal activity in the district as they contain fragments of quartz-veined granitoids. The biotite breccias are generally closely associated with, but are cut by quartz porphyry dikes. Locally, the biotite-rich breccias grade into a Cu-mineralized biotite crackle breccias containing fragments of quartz porphyries. The early quartz veins and the biotite crackles controlled the distribution of the pervasive biotitization of hornblende(Roberts, 1975, Dilles et al., 1999).

The quartz porphyries occur as a swarm of steeply south-dipping, east-west striking dikes extending from the Anaconda Dome to the Continental pit (Meyer et al., 1968; Roberts, 1975; and Reed, 1979a, b) and coalesce into larger plugs sampled in deep drilling at ~2 km depth in the center of the district. The quartz porphyry dikes are cut by the Early Dark Micaceous, quartz, and quartz-molybdenite veins, all of which are enclosed within the broad 6 km by 2 km zone of the pervasive biotitization of

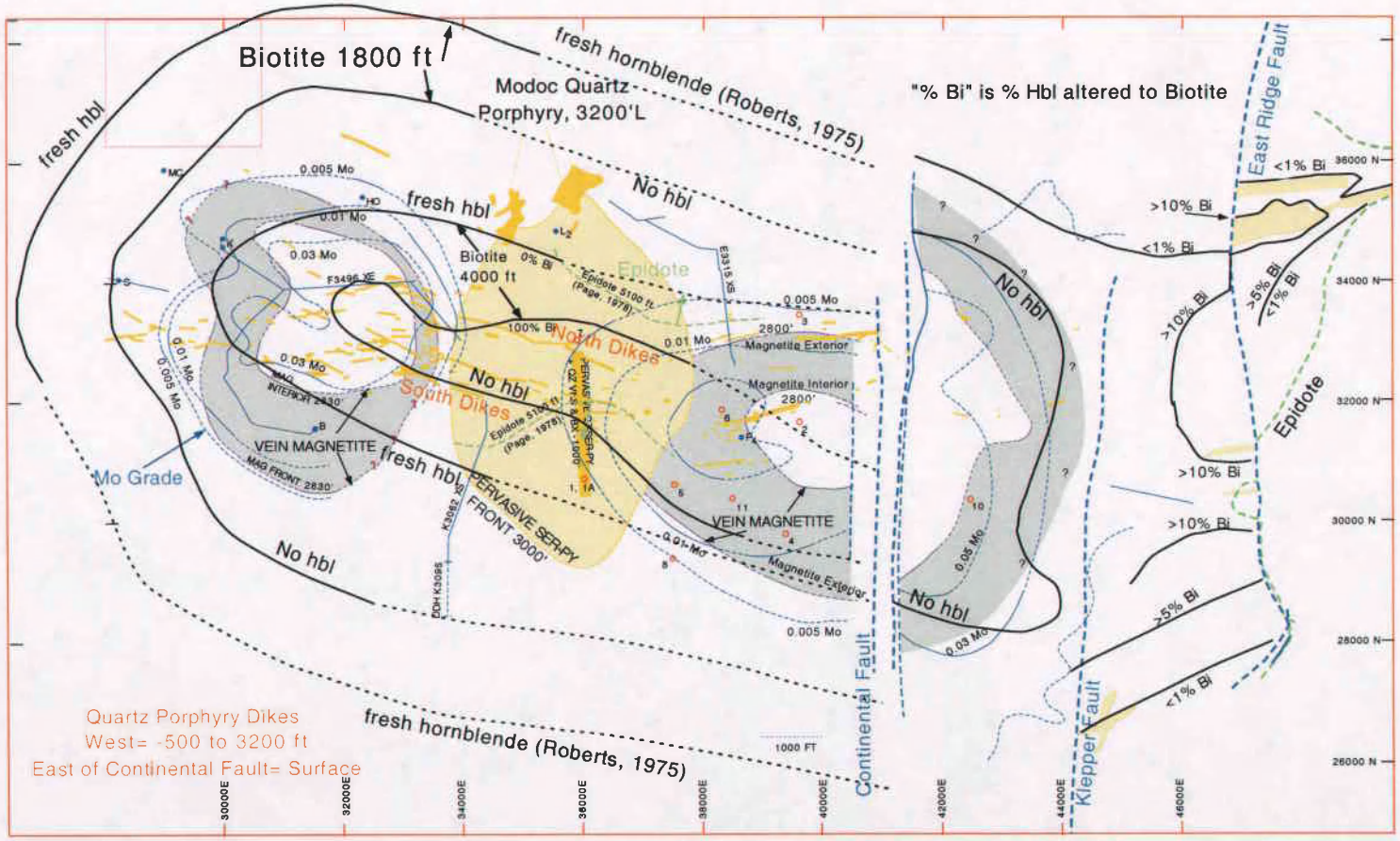

Fig. 2a. Plan map showing the pre-Main Stage geology, Cu-Mo mineralization, and alteration, including the distribution of pervasive biotitic alteration of hornblende, two pre-Main Stage domes, and the GS dome. After Reed (1979), Roberts (1975), and Dilles et al., (1999).

Figure 2b: Simplified east-west cross section of the Butte district. It shows the two pre-Main Stage centers of mineralization, the Pittsmont and Anaconda domes and the pervasive gray-sericitic (GS) alteration, which has an intermediate age between the pre-Main Stage and Main Stage based on vein cutting relations. The Continental fault, a post-ore normal fault, has offset the "Pittsmont" pre-Main Stage Dome about 1070-1370 meters downward relative to the Continental Pit area. The black vertical lines labeled "DDH" are the locations of several deep drill holes and the red dots are the sample locations that are used in this study (after Reed, 1999).

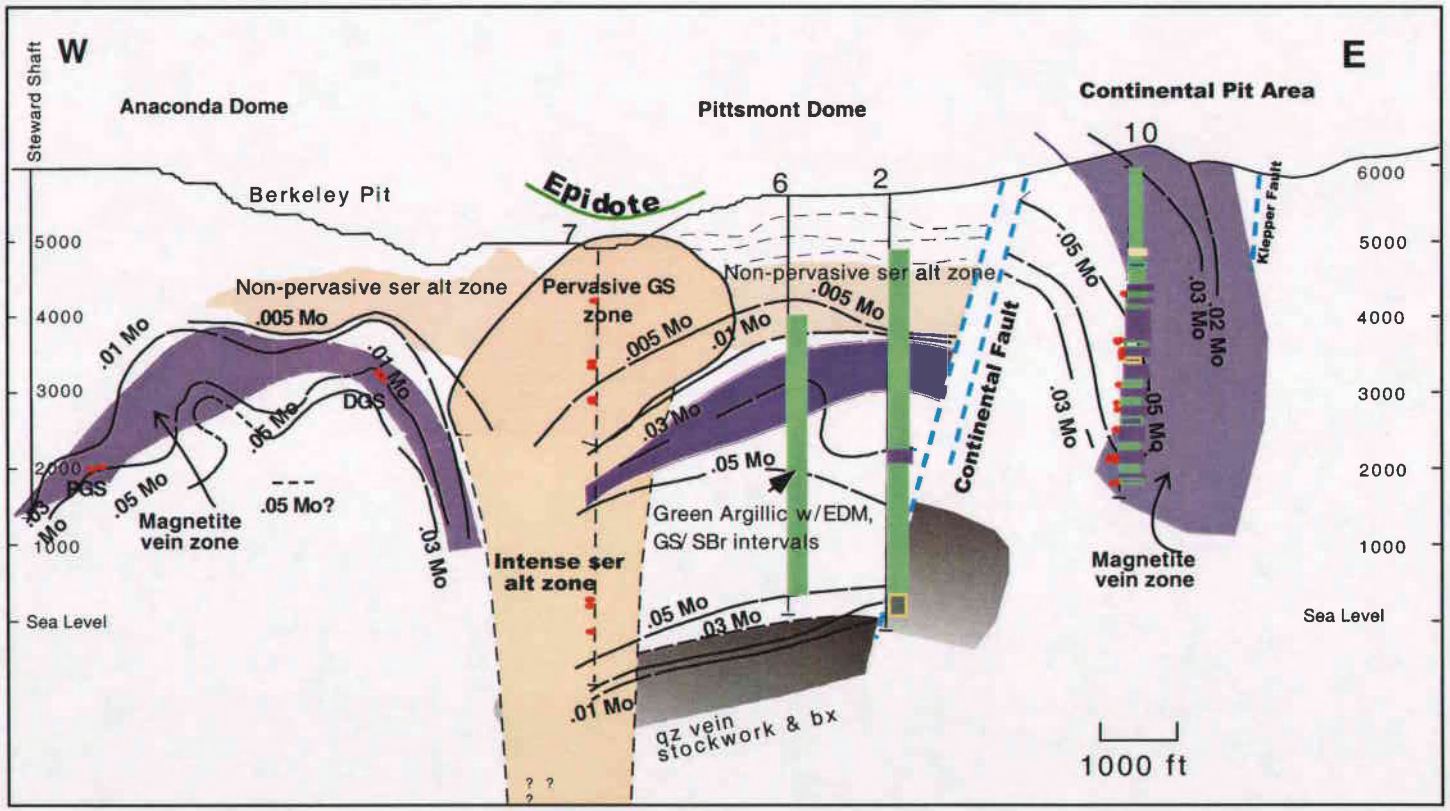
W
E
Steward Shaft
Anaconda Dome
Pittsmont Dome
Continental Pit Area
Berkeley Pit
Epidote
Non-pervasive ser alt zone
.005 Mo
Pervasive GS zone
Non-pervasive ser alt zone
.01 Mo
.005 Mo
.01 Mo
.03 Mo
DGS
.05 Mo
.05 Mo
DGS
.05 Mo?
.05 Mo
Magnetite vein zone
.03 Mo
Intense ser alt zone
Green Argillic w/EDM, GS/ SBr intervals
.05 Mo
.03 Mo
.01 Mo
qz vein stockwork & bx
Continental Fault
.05 Mo
.03 Mo
.03 Mo
.02 Mo
.05 Mo
Klepper Fault
Magnetite vein zone
Sea Level
Sea Level
1000 ft
5000
4000
3000
2000
1000
6000
5000
4000
3000
2000
1000
7
6
2
10

hornblende (Fig. 2). On the basis of detailed core logging and mapping, the biotite-rich igneous breccias and quartz porphyry dikes were emplaced synchronously with initiation of K-silicate alteration and Cu-Mo mineralization (Brimhall, 1977; Reed, 1979). This early, high temperature, K-silicate alteration and Cu-Mo mineralization is termed the pre-Main Stage, and available isotopic age data indicate brackets of 75 Ma to 63 Ma (Martin et al., 1999, Snee et al., 1999). Sericitic alteration with pyrite but no Cu mineralization followed and is in turn cut by Main Stage veins (Meyer et al., 1968). The age of sericitic alteration is 62.5 to 64 Ma (Snee et al., 1999) based on Ar-Ar age dating of sericite.

Post-mineralization events

Following mineralization, rhyodacite dikes with a K-Ar age of ~58.5 Ma cut the Main Stage veins (Martin et al., 1999). Eocene magmatism includes rhyolite dikes of Big Butte at 51 Ma and eruption of the associated Lowland Creek Volcanics between 48 and 52 Ma (Smedes, 1974; Proffett, 1974; Snee et al., 1999; L.W. Snee and F. Dudes, written communication, 1997). Basin-and-Range normal faults post-date the volcanics and are late Cenozoic age. These faults have resulted in tilting of Lowland Creek Volcanics between 25° and 50° to the west or northwest along the northwestern margin of the district (Proffett, 1974; Houston et al., 1999). The amount of westward tilt of the Butte district is not precisely known, an estimate of 25° to 30° W tilt was given by Proffett (1979) based on geologic studies, whereas Geissman et al. (1980) gave an estimate of 5° to 12° W based on paleomagnetic studies.

The Continental fault passes through the eastern part of the district and is a westward dipping normal fault that has 1070 to 1370 meters. It has displaced the "Pittsmont Dome" downward on the west relative to the Continental area to the east (Fig. 1). East of this fault, the deep and eastern peripheral part of the district has been

only minimally affected by the elsewhere-widespread Main Stage fluids, and provides us the best samples to study the early K-silicate alteration.

Geochronology

Previous geochronology by Meyer et al. (1968) yielded K-Ar ages of 72-73 Ma for the Butte Quartz Monzonite, 62.8± 2.0 Ma for the Early Dark Micaceous biotite, and 57.5 to 58.0 Ma for the hydrothermal sericite in the Main Stage vein selvages. These data suggest that the biotite breccias, quartz porphyries, and pre-Main Stage mineralization are about 10 m.y. younger than the host rock, the Butte Quartz Monzonite, and the Main Stage mineralization is about 5 m.y. younger than the pre-Main Stage porphyry copper deposits.

Recent preliminary U-Pb ages of zircon and sphene, and one ^{40}Ar-^{39}Ar age of hornblende from the Butte Quartz Monzonite in the Butte district suggest a crystallization age of approximately 76.5 Ma for the Butte Quartz Monzonite (Martin et al., 1999, Snee et al., 1999). In addition, fractions of zircon from the Modoc quartz porphyry yield an age of 75.6 Ma. Single zircons from three quartz porphyry dikes yield preliminary dates of 72 to 69 Ma that is similar to one K-feldspar and biotite age obtained by Ar-Ar dating near the eastern limit of pre-Main Stage hydrothermal alteration. The large difference in these zircon dates could indicate that porphyry intrusions associated with Butte Cu-Mo mineralization span several million years from 75.6 Ma to 69 Ma, or younger, if the zircon dates represent crystallization ages. However, this interpretation might not be true due to the possibilities that the zircons in the quartz porphyry could be represented by mixtures of newly crystallized zircon (<69 Ma) with inherited Butte Quartz Monzonite zircon (76.5 Ma), which are not optically distinguishable from the newly crystallized zircons, or the younger ages (72 & 69 Ma) might be due to lead loss.

All the dated hydrothermal micas, from pre-Main Stage K-silicate alteration, gray-sericitic, and Main Stage mineralization yield ^{40}Ar-^{39}Ar ages ranging from 64 to 61 Ma (Snee et al., 1999). Despite the fact that hydrothermal biotite must be approximately synchronous with quartz porphyry emplacement, all but one hydrothermal biotite yield much younger ages of 63 to 64 Ma.

The geochronologic data presently available (Table 1) are ambiguous about the absolute age of pre-Main Stage K-silicate alteration, and whether the gray-sericitic alteration represents the end stage of pre-Main Stage mineralization, or a deep feeder for the Main Stage mineralization, or a transition in a continuum from pre-Main Stage to Main Stage. Alternatively, all the ^{40}Ar-^{39}Ar ages of the hydrothermal micas from both pre-Main Stage K-silicate and gray-sericitic alterations could have been reset by the later thermal Main Stage event (~64 Ma).

In summary, the major intrusive activities and mineralization (alteration) sequences in the Butte district are listed in Table 1, which integrates the geological observations, dating, and fluid inclusion results.

Table 1. Time and temperature of major intrusive and mineralization events

Major Event	Age (Ma)	Temperature (° C)
Butte Quartz Monzonite Intrusive	76	700
Quartz Porphyry Dikes and Associated K-silicate Alteration	76-69?	550-650
Gray-Sericitic Alteration	<69, >64	400
Main Stage mineralization	<64, >58	250-300
Green, White Argillic Alteration	?	150-200

Three-dimensional geological data base

The Butte district was the birthplace of pioneering studies of the geology of ore deposits by Sales (1914), Sales and Meyer (1948, 1949), and Meyer et al. (1968) under the auspices of the Anaconda Mining Company. Beginning with these early studies, the Butte district represents a 100-year data of surface and underground geology mapping and laboratory studies extending to the present (Howard, 1972; Brimhall, 1972, 1977; Roberts, 1975; Page, 1979, Proffett, 1974, and Houston et al., 1999). In the late 1970's, a deep drilling program was sponsored by Anaconda in which ten deep drill holes with a total of 18,000 meters of core were drilled in the center of the district to explore the deep parts of the hydrothermal system (Fig. 1). The geological investigations of drill hole data were summarized by Reed (1979a, b, 1980, 1981). Since 1985, Montana Resources, the new owners, has continued to mine porphyry copper mineralization by open-pit techniques in the East Continental area, which was the bottom part of the porphyry system. Together, it allows us to sample a region that is more than 2 km vertically by 7 km width exposured in surface, drill holes, and underground workings, and these provide us an excellent access to this three-dimensional hydrothermal system.

Mineralization and Hydrothermal Alteration

Pre-Main Stage porphyry Cu-Mo system

The Anaconda Dome and Pittsmont Dome-Continental area are two pre-Main Stage mineralization centers that straddle the quartz porphyry dike swarm (Fig. 2a & 2b). The two centers lie on an axis that strikes approximately S80°E and both contain the same types of alteration and veins related to copper and molybdenum mineralization (Reed,

Table 2 Relationships among alteration types, sulfides, and vein minerals of the pre-Main Stage and Main Stage in the Butte, Montana (After Reed, 1979b)

Alteration Name	Silicate Alteration	Disseminated Sulfides	Associated Veins
Pre-Main Stage			
Pervasive biotitic	hbl±bi-->2nd bi	ccp±py	qtz, anh, mb, or, ccp±mt±py
Early Dark Micaceous (EDM)	hbl±bi-->2nd bi plag-->or, ser, anh, carb±and±cor±plag	ccp±py	qtz, anh, mb, or, ccp±mt±py
Sericite, secondary biotite (SBb--weak EDM)	bi-->2nd bi plag-->green ser, 2nd bi	py, ccp±mt	qtz, py, ccp±mb±mt
Pale green sericitic (PGS)	bi-->ser±chl±carb feld-->green ser ± chl texture destroyed	py±ccp±mt	qtz, py±ccp±mb±mt
Dark green sericitic (DGS)	bi-->chl feld-->green ser±chl texture intact	py±ccp	qtz, py±ccp (±minor mb,mt)
Dark green sericitic with fresh relict rock K-feldspar	bi-->chl plag-->green ser K-feldspar-->fresh	py±ccp	qtz, py±ccp (±minor mb,mt)
Quartz-Mo veinlets	weak plag-->K-feldspar		qtz, mb, ±ccp,±py
Propylitic (Prop)	bi-->chl, ep plag-->ser, ep	py, ccp, sl	qtz, py, ccp, gn, sl
Gray sericitic (GS)	feld-->grey ser bi-->ser, chl (colorless)	py(±trace ccp)	qtz, py (±trace ccp)
Sericitic with remnant igneous biotite (SBr)	bi-->fresh plag-->green ser or-->green ser or fresh	py± ccp	qtz, py±ccp±mb
Main Stage			
Advanced argillic	pyrophlite, dickite, kaolinite	py±cc±bn	qtz, py, cc, bn, en
White sericitic	bi, feld-->ser texture may bedestroyed	py±cc±bn	qtz, py, cc, bn
White argillic (WA)	bi-->fresh feld (plag)-->kaolinite	±py ± ccp	none
Green argillic (GA)	bi-->fresh feld (plag)-->green mont.	±py ± ccp	none
Propylitic	bi-->chl + ep plag-->ser + ep	py, ccp, sl	qtz, py, ccp, gn

Abbreviation

hbl: hornblende; bi: biotite; 2nd: secondary; plag: plagioclase; or: orthclase; ser: sericite; anh: anhydrite; carb; carbonate; and: andalusite; cor:corundum; chl: chlorite; qtz: quartz; py: pyrite; ccp: chalcopyrite; mb: molybdenite; mt: magnetite; bn: bornite; qz: quartz; sl: sphalerite; en: enargite; cc: chalcocite;

1979a, b). The shapes of the two domes are defined by the Mo grade contours, by zones of magnetite veinlets, and other distributions of alteration minerals (Fig. 2). The pre-Main Stage is characterized by two alteration series and related veins and sulfides (Reed, 1979a,b, Table 2). The earliest high temperature event resulted in the first series of K-silicate alteration that is characterized by the pervasive alteration of hornblende to biotite, which forms a broad envelope over the tops of the Anaconda and Pittsmont domes (Fig. 2a, Roberts, 1975). The zone of biotitization encloses all first and second series alteration types. The earliest and innermost of these is the first series Early Dark Micaceous (Meyer, 1965) veinlets and narrow (<5 cm) alteration halos that contain Cu-Fe sulfides (ca. 0.5 to 0.8 wt. % Cu), biotite, K-feldspar, sericite (muscovite), anhydrite, and other silicates formed at 550° to 600 °C (Roberts, 1975). The Early Dark Micaceous alteration grades upward and outward into a contemporaneous to slightly younger, but more poorly documented, second hydrothermal alteration series that consist of pale green sericitic, dark green sericite-chlorite and outermost propylitic epidote-chlorite alteration types (Reed, 1979). Quartz ± molybdenite veinlets with narrow or non-existent alteration selvages cut and post-date the veinlets related to the Early Dark Micaceous, pale green sericitic, dark green sericite-chlorite alteration, but do not extend into the upper and outer propylitic zones. Fluid inclusion data (Roberts, 1975; Rusk et al., 1999) suggest that pre-Main Stage alteration series described above likely occurred at pressures of 1.7 - 2.0 kb, which corresponds to a 5-8 km depth assuming lithostatic pressure.

Chalcopyrite is the only abundant Cu-bearing mineral in the pre-Main Stage assemblages, and is generally in stockwork veinlets and their envelopes. In the Cu-mineralized interior zone, pyrite is approximately equal in abundance to chalcopyrite (Brimhall, 1977) and principally chalcopyrite is found outside of the Early Dark Micaceous veinlet selvages, but is not very abundant. Minerals in these early veinlets

include quartz, chalcopyrite, pyrite, molybdenite, sericite, biotite, anhydrite, carbonate, magnetite, fluorite, and K-feldspar. Molybdenite is abundant in the second pre-Main Stage mineralization series, consisting of quartz veinlets, which cut the chalcopyrite-bearing veinlets and commonly lack an alteration selvage.

Gray sericitic alteration

Between Steward Dome and Pittsmont Dome, and partially overlying the western part of Pittsmont Dome, lies a bulb-like volume of rock that is pervasively altered to quartz, sericite, and pyrite, and is characterized by a stockwork of quartz-pyrite veinlets with overlapping sericitic alteration halos (Fig. 2). This pervasive sericite zone yields laterally into an apron of partially sericitized ground that covers most of the Pittsmont and Anaconda Domes above and outside of the regions of principal Cu-Mo mineralization (Fig. 2). At the deep level, the pervasive sericite zone is more characterized by intense quartz-vein stockwork and breccia (Fig. 3). Vein cutting relations show that the gray-sericitic veinlets cut the chalcopyrite-bearing and quartz-molybdenite veins, but are cut by the Main Stage veins, thereby constituting the third distinct mineralization stage. The gray-sericitic zone contains only a trace of chalcopyrite (<0.1 wt. % Cu).

Main Stage Cu-As-Zn-Pb vein system

The fourth mineralization series at Butte is the youngest event. The Main Stage consists of giant fissure-veins containing high-grade copper, zinc, lead, silver, and manganese ores. These large Main Stage veins are bordered by alteration halos zoned outward from an inner, local kaolinite-dickite advanced argillic zone, to a "white" sericitic zone, to a well-developed intermediate argillic alteration zone (kaolinite or

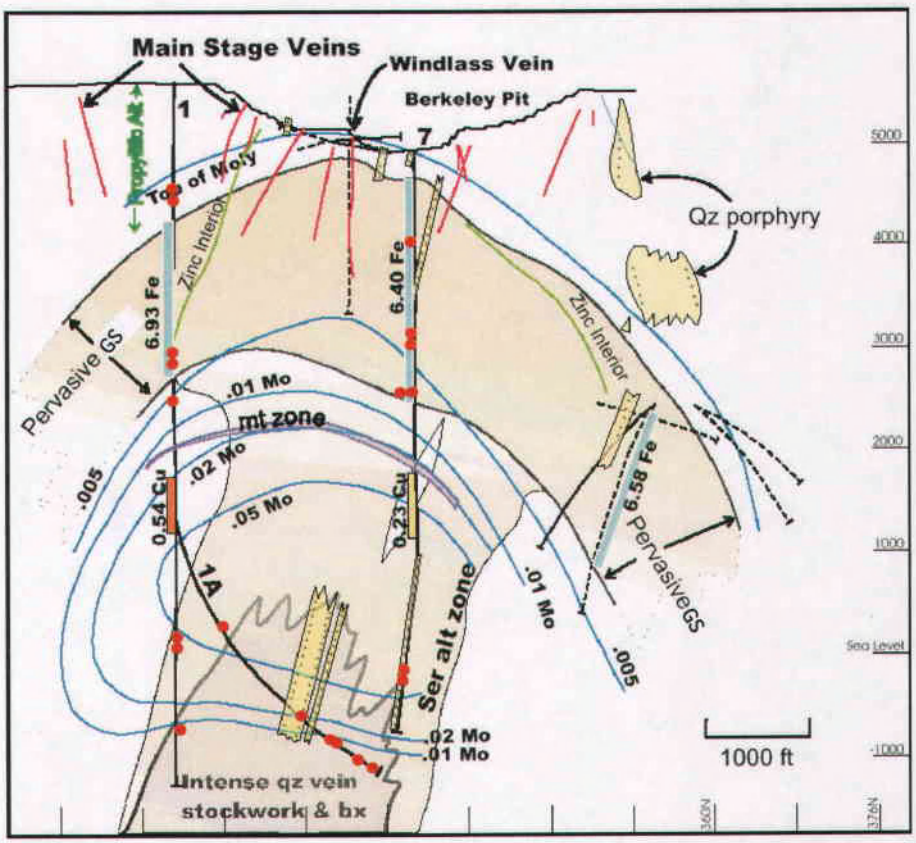

Fig. 3. Simplified north-south geological cross section shown in Figure 1. It crosses DDH 7 to DDH 1&1A and shows the younger, mushroom shaped Gray-Sericitic alteration and locations of isotopic samples (dots).

smectite), to an outer propylitic zone (Sales and Meyer, 1948, 1949; Meyer et al., 1968; Meyer and Hemley, 1967). The zoned alteration halos around Main Stage veins interpreted by Sales and Meyer as having developed synchronously as acid fluid diffused into the wallrock from the vein channel following a gradient of increasing pH and $[K^+]/[H^+]$ of the fluid (Meyer and Hemley, 1967). The isotopic data (see below), alteration distributions, and some mineralogic data suggest that the different assemblages in the halos may not have developed at the same time. Propylitic alteration is widespread, and is not clearly zoned around Main Stage veins. As noted in Table 2, it form a broad outer zone around the pre-Main Stage biotite-alteration zone. The outer green argillic alteration contains montmorillonite, a mineral that typically forms in geothermal systems at <160-180°C (Reyes, 1990), whereas pyrophyllite in the inner selvage is stable only above ~260°C.

The Main Stage quartz-sulfide veins were mostly developed in the central part of the Butte district, where they are superimposed on the earlier pre-Main Stage porphyry Cu-Mo mineralization, but they also extend several kilometers west and northwest beyond the limits of pre-Main Stage hydrothermal biotite (Fig. 2). To the east, in the Pittsmont Dome region, however, Main Stage veins are much smaller and fewer (Fig. 1).

Post-Main Stage

Post Main Stage alteration was noted by early workers at Butte (Meyer et al., 1968) who suggested that argillic alteration was present along faults of the Rarus and other fault systems that cut Main Stage veins and are not occupied by (or cut by) any Main Stage veins. Similarly, post-Main Stage rhyodacite dikes are affected by argillic alteration (J.M. Proffett, personal commun., 1999; Sheppard and Taylor, 1974). In the present study, argillic alteration was logged in much of the deep drill core where igneous plagioclase of the Butte Quartz Monzonite was preserved during pre-Main Stage

and Main Stage alteration. This argillic alteration consists principally of "green argillic" alteration characterized by montmorillonite or other smectite clays, with some zones of "white argillic" alteration where kaolinite is the principal clay. White and green argillic alteration zones are not apparently distributed as selvages to well-developed Main Stage veins, or as broad zones on the 10 to 100 m scale near these veins. Based on these observations, we offer the reinterpretation that much of the green argillic alteration may represent a low-temperature (<200°C) hydrothermal event that post-dates the Main Stage. Below, we illustrate the isotopic effects of this alteration.

Alteration assemblages sampled for isotopic study

Five of the 13 types of alteration types listed in Table 2 have been studied here using isotopic analyses; their mineralogy is presented below.

Pervasive biotitazation of hornblende: It is about a 2 by 5 km zone, as shown in Figure 1 where primary hornblende is generally replaced by secondary biotite and K-feldspar, quartz, sulfide(s), rutile, ± anhydrite; igneous biotite is either fresh or partly replaced along its rim by secondary biotite and minor K-feldspar, quartz, and sulfide(s). Plagioclase is slightly altered to biotite or sericite, and igneous K-feldspar is unaltered.

Early Dark Micaceous (<1 to 5 cm envelope on veinlets, Fig. 2): Primary hornblende is replaced by secondary green and brown biotite and sericite, quartz, sulfide(s), and rutile; igneous biotite is relict but partly replaced on its rim by secondary biotite and sericite, quartz, secondary K-feldspar, minor sulfide(s), and rutile; and both plagioclase and K-feldspar are replaced by sericite, fine-grained biotite, quartz, secondary K-feldspar, ± sulfide(s), and oxide(s).

Gray-sericitic (Figs. 2&3): Hydrothermal sericite, quartz, pyrite, and rutile have replaced all rock minerals and destroyed the rock texture. Locally, muscovite pseudomorphs of igneous biotite is recognizable.

Green argillic (superimposed on pre-Main Stage): Minerals of the earlier pre-Main Stage alteration are generally preserved, except that most of the remaining plagioclase is replaced by montmorillonite (Na-smectite), ± kaolinite, illite.

White argillic (superimposed on pre-Main Stage): Relict igneous plagioclase is partly to completely replaced by kaolinite, ± montmorillonite, sericite.

X-ray diffraction analyses on three clay minerals from samples 11148-4790.5, 11148-4219.5, and Bu96004 show that all the separates have more or less mixed mineral content of kaolinite, montmorillonite, and illite. For example, in sample 11148-4790.5, the percentage of these minerals in the separate is 60% kaolinite, 10% montmorillonite, and 30% illite. For sample 11148-4219.5, there are 60% montmorillonite, 8% kaolinite, and 27% illite plus 5% MGchl in a <2μm grain size separate; and the percentage of minerals is 35% kaolinite, 15% montmorillonite, and 50% illite (mica) in a coarse grain size separate (hand picked). Sample Bu96004, on the other hand, is montmorillonite dominated with about 10% of illite and <10% kaolinite mixed together.

Analytical Procedures

Electron microprobe

The CAMECA SX-50 electron microprobe at Oregon Stage University was used to determine chemical compositions of hornblende, biotite, and sericite. A beam current of 30.1 nA and an accelerating voltage of 15.1 kV were used. The counting time was 10 seconds for major elements, 20 seconds for F, Ba, Ti, and Fe, and 30 seconds for Rb, respectively. The PAP correction procedure was also used. Natural and synthetic mineral standards were analyzed at beginning of each run and all the standards used for our analyses are listed in Appendix A. Relative analytical error, based on replicate

analyses, is about 1 percent for major elements, and 5-10 percent for minor elements, respectively.

Oxygen and hydrogen isotopes

A total of 147 mineral separates were analyzed for oxygen and/or hydrogen isotopic compositions from 62 samples, as described below. These mineral separates include hornblende, biotite, K-feldspar, clay, sericite, and quartz. These minerals were purified by crushing, sieving, hand-picking, and in some cases, heavy liquids. The purity is > 99 percent and the principal contaminants are intergrown rutile in some biotite grains and intergrown quartz in some sericite grains. The clay minerals used for hydrogen isotopic analyses were separated by centrifuge to <2μm grain size, except the kaolinite-rich clay sample 11148-4219.5, which was hand-picked.

The gases used for $^{18}O/^{16}O$ and D/H analyses were extracted in the stable isotope laboratory in the Geosciences Department at Oregon State University, except for eight samples, 11135-3841, 11135-3586, 10778-4, 10772-31, 10854-643, 10759-336, 11170-1767, and 11170-2423, which were analyzed at the Geological Survey of Japan in Tskuba. A laser-extraction vacuum line, modified from the design of Sharp (1989), was used to extract oxygen gases from silicates. A small amount of silicate (2-5 mg) was heated by the 25 watt CO_2 laser and reacted with the ClF_3 reagent to release O_2. The oxygen gas was then converted to CO_2 by reaction with a hot carbon rod in the presence of platinum. The CO_2 was collected in sealed tubes and analyzed for $^{18}O/^{16}O$ by mass spectrometry at the College of Oceanography and Atmospheric Sciences, Oregon State University, or Washington State University.

The standard uranium reduction technique was used for extraction of hydrogen from minerals (Bigeleisen et al., 1952). About 50 to 100 mg of hydrous minerals (or 20 to 40 mg of clay minerals) wrapped in Mo foil were placed in quartz-tubes and pre-heated at

150 -180 °C overnight under vacuum to remove surface and interlayer water. The samples then were step-heated to 1250 °C to release the structural water, which was converted by reaction with hot uranium (~770 °C) to H_2 gas. The D/H ratios of the H_2 samples were determined by mass spectrometry at Washington State University.

All isotope analyses are reported as δ–values in per mil relative to the standard mean ocean water (V-SMOW). Replicate oxygen analyses for NBS-30 biotite yield $\delta^{18}O$ of 5.0 ± 0.3 ‰ (n=32) (1σ), for UWG2 garnet yield $\delta^{18}O$ of 5.8 ± 0.3 ‰ (n=6), for NCSU quartz yield $\delta^{18}O$ values of 10.7 ± 0.6 ‰ (n=22), and for NBS-28 silica glass yield $\delta^{18}O$ of 9.3 ± 0.1 ‰ (n=3). The gas yields for quartz standards are rather low (~75%), reflecting the difficulty of analyzing quartz with a laser. Therefore, an empirical correction of +0.5 ‰ on oxygen isotopic compositions has been made to quartz reported in this study.

Replicate hydrogen analyses of NBS-30 biotite, in our lab, yields δD of -59 ± 7 ‰ (n =12), which is about 6 ‰ heavier than the accepted value of -65 ‰. Our lab standard BuD96014 (Butte Quartz Monzonite) yields a δD value of -156 ± 6 ‰ (n=12). The Misasa sericite standard yields a δD value of 56 ± 6 ‰ (n=6) in our lab, and is ~4 per mil heavier than the δD values of 60 ± 1 ‰ obtained by Okayama University in Japan. Whereas we have not made any lab correction for the unknowns, a 5 ‰ reduction may be appropriate.

Replicate analyses (reported at 1 std dev) for a variety of mineral unknowns (hornblende, biotite, K-feldspar, sericite, quartz, and clay) yield generally small (±0.2‰) standard deviations for $\delta^{18}O$ with the exception of a few samples (Table 3 & 4) that have the standard deviation about 1‰. The hydrogen replicate analyses (hornblende, biotite, sericite) have a much larger range of standard deviations from 1 to 16 ‰. These large standard deviations suggest some D/H isotopic heterogeneity in individual mineral separates of the unknowns.

Composition of Hydrous Silicates

Biotite data

Roberts (1975) noted variations in Fe/Fe+Mg and TiO_2 of both hydrothermal biotite and relict igneous biotite in the zone of pervasive alteration of hornblende to biotite. Here we have performed additional analyses to understand the compositional variations, in particular to see if these variations are due to high-temperature K-silicate alteration, or due to low-temperature argillic alteration.

Electron microprobe analyses of biotites from different parageneses were performed to document the chemical compositions of each biotite type and to understand under the conditions when the biotite had last equilibrated with hydrothermal fluid. In particular, we wanted to test the possibility that D/H and $^{18}O/^{16}O$ isotopic exchange with low temperature, acidic fluids may have changed compositions of earlier-formed, high-temperature biotite.

There are three main classes of biotite: igneous biotite in fresh Butte Quartz Monzonite, biotite in K-silicate-altered rock in which all hornblende is altered to biotite and other minerals, and biotite in K-silicate altered rock where plagioclase is partly replaced by later montmorillonite or kaolinite at low-temperature. In the last two classes of altered rocks, the biotite can be further subdivided into: 1) relict igneous biotite, recognized by its large grain size (0.5-5 mm) and book-like form; and 2) hydrothermal biotite, recognized by its fine-grain size (0.1 to 0.5 mm) and occurrence as clots and aggregates of disoriented "shreddy" flakes intergrown with quartz and minor rutile, sulfide, and other minerals. The latter occupied former igneous hornblende sites.

Compositions of all three main biotite classes are distinct, and for some chemical parameters the relict igneous and hydrothermal biotite in altered rocks can be further

distinguished. Igneous biotite has higher values of molar Fe/(Fe+Mg) and TiO_2, compared to biotite from hydrothermally altered rocks (Fig. 4a). In both K-silicate samples and K-silicate samples with an argillic overprint, the molar Fe/(Fe+Mg) of relict igneous and hydrothermal biotite are similar. However, in these samples, TiO_2 is slightly more elevated in the relict igneous biotite relative to hydrothermal biotite and is broadly the same in both samples with and without argillic alteration. In K-silicate samples, Fe/Fe+Mg ranges from 0.36 to 0.45, whereas in argillically altered K-silicate samples, Fe/(Fe+Mg) is in generally lower and ranges from 0.18 to 0.42.

The biotite compositions from this study (Fig. 4a) are generally similar to microprobe analyses by Roberts (1975) (Fig. 4b). Roberts (1975) did not recognize the effect of reduced Fe/(Fe+Mg) due to late argillic alteration, but his data group IIIa (hydrothermal biotite with low Fe/Mg) are consistent with this origin because they overlap with the compositions we have reported (Fig. 4a &4b).

The fluorine content of biotite increases significantly from fresh Butte Quartz Monzonite, to K-silicate altered rock, and to K-silicate altered rock with argillic alteration overprint (Fig. 4c), which indicates F was added by hydrothermal fluids from both high temperature K-silicate alteration and low temperature argillic alteration. Chlorine, on the other hand, in these samples shows only a slight decrease from igneous biotite, to K-silicate biotite, and to K-silicate biotite overprinted by argillic alteration. Similar to the Fe/(Fe+Mg) ratio, there are no obvious differences in F and Cl content between relict igneous biotite and coexisting hydrothermal biotite within the same alteration type. These data suggest that hydrothermal and igneous biotite apparently were chemically equilibrated with respect to F, Cl, and OH in the OH-site.

Hydrothermal biotites apparently have lower Ti, Fe/Fe+Mg, and Cl but higher F (and Al) relative to fresh igneous biotite from Butte Quartz Monzonite. Biotite was apparently preserved as a stable mineral during the low temperature argillic alteration

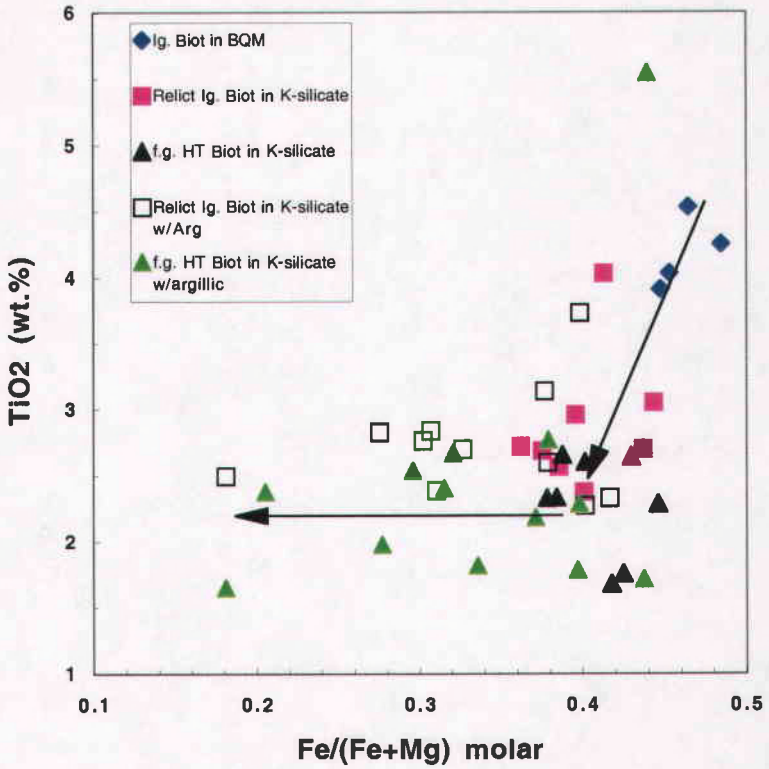

Fig. 4a. Composition of biotites from BQM, K-silicate alteration, and K-silicate with argillic alteration overprint.

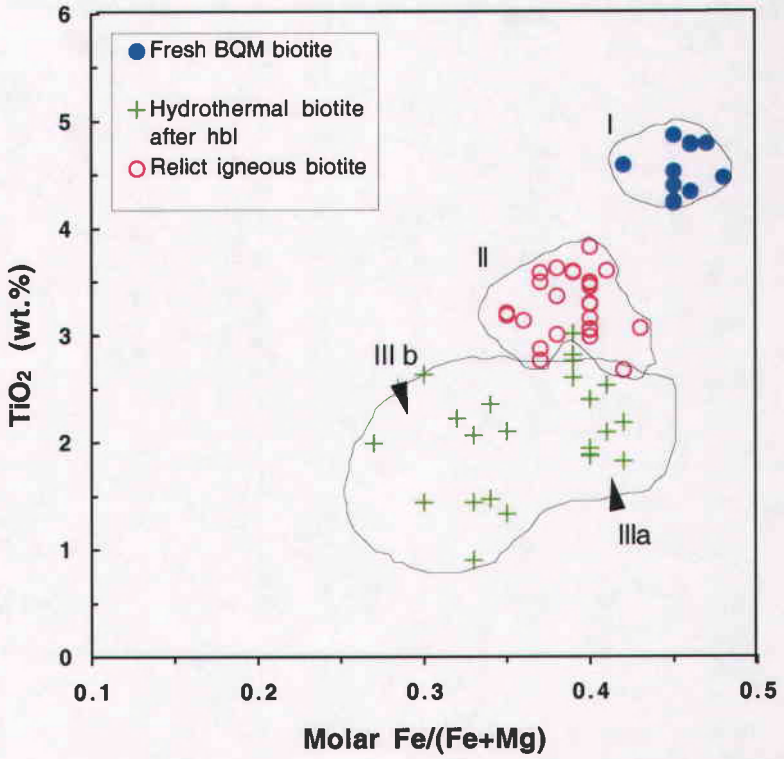

Fig. 4b. Composition of biotites with different origin. Microprobe data from Roberts, 1975.

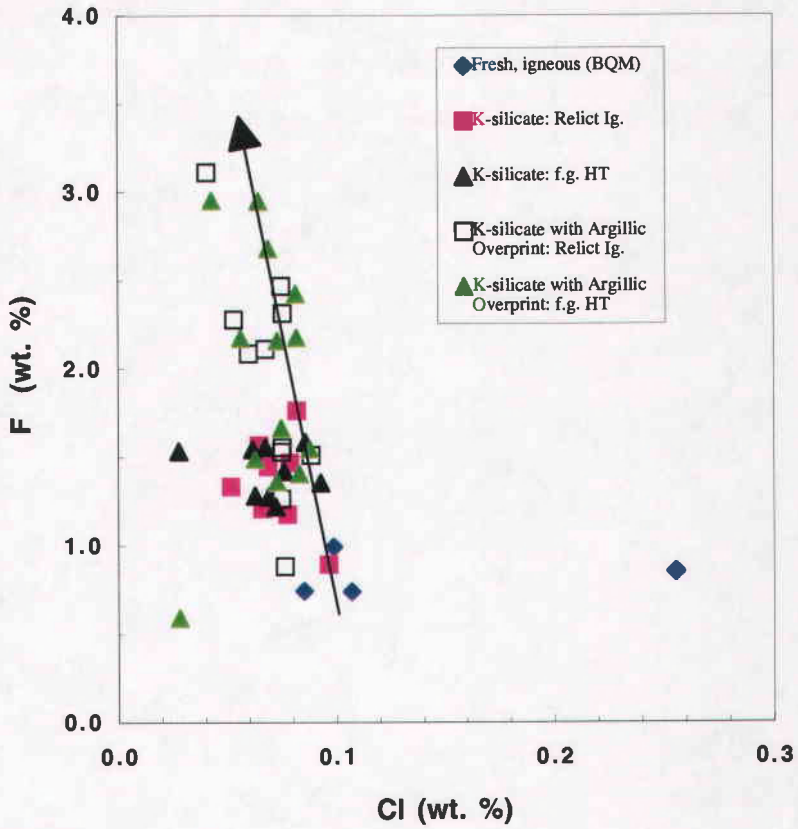

Fig. 4c. Variation of F and Cl contents from fresh igneous biotite (BQM), to high-T hydrothermal biotite (K-silicate alteration), and to low-T argillically altered biotite (K-silicate with argillic alteration overprint).

which occurred at a temperature below which biotite forms in nature (>270°C, Reyes, 1990). However, in argillically altered samples, Fe/Fe+Mg and Cl concentrations are reduced whereas Al and F are increased. TiO_2 content is not changed, apparently because the low-temperature alteration was not capable of removing Ti from the biotite crystal structure and therefore, the TiO_2 contents reflect high-temperature formation. The increase of F/Cl is consistent with F/Cl partitioning theory in which F is increasingly partitioned relative to Cl into biotite as temperature declines in equilibrium with an aqueous fluid of fixed composition (Stormer and Carmichael, 1971).

Sericite data

Microprobe analyses of Butte sericite from various alteration types from Page (1979), together with the gray-sericitic from this study are shown in Figures 5a and 5b. (see Appendix B-b for detailed data). In general, compositions of sericite vary significantly with the paragenesis and alteration assemblage but also have considerable overlap among different alteration groups.

According to Page (1979), sericite from the pale-green sericitic (PGS) alteration exhibits a large variation in the Al/Si ratios from 0.72 to 0.94, but a relatively narrow range of K_2O content (Fig. 5a). Further, the coarse-grained sericite has an Al/Si ratio of 0.93 which is close to the 0.96 of the end member of muscovite whereas fine-grained sericite has much lower Al/Si ratios. Thus considerable substitution of Fe^{2+} or Mg to maintain charge balance should be expected. In contrast to PGS, sericite from dark-green-sericitic alteration (DGS) has a smaller variation in the Al/Si ratios from 0.68 to 0.78, excluding one sample (Al/Si~0.9), but a relatively wider range of K_2O contents (Fig. 5a). These composition ranges are in general close to illite.

Microprobe analyses of sericite from the gray-sericitic alteration from this study overlap with those analyzed by Page (1979). The compositions lie intermediate between

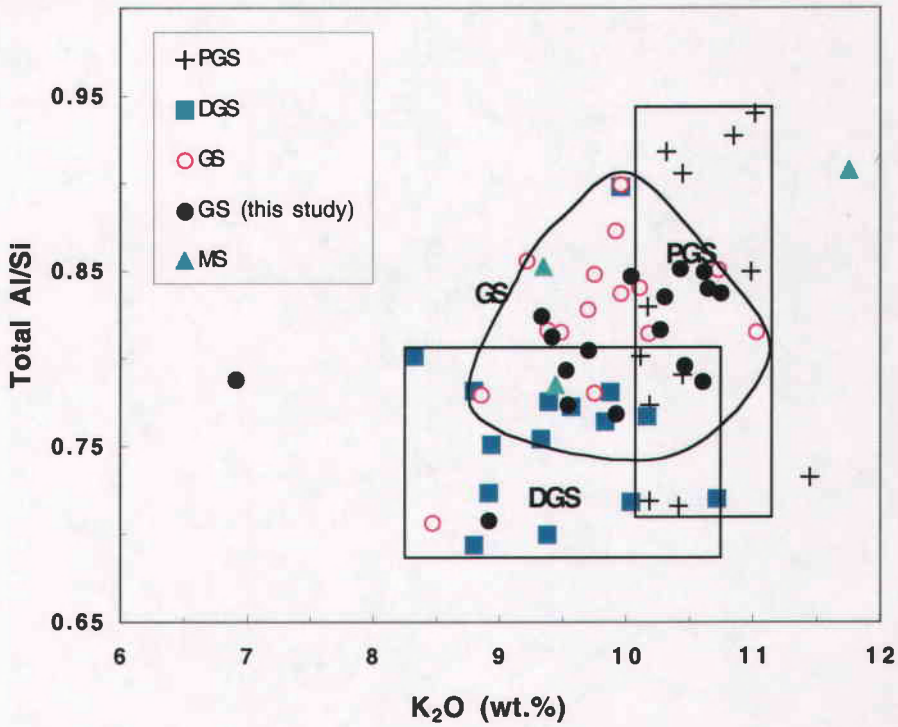

Fig. 5a. K_2O versus molar Al/Si for Butte sericites. Microprobe data from Page (1979) and this study.

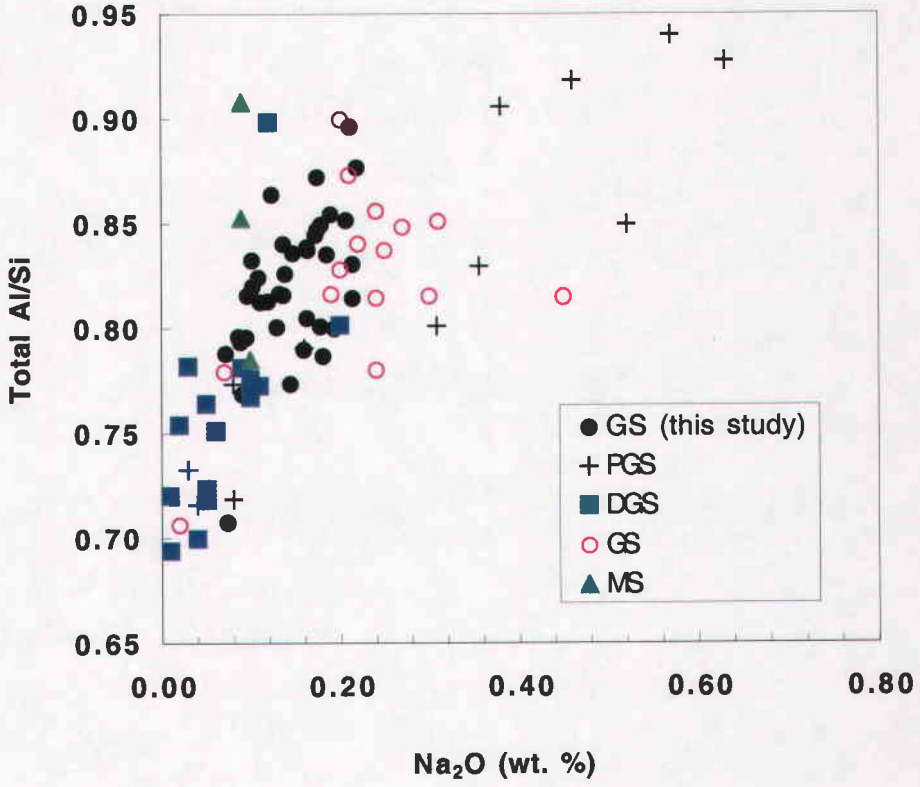

Fig. 5b. Na_2O versus molar Al/Si for Butte sericites. Microprobe data from Page (1979) and this study.

the dark-green sericitic and pale-green sericitic alteration and have a similar range in both Al/Si ratio (0.76-0.90) and K_2O content (8.5-11wt.%), with a few exceptions (Fig. 5a).

The composition variation of sericite from PGS, to GS, and to DGS may suggest that sericite from the gray-sericitic alteration may have formed at a lower temperature than pale-green sericite, but at a higher temperature than sericite from the dark-green sericitic alteration. However, there were only three analyses from Main Stage sericite (Fig. 5a), which are too sparse to allow a sound interpretation.

The Na_2O content for the sericites from Butte display similar patterns compared to K_2O when plotted against molar Al/Si ratio (Fig. 5b). In general, these sericites exhibit a weak positive correlation between the Al/Si ratio and the Na_2O content. PGS sericites have a higher Na_2O content compared to DGS. Again, the gray sericites have compositions intermediate between PGS and DGS sericites. However, the data from this study exhibit a narrower range and generally lower Na_2O content than those reported by Page (1979).

It is interesting to note that the fine-grained sericite from PGS is significantly different from the rest of PGS sericites, but falls into the range of DGS sericite. We speculate that these fine-grained sericites might have exchanged cations with later hydrothermal fluids (of DGS?) because the smaller grain size would generally facilitate reaction exchange relative to the minerals with larger grain size.

Microprobe analyses of GS sericite from this study are shown again in Figure 5c (Al/Si vs K_2O) and Figure 5d (Al/Si vs Na_2O), but are further divided into two subgroups: pervasive gray-sericitic alteration and non-pervasive sericitic alteration with argillic superimposed on plagioclase site outside sericite envelope. There is no distinction in these compositions between the two alteration assemblages, which may suggest that the later argillic alteration had little effect on these compositions of the GS sericite.

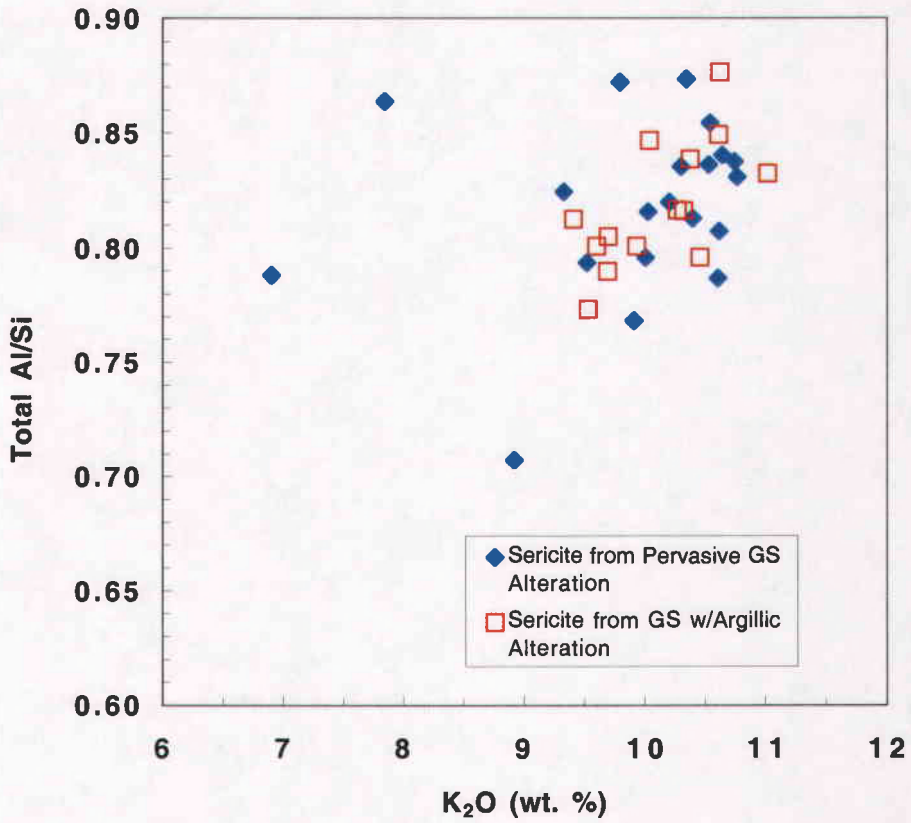

Fig. 5c. Compositional variation of K_2O versus molar Al/Si ratio of sericite from pervasive GS alteration and non-pervasive GS alteration

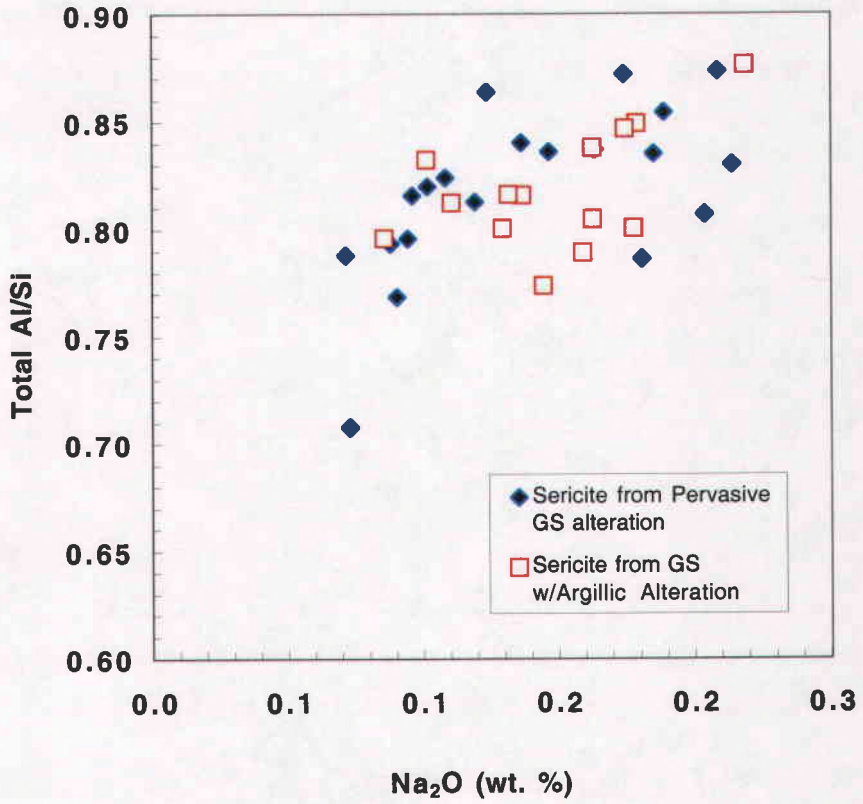

Fig. 5d. Compositional variationof Na_2O versus molar Al/Si ratio of sericite from pervasive GS alteration and non-pervasive GS alteration.

Oxygen and Hydrogen Isotope Data

Sample selection for K-silicate alteration

In this study, rock samples were selected from both surface exposures and deep drill holes and can be divided into three groups: four samples of unaltered Butte Quartz Monzonite, seven samples of biotite from K-silicate alteration, and twenty samples of K-silicate alteration with later argillic superimposed (Figs. 1, 2b & 3). The fresh Butte Quartz Monzonite samples were chosen to determine the original isotopic composition of the host rock. Biotite-altered Butte Quartz Monzonite and K-silicate altered samples, including the biotite breccia sample, were selected to investigate the pre-Main Stage "Early Dark Micaceous" type fluid isotopic compositions in rock with otherwise fresh plagioclase and hydrothermal biotite replaced hornblende. Twenty samples with late argillic alteration superimposed on K-silicate assemblages were studied to determine the effect of late argillic fluids on early pre-Main Stage alteration minerals.

Within each group, pairs or triplets of coexisting mineral were analyzed (Table 3) in order to check the state of the isotopic equilibrium bewteen minerals during each alteration event: early K-silicate alteration and later argillic alteration. The hydrothermal biotite replacing igneous hornblende would usually be the ideal alteration product for determining isotope compositions ($^{18}O/^{16}O$ and D/H) of the K-silicate alteration. However, because the hydrothermal biotite from hornblende sites is always intergrown with fine-grained quartz, separation of pure biotite from quartz in the laboratory is extremely difficult. Instead, the relict igneous biotite in K-silicate altered rocks was used to determine the isotopic compositions of the early high-temperature hydrothermal fluids because the relict igneous biotite was also in isotopic as well as compositional equilibrium with the high-temperature, K-silicate hydrothermal fluids. Further, the relict igneous biotite and the hydrothermal biotite in argillized K-silicate alteration may have

Table 3. Oxygen and Hydrogen Isotopic Data from Fresh Rock and pre-Main Stage K-silicate Alteration Assemblages

Sample	Location	Alteration	% chl in biotite % clay in plag	Mineral Analyzed	Measured isotopic values $\delta^{18}O$ (‰, SMOW)	 δD (‰, SMOW)	Measured H2O (wt %)	Calculated isotopic values of fluids T (°C)	 $\delta^{18}O$ (‰, SMOW)	 δD (‰, SMOW)
Butte Quartz Monzonite (BQM)										
Bu214	Elk Park	Fresh	1% chl	Biotite	4.1	-88 ± 12(2)	2.8 ± 0.0	700	6.7	-61
				Hornblende	5.2	-68 ± 1(2)	1.9 ± 0.0	700	7.4	-45
				K-feldspar	7.6			700	7.1	
				Quartz	8.6			700	7.5	
Bu211	I-15 roadcut	Fresh	3-5% chl	Biotite	5.6 ± 0.1(2)	-119	2.8	700	8.3	-91
				Hornblende	6.0 ± 0.2(3)	-110	1.7	700	8.2	-87
				K-feldspar	8.4			700	7.9	
				Quartz	8.7			700	7.6	
Bu96001	I-15 roadcut	Fresh	5% chl	Biotite	4.1 ± 0.0(2)	-165	2.9	700	6.8	-135
				Hornblende	5.6	-149	2.0	700	7.9	-126
				K-feldspar	7.9			700	7.3	
				Quartz	8.7			700	7.7	
BuD96014	Berkeley pit, North ramp	Fresh	up to 5% chl	Biotite	4.1 ± 0.3(2)	-156 ± 6 (2)	3.0 ± 0.1	700	6.5	-125
				Hornblende	5.3 ± 0.3(2)	-146	1.9	700	7.4	-123
				K-feldspar	7.5 ± 0.1(2)			700	7.0	
				Quartz	8.9			700	7.8	
K- Silicate Alteration										
11172-2200	DDH 10	PB		Ig bi	5.2 ± 0.0(2)	-124	2.5	550	7.7	-92
				HT bi	5.4	-114a	1.5c	550	7.9	-83
				K-feldspar	8.2 ± 0.2(2)			550	7.0	
11172-2934	DDH 10	PB	± chl	Ig bi	5.0	-96 ± 8(2)	2.4 ± 0.0	550	7.4	-64
				HT bi	4.4	-93a	1.6c	550	6.9	-62
				K-feldspar	8.2			550	7.1	
				Quartz	9.6			550	7.7	
11172-3920	DDH 10	PB	1% chl	Ig bi	4.5 ± 0.2(2)	-94	2.7	550	7.2	-60
				HT bi		-88a	1.9c	550	6.8	-55
				K-feldspar	8.3			550	7.1	
				Quartz	8.9			550	7.0	
11172-4005	DDH 10	PB	<5% chl	Biotite	5.2	-77	2.4	550	7.7	-47
				K-feldspar	7.8			550	6.6	
11172-4166	DDH 10	PB	10-20% calc	Biotite	4.7	-93	2.7	550	7.2	-59
				HT bi		-117 ± 4(2)a	1.7 ± 0.1c	550		-83
				K-feldspar	6.4 ± 0.2(2)			550	5.2	
				Quartz	9.5			550	7.6	

TABLE 3 (Continued)

Bu96017	Continental Mine, 5680 elevation	PB		Biotite	5.7 ± 0.2(2)	-86b	2.2	550	8.1	-55
				K-feldspar	8.9			550	7.7	
Bu96018	Continental Mine, 5680 elevation	BB	± chl	Biotite	4.7	-130	2.8	550	7.2	-98
				K-feldspar	8.2			550	7.1	
				Quartz	10.0			550	8.1	
K-Silicate Alteration with Argillic Superimposed										
Bu96004	Continental Mine, 5680 elevation	EDM/GA	30% mont	HT bi	6.9	-126b	1.6c	550	9.4	-92
				Mont-rich	7.8	-109	5.4	150	-2.4	-97
				K-feldspar	8.4 ± 0.4(2)			550	7.4	
Bu96006	Continental Mine, 5680 elevation	PB/Porp	5-10% chl	Biotite	3.0	-132b	2.6	550	5.5	-101
				K-feldspar	6.1			550	5.1	
Bu96007	Continental Mine, 5680 elevation	PB/WA	70-90 kao	Biotite	-0.3 ± 0.2(2)	-129b	2.9	550	2.0	-100
				K-feldspar	4.0 ± 1.0(2)			550	2.3	
Bu96009	Continental Mine, 5680 elevation	PB/A (?)	<50% kao	Ig bi	3.5	-144	2.4	550	6.0	-123
				HT bi		-145a	1.9c	550		-113
				K-feldspar	7.5			550	6.3	
Bu96015	Continental Mine, 5680 elevation	PB/GA	60% mont	Biotite	6.2	-120b	2.2	550	8.7	-93
				K-feldspar	9.6			550	8.6	
Bu96016	Continental Mine, 5680 elevation	PB/GA±WA	10% clay,10% calc & <5% chl	Biotite	-2.0 ± 0.4(2)	-152	2.8	550	0.5	-122
				HT bi		-152a	2.2c	550		-119
11135-3481	DDH 2	EDM/A	~5% cavities ± calc	Ig bi	0.1	-135	2.4	550	2.6	-122
				HT bi		-147a	1.8c	550		-119
11135-3586	DDH 2	BB/A	2-10% clay, ± chl	HT bi	-1.7	-133a	2.3c	550	0.8	-105
11135-4966	DDH 2	BB/A	40-60% clay	Biotite	6.0 ± 0.1(2)	-116b	1.8c	550	8.6	-89
				K-feldspar	8.1			550	6.9	
11148-4219.5	DDH 3	EDM/WA/GA	~10% chl	Biotite	4.9	-130b	2.3c	550	7.4	-103
			10-20% mont+kao	K-feldspar	8.7			550	7.6	
				Kao-rich	5.8	-118	7.2	150	-2.9	-98
				Mont-rich		-109	4.6	150		-97
11148-4790.5	DDH 3	PB/WA	± chl	Biotite	-0.4	-158b	2.6	550	2.1	-131
			90% kao ± mont	K-feldspar	2.5			550	1.5	
				Kao-rich	0.5 ± 0.1(2)	-133	8.7	150	-8.2	-113
11171-3367	DDH 8	BB	± chl	HT bi		-129a	1.0c	550		-103
11171-4911	DDH 8	PB/GA	± chl,	Biotite	5.6	-137 ± 16(2)b	1.7± 0.1	550	8.1	-112
			>90% mont ± kao	K-feldspar	8.9			550	7.9	
5-3449	DDH 5	BB/GA?	?	Biotite	5.9	-159	2.1	550	8.4	-131
5-4369	DDH 5	PB/GA?	?	Biotite	6.3 ± 0.3(2)	-150	2.2	550	8.8	-122
11172-1865	Continental Mine, DDH 10	PB/GA	5-10% mont	Ig bi	5.8 ± 0.0(2)	-115	2.3	550	8.3	-84
				HT bi		-115a	1.6c	550	7.6	-84
				K-feldspar	8.8 ± 0.1(2)			550	7.6	
11172-1863	Continental Mine, DDH 10	PB/GA?		Biotite	5.2			550	7.7	
				Muscvite	7.0			550	7.3	

TABLE 3 (Continued)

5-4680	DDH 5	BB/GA?	?	White mica	2.8		550	3.0	
11135-1377	DDH 2	BB/A??	?	Biotite	0.4		550	2.9	
				White mica	5.3		550	5.5	
11135-4206	DDH 2	BB/A??	?	Biotite	1.7		550	4.2	
				White mica	6.1		550	6.3	
Pale Green Sericitic and Dark Green Sericitic Alteration									
10778-4	Anaconda Dome	PGS	?	Sericite	6.4	-156	300	3.0	-113
10772-31	Anaconda Dome	PGS	?	Sericite	6.0	-161	300	2.6	-119
10854-643	Anaconda Dome	DGS	?	Chlorite	3.4± 0.1(2)	-115	300	4.4	-52
10759-336	Anaconda Dome	DGS	?	Chlorite	3.3± 0.7(2)	-124	300	4.3	-63

Abbreviations: PB: pervasive biotitization of hornblende; BB: biotite breccia; EDM; early dark micecaous; Prop: propylitic; A: argillic; GA: green argillic; WA: white argillic; Ig bi: igneous biotite; HT bi: hydrothermal biotite; DDH: deep drill hole; chl: chlorite; plag: plagioclase; mont:montmorillnite; kao: kaolinite; calc: calcite

Notes

a. Hydrogen isotopic compositions were obtained from hydrothermal biotite mixed with quartz.
b. Hydrogen isotopic compositions were obtained from mixture of relict igneous biotite, hydrothermal biotite and quartz.
c. Measured water content from mixture of hydrothermal biotite and quartz and/or relict igneous biotite. Percentage of these minerals are not determined.

1. $1000\ln \alpha$ biot-H2O= 0.41 $(10^6/T^2)$ -3.10 (?) (T: 500-800 °C) Bottinga and Javoy (1973) and Javoy (1977)--Oxygen
2. $1000\ln \alpha$ hbl-H2O = -2.3 $(10^6/T^2)$--Oxygen
3. $1000\ln \alpha$ kspar-H2O = 1.59 $(10^6/T^2)$ – 1.16, (T: 500-800°C) Matsuhisa et al. (1979)--Oxygen
4. $1000\ln \alpha$ qtz-H2O = 2.05 $(10^6/T^2)$ - 1.14, (T: 500-800 °C) Matsuhisa et al. (1979)--Oxygen
5. $1000\ln \alpha$ kao-H2O = 2.76 $(10^6/T^2)$ - 6.75, (T< 150-350 °C) Sheppard and Gilg (1996)---Oxygen
6. $1000\ln \alpha$ mont-H2O = 2.55 $(10^6/T^2)$ – 4.05, (T: 0-350 °C) Sheppard and Gilg (1996)---Oxygen
7. $1000\ln \alpha$ ill/mus-H2O =2.39 $(10^6/T^2)$ – 3.76, (T: 0-700 °C) Sheppard and Gilg (1996)---Oxygen
8. $1000\ln \alpha$ hbl-H2O = -23.1, (T: 350-805°C) Graham et al. (1984)—Hydrogen
9. $1000\ln \alpha$ mica-H2O = $-22.4(10^6/T^2) + 28.2 + (2X_{Al}-4X_{Mg}-68X_{Fe})$, (T: 450-850 °C) Suzuoki and Epstein (1976)—Hydrogen
10. $1000\ln \alpha$ mica-H2O = $-22.4(10^6/T^2) + 28.2 + C$ (where C=32.2) (T: 450-850 °C) Suzuoki and Epstein (1976)—Hydrogen
11. $1000\ln \alpha$ kao-H2O =-2.2 $(10^6/T^2)$ - 7.7, (T: 0-330 °C) Sheppard and Gilg (1996)--Hydrogen
12. $1000\ln \alpha$ mont-H2O =-12.5, (T =~ 150 °C) Capuano (1992) -Hydrogen

been re-equilibrated isotopically with the late argillic hydrothermal fluids and therefore, they should posses different isotopic compositions from non-argillized K-silicate samples.

Oxygen isotope data of BQM and K-silicate minerals

Butte Quartz Monzonite: We examined unaltered Butte Quartz Monzonite, the host rock to all ores at Butte, to obtain the pre-alteration isotope compositions. The oxygen isotopic compositions of minerals from fresh Butte Quartz Monzonite at Butte yield values typical of granites.

The four hornblende samples have a narrow range of $\delta^{18}O$ values from 5.1 to 6.0 per mil, whereas the coexisting biotite possesses a slightly wider range of $\delta^{18}O$ values from 3.9 to 5.7 per mil (Fig. 6a, Table 3). These data show that hornblende is isotopically heavier than biotite by about 0.9 to 1.5 per mil, except for one sample (Bu211), where they differ by only 0.3 per mil. These analyses and the observed hornblende-biotite fractionation are in agreement with previous oxygen isotope studies of coexisting hornblende and biotite from the Boulder batholith ($\Delta_{Hbl\text{-}Biot} = 1.5$ ‰) by Taylor and Epstein (1962), Shieh and Taylor (1969), and Sheppard and Taylor (1974), and apparently reflect the equilibrium ^{18}O fractionation between hornblende and biotite in granitic systems (Taylor, 1974). K-feldspar samples from the four fresh Butte Quartz Monzonite samples yield $\delta^{18}O$ values of 7.4 to 7.9 per mil. These are isotopically heavier than the coexisting hornblende and biotite, and are consistent with the equilibrium fractionation of $\Delta_{Ksp\text{-}Biot} = 3.5$ - 3.7 per mil. The $\delta^{18}O$ values from four rock quartz samples are within a narrow range (8.6- 8.9‰) and are also isotopically heavier relative to the rest of co-existing minerals.

K-silicate alteration: Biotite from the seven K-silicate alteration samples yields oxygen isotope compositions ranging from 4.4 to 5.7 per mill (Fig. 6b, Table 3). The

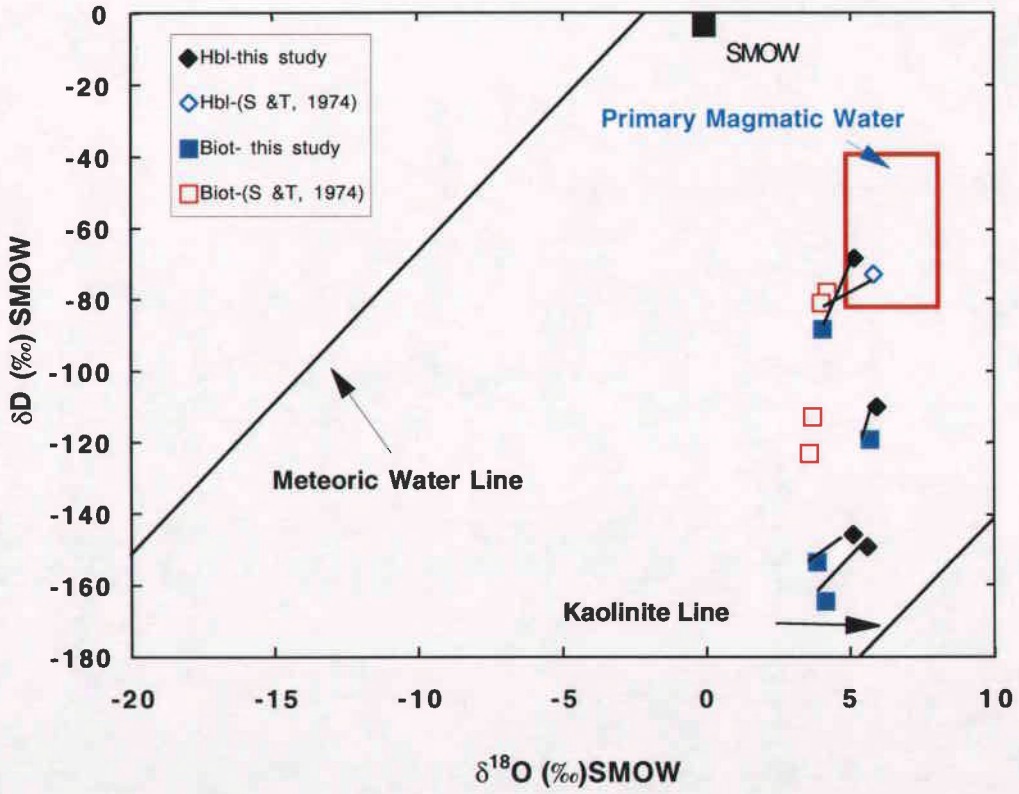

Fig. 6a. $\delta^{18}O$ versus δD of hornblende and biotite from the freshest samples of Butte Quartz Monzonite from the Butte district (data from Sheppard & Taylor 1974 (S&T) and this study; lines connect coexisting minerals).

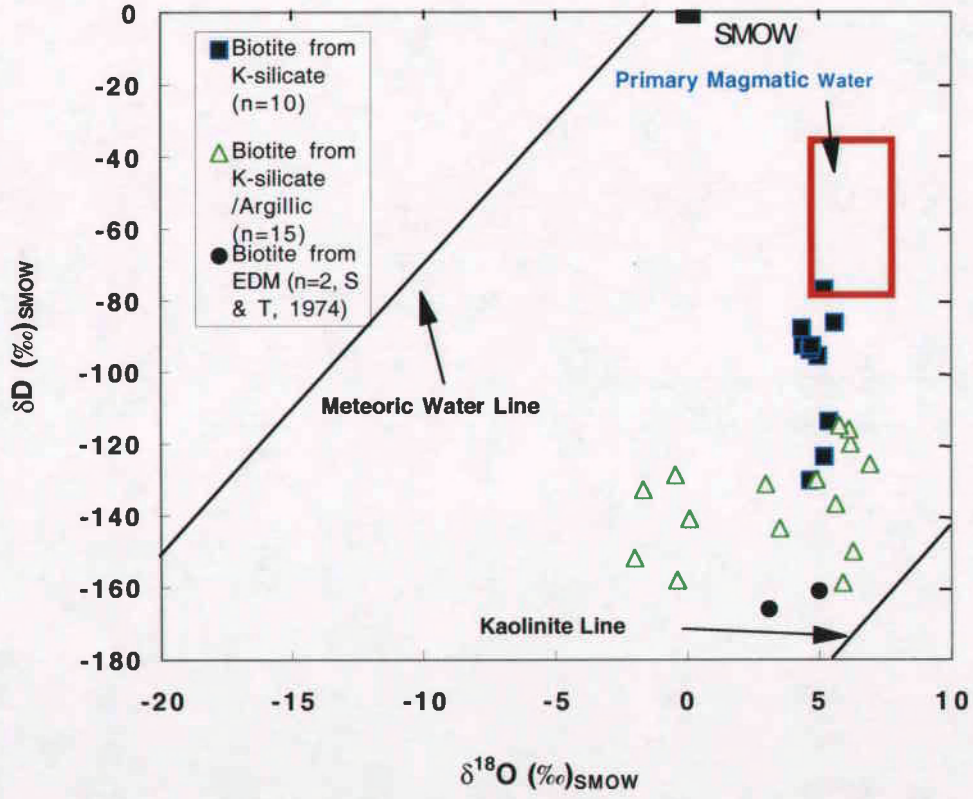

Fig. 6b. Oxygen and hydrogen isotopic compositions of hydrothermal biotite from early K-silicate alteration. Two samples from Sheppard and Taylor (1974) are also included.

mean $\delta^{18}O$ value of 5.0 per mil (±0.4‰, n=7) is slightly ^{18}O-enriched relative to the Butte Quartz Monzonite biotite which has a mean $\delta^{18}O$ value of 4.3 per mil (n=4). For two samples, both hydrothermal biotite (replacing hornblende) and relict igneous biotite in the K- silicate alteration zone have been analyzed separately and yield similar oxygen isotope compositions (11172-2200: $\delta^{18}O_{\text{HT Biot.}}$ = 5.4 ‰, $\delta^{18}O_{\text{Relict Biot.}}$ = 5.2 ‰; 11172-2934: $\delta^{18}O_{\text{HT Biot.}}$ = 4.4 ‰, $\delta^{18}O_{\text{Relict Biot.}}$ = 4.9 ‰, Table 3). These data indicate that oxygen isotopic equilibrium was likely established between relict igneous and hydrothermal biotite, and that relict igneous biotite was ^{18}O-enriched via K-silicate alteration by ~0.5 to 1.0 per mil relative to fresh rock biotite.

Oxygen isotope compositions of relict igneous K-feldspar in the K-silicate alteration samples ($\delta^{18}O$= 8.0±0.8‰) are similar to that of K-feldspar from biotite breccia ($\delta^{18}O$ = 8.2 ‰). Most of these K-feldspars are slightly ^{18}O-enriched relative to the fresh Butte Quartz Monzonite K-feldspar (7.5 to 8.4 ‰), excluding sample 11172-4166 which possesses a lighter $\delta^{18}O$ value of 6.4 ‰ (Fig. 7, Table 3). The fractionation between K-feldspar and biotite in these K-silicate alteration samples is about 3 per mil, except for sample 11172-4166, which is 1.7 per mil. Similar to other K-silicate minerals, the three quartz samples from quartz veinlets are also ^{18}O-enriched (~0.5 ‰) relative to those of BQM samples. Possible, but speculative, explanations are either the K-silicate alteration fluid was ^{18}O-enriched, or K-silicate alteration was formed at lower temperatures than BQM.

K-silicate with argillic alteration: In contrast to the relatively uniform $\delta^{18}O$ values of minerals from K-silicate alteration, the oxygen isotope compositions of minerals from K-silicate altered samples that were affected by later argillic alteration are highly variable. Biotite from these samples gives a wide range of $\delta^{18}O$ values from -2.0 to 6.9 per mil (Fig. 6b, Table 3). In addition, these biotite samples can be divided into two groups based on the alteration type and their oxygen isotope compositions: (a) white

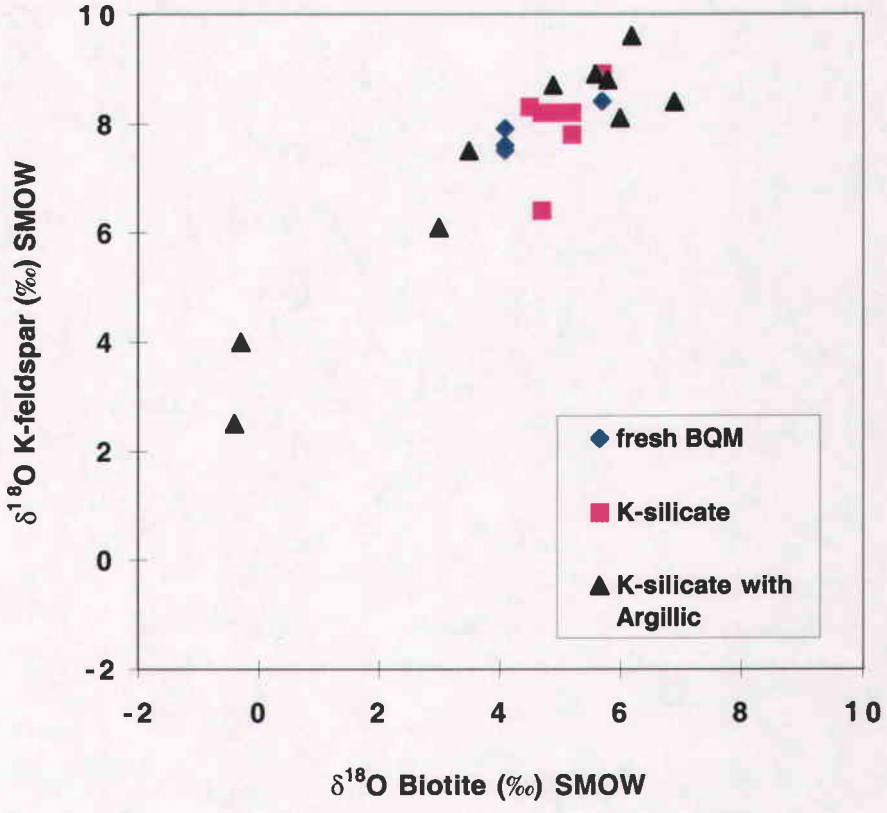

Fig. 7. Oxygen isotope compositions of biotite-K-feldspar pairs from samples of BQM, K-silicate alteration, and K-silicate with argillic alteration overprint.

argillic (4 samples): $\delta^{18}O$ similar to or slightly enriched relative to typical K-silicate alteration samples and (b) green argillic (10 samples): ^{18}O-depleted relative to typical K-silicate alteration samples (Fig. 6b). Ten K-feldspars from the argillized K-silicate alteration group also show a large isotopic variation ($\delta^{18}O_{Kspar}$ = 2.5 ‰ to 9.6 ‰) (Fig. 7). The fractionation between K-feldspar and biotite in the argillically altered K-silicate samples ranges from 1.5 to 3.8 ‰.

$\delta^{18}O$ versus composition of biotite: The ^{18}O-isotopic composition of biotite from fresh rock, K-silicate, and K-silicate with argillic alteration was plotted against its TiO_2 content (Fig. 8a) and Fe/(Fe+Mg) ratios (Fig. 8b). The K-silicate biotite is slightly enriched in ^{18}O, but depleted in TiO_2 relative to the fresh rock biotite. Subsequent argillic alteration produced a wide range of $\delta^{18}O$, but did not modify the TiO_2 content of biotite. The Fe/(Fe+Mg) ratios of biotite in argillically altered samples are either similar or reduced relative to K-silicate biotite. These variations are seen for both biotite samples that are ^{18}O-enriched (mont) and ^{18}O-depleted (kaol) by argillic alteration relative to K-silicate biotite. One exception is the sample Bu96016 which is ^{18}O-depleted but with a similar Fe/(Fe+Mg) ratio to the K-silicate biotite (Table 3). This sample contains both montmorillonite and kaolinite, but is dominated by montmorillonite of green argillic alteration.

$\delta^{18}O$ of clay minerals: Clay minerals from three samples that are strongly argillic-altered and were likely formed by late hydrothermal fluids, yield $\delta^{18}O$ values of 0.5 per mil for 11148-4790.5, 5.8 per mil for 11148-4219.5, and 7.8 per mil for Bu96004, respectively. XRD analyses illustrate that they are mixed samples. Sample 11148-4790.5 is dominated by kaolinite, sample 11148-4219.5 is enriched with both kaolinite and montmorillonite (1:1), and sample Bu96004 is montmorillonite-rich. Therefore, the $\delta^{18}O$ values of these clay samples represent mixed isotopic compositions. This large isotopic variation (0.5-7.8‰) among these three argillized K-silicate alteration samples

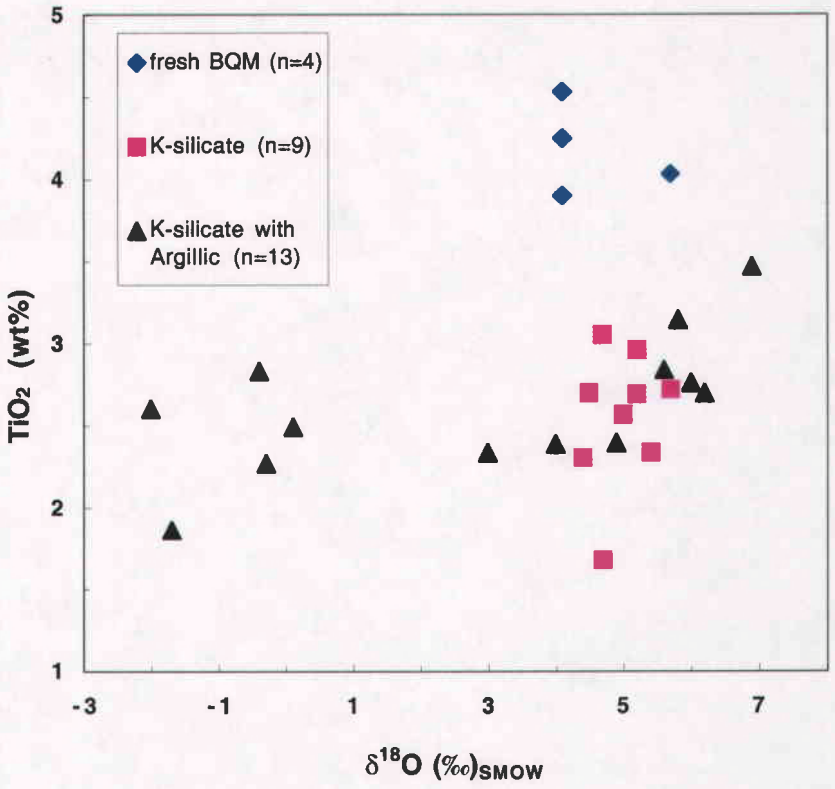

Fig. 8a. Relationship between TiO_2 content and $\delta^{18}O$ values of biotites samples from BQM, K-silicate alteration, and K-silicate with argillic alteration overprinted.

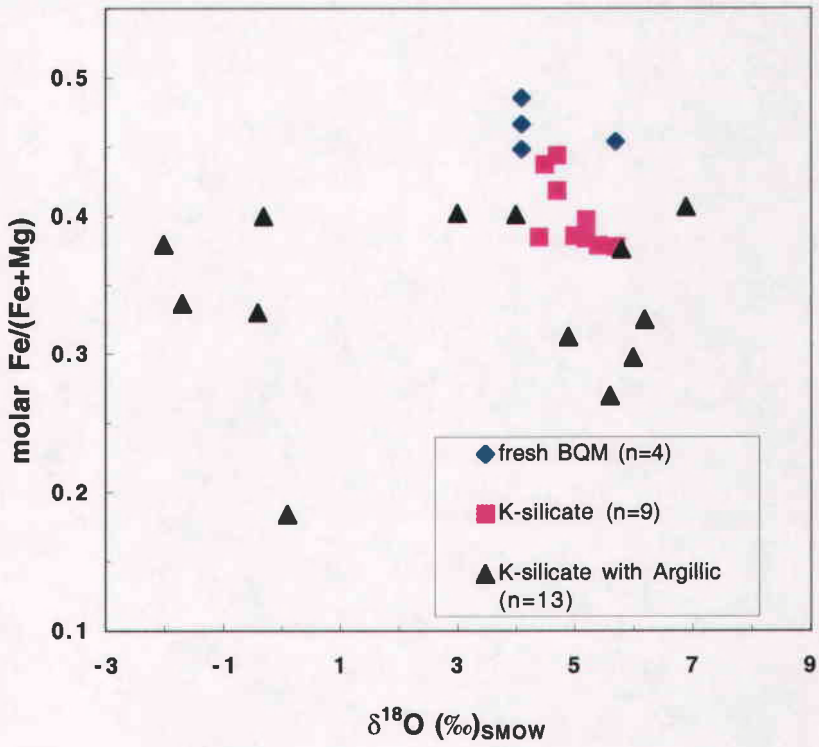

Fig. 8b. Relationship between Fe/(Fe+Mg) ratio and $\delta^{18}O$ values of biotite samples from BQM, K-silicate alteration, and K-silicate with argillic alteration overprint.

is in good agreement with the wide range of oxygen isotope composition of clays and micas from the Main Stage mineral assemblages ($\delta^{18}O$ = -9 to +12 ‰), reported previously by Sheppard and Taylor (1974), apparently reflecting various degrees of exchange of meteoric waters with wallrocks, as explained below.

Hydrogen isotopic compositions

Butte Quartz Monzonite: Both hornblende and biotite in the four fresh Butte Quartz Monzonite samples show a wide range of hydrogen isotopic compositions (Fig. 6a, Table 3). The δD values of hornblende are -68 per mil for Bu214, -110 per mil for Bu211, -146 per mil for Bu96001, and -149 per mil for Bu96014, and the coexisting biotite has slightly lighter δD values of -88, -119, -156, and -165 per mil, respectively. Previous data (Sheppard and Taylor, 1974) show a similar pattern but our data have extended this range toward D-depletion. The small variation in the measured fractionation of 9-20 ‰ between hornblende and biotite of these samples shown in Figure 9 suggests a hydrogen isotopic equilibrium between these two hydrous-minerals and the coexisting aqueous fluid which might be the original magmatic fluid or a late meteoric fluid. It is noteworthy that the apparent fractionation between these two co-existing minerals here is larger than the fractionation of 5-6 ‰ at 700 °C obtained from laboratory experiments (Suzuoki and Epstein, 1976; Graham et al., 1984) between hornblende and biotite.

K-silicate alteration: The seven K-silicate alteration samples selected for this study are all from Continental area (deep drill hole #10 and surface samples at the 5680 feet (1731 meters elevation), where there is little evidence of either the Main Stage alteration and mineralization, or the argillic alteration. The δD values of biotite from these samples range from -77 to -130 per mil (Fig. 6b, Table 3), and they are all significantly isotopically heavier than the two δD values of -160 and -166 per mil from K-silicate

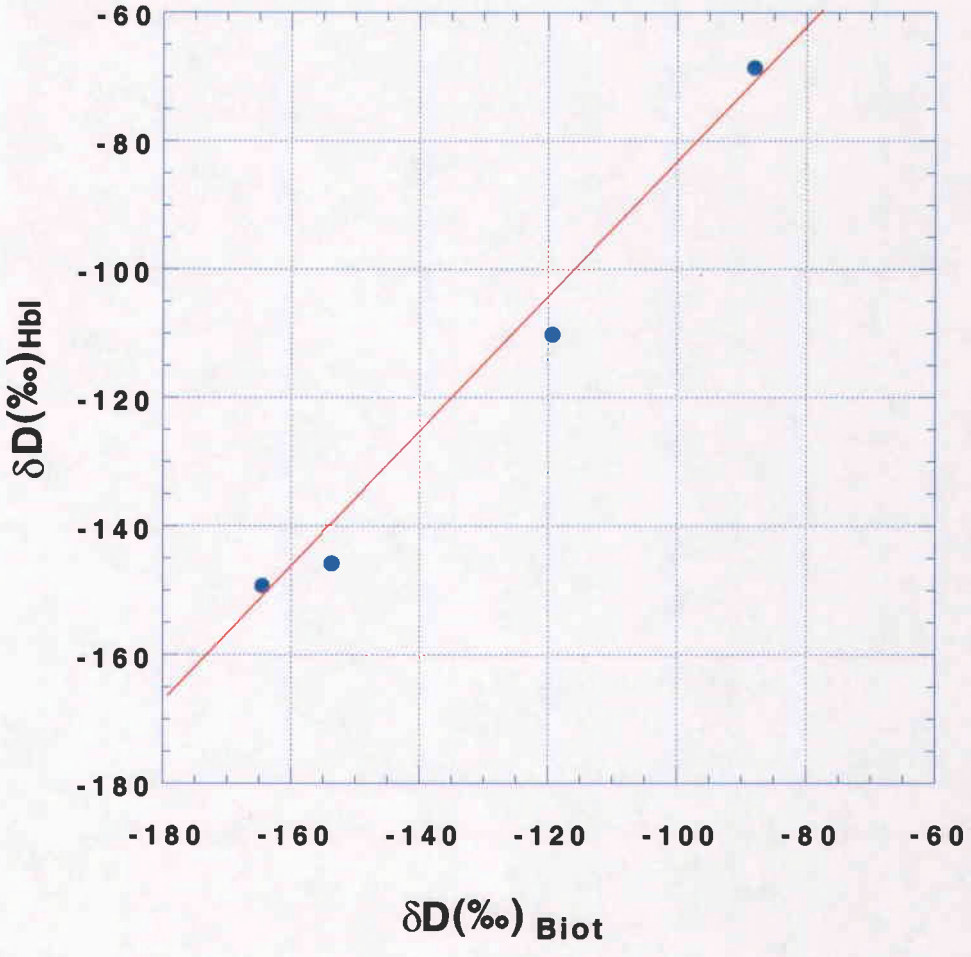

Fig. 9. Hydrogen isotope compositions of biotite-hornblende pairs from BQM

reported previously (Sheppard and Taylor, 1974). The δD values of these seven samples apparently fall into two subgroups: four samples with δD > -94 per mil and three samples with δD < -117 per mil (Fig. 6b).

The δD values of co-existing relict biotite and secondary biotite pairs from four K-silicate samples of 11172-2200, 11172-2934, 11172-3920, and 11172-4166 are shown in Figure 10. The δD differences between the relict biotite and the secondary biotite in samples 11172-2934 and 11172-3920 are small (< 6 ‰), whereas the δD difference in samples 11172-2200 and 11172-4166 are 10 and 25 per mil, respectively. The small difference (< 6 ‰) between these two biotite minerals in the first two samples strongly suggests that hydrogen isotope in the relict igneous biotite of Butte Quartz Monzonite has reequilibrated with the K-silicate hydrothermal alteration fluids, which formed the secondary biotite. However, it is less convincing that re-equilibration was also occurred in the last two samples where the δD differences are relatively large. Perhaps, the δD values of these two samples have been affected by later alteration events.

In general, biotite from the K-silicate alteration contains about 2.5 weight percent water which is slightly less than that in fresh rock biotite (2.9 wt. %). Calculated formula water of biotite in K-silicate alteration ranges from 3.4 to 3.7 weight percent and in Butte Quartz Monzonite is about 3.7 weight percent based on microprobe data. The calculated water content is about 1 weight percent higher than that measured values in these biotites. It may suggest that there are other substitutes at the anion sites besides Cl, F.

K-silicate with argillic alteration: A total of twenty-three mineral separates from sixteen partly argillically altered samples of K-silicate alteration have been analyzed for hydrogen isotopic compositions (Table 3). These include three relict biotite-secondary biotite pairs (samples Bu96009, Bu96016, and 11172-1865) and four coexisting clay minerals (samples Bu96004, 11148-4219.5, and 11148-4790.5). Sample Bu96006 was

originally classified into this group, however, further petrologic study has not found clay mineral(s) in this sample (see Appendix C).

The hydrogen isotopic compositions of biotite for the argillically altered samples of K-silicate alteration fall between -115 and -159 per mil (Fig. 6b, Table 3). These argillically altered samples are mostly isotopically lighter in δD values relative to the unaltered K-silicate samples. However, the δD values of the subgroup (< -117 ‰) from the K-silicate alteration samples are overlap with several D-rich samples within this argillically altered group.

As stated above, the relict igneous biotite-secondary biotite pairs were analyzed to check the state of hydrogen isotopic equilibrium between these two minerals. The δD values of relict biotite and hydrothermal biotite are -144 per mil and -145 per mil for sample Bu96009, -152 per mil and -152 per mil for sample Bu96016, and -115 per mil and -115 per mil for sample 11172-1865, respectively (Table 3). It is important to note that the difference in δD values between each of these biotite pairs is very small (≤1 ‰) (Figure 10). Thus, the analyses of the three relict biotite-hydrothermal biotite pairs indicate the hydrogen isotopic compositions of biotite in these argillically altered samples have attained isotopic equilibrium not only with each other but also with the associated aqueous fluids.

The hydrogen isotopic compositions of biotite in the argillically altered samples of K-silicate alteration are plotted against the estimated percentage of clay content in plagioclase sites in Figure 11. The four samples of 11171-3367, 11172-1865, 11135-3481, and 11135-3586 are less argillically altered relative to the other samples of Bu96004, Bu96009, Bu96015, 11148-4219.5, 11148-4790.5, and 11171-4911 (Fig. 11, Table 3). Direct observations of the hand samples show that these six samples contain either strong white, or green argillic alteration, or both. However, in general as shown in Figure 11, there is no correlation between the clay content of plagioclase

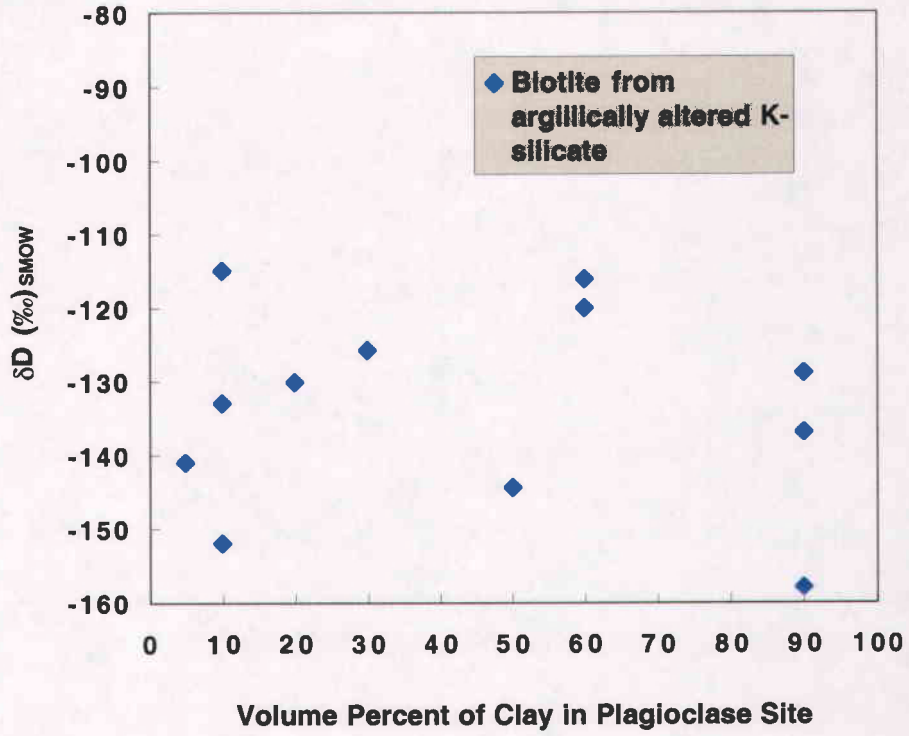

Fig. 11. Relationship between precentage of clay replacing plagioclase and the δD values of the co-existing biotite from K-silicate with argillic alteration overprinted samples.

and the δD value of the biotite in these samples. Although biotite from samples containing kaolinite generally have lighter δD values (by ~10-20‰) than those from samples rich in montmorillonite, data presented here are too few to draw any definitive conclusions.

The hydrogen isotopic composition of biotite from fresh rock, K-silicate, and K-silicate with argillic alteration was plotted against its Fe/(Fe+Mg) ratio in Figure 12. In general, there is a weak correlation between the δD values and the Fe/(Fe+Mg) ratio that the variation in the δD values of the biotite from all samples decreases with decreasing Fe/(Fe+Mg) ratio. The highest Fe/(Fe+Mg) ratios are from the four BQM samples that have similar values of 0.44-0.48. The next highest Fe/(Fe+Mg) ratios come from these seven K-silicate biotite samples that fall in a narrow range, but the ratio of the sixteen altered K-silicate biotite samples spans much wider range from 0.18 to 0.43, similar to the wide range of $\delta^{18}O$ values of these samples as shown in Figure 8a.

Montmorillonite-rich clay from sample Bu96004 yields a hydrogen isotopic composition of -109 per mil with estimated water content of 5.4 weight percent. Kaolinite-rich clay from sample 11148-4790.5 yields a δD value of -133 per mil with an estimated water content of 8.7 weight percent. The hydrogen isotopic compositions of montmorillonite-rich clay and kaolinite-rich clay, both from sample 11148-4219.5, are -109 and -118 per mil with water contents of 4.6 weight percent and 7.2 weight percent, respectively. These values are obtained from mixture samples and therefore should represent the bulk compositions, in terms of isotopic and water content, of these samples.

Gray-sericitic alteration

A total of twenty-seven samples (64 of separates) of gray-sericitic alteration have been selected for both oxygen and hydrogen isotopic composition analyses to

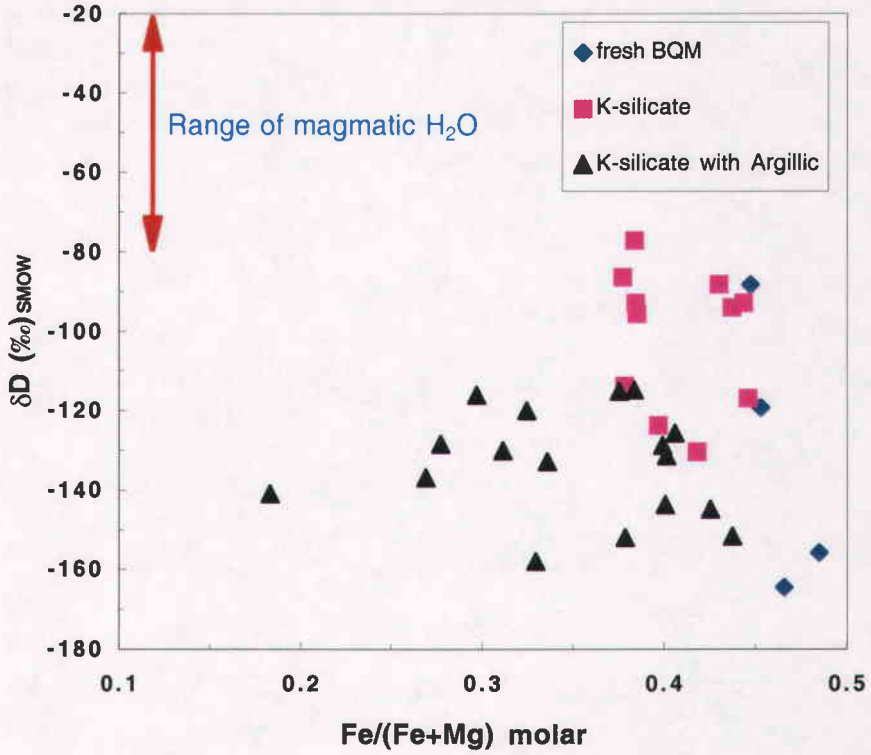

Fig. 12. Relationship between Fe/(Fe+Mg) ratio and δD values of biotite from samples of fresh rock BQM, K-silicate alteration, and K-silicate with argillic alteration overprint.

investigate the hydrothermal history at Butte (Fig. 13). Most of these samples are from deep drill holes 1, 1A, and 7 (Fig. 3). These samples can be in general classified into two groups based on their petrographic characteristics: pervasive gray-sericitic alteration and non-pervasive sericite alteration with Main Stage white sericite overprint and/or with argillic alteration of plagioclase outside the sericitic envelopes (Table 4).

Oxygen isotope data: The oxygen isotopic compositions of sericite from the gray-sericitic alteration lie within a narrow range from 6.4 to 9.5 per mil (Fig. 13). For eleven samples, oxygen isotope analyses have been performed on both the sericite that replaced igneous biotite grains and the coexisting fine-grained sericite that replaced feldspar. In general, the two coexisting sericites have similar isotopic compositions, although the fine-grained sericites ($\delta^{18}O_{mean}$ = 8.1 ‰) are slightly isotopically heavier than the sericite that pseudomorphs biotite (Fig. 14a, $\delta^{18}O_{mean}$ = 7.8 ‰). This small $\delta^{18}O$ difference (up to ~1 ‰) could be caused by minor impurity (5 to 35 vol.%) of isotopically heavier quartz ($\Delta_{qz\text{-}ser}$ = ~3 ‰) that forms a fine intergrowth with the fine-grained sericite. Alternatively, these fine-grained sericites, which are more susceptible to isotopic exchange, may have been enriched preferentially by partial re-equilibration with later, lower temperature aqueous fluids.

Oxygen isotope analyses have also been performed on quartz from the quartz-pyrite veins and hydrothermal wall rock sericite from the vein's alteration selvage (Fig. 14b). The vein quartz yields $\delta^{18}O$ values ranging from 9.1 to 11.8 per mil with a mean of 10.6 ± 0.6 per mil (n=24), whereas the sericites have a mean $\delta^{18}O$ value of 8.0 ± 0.9 per mil (n=36). As shown in Figure 14b, the coexisting vein quartz and wall rock sericite pseudomorphs of igneous biotite are positively correlated. The observed fractionation between the co-existing quartz and sericite are from 1.8 to 4.0 per mil (all but two samples) with an average $\Delta_{qz\text{-}ser}$ = ~3 per mil (Fig. 14b). This value corresponds to an apparent equilibrium temperature of 360°C using fractionation factors

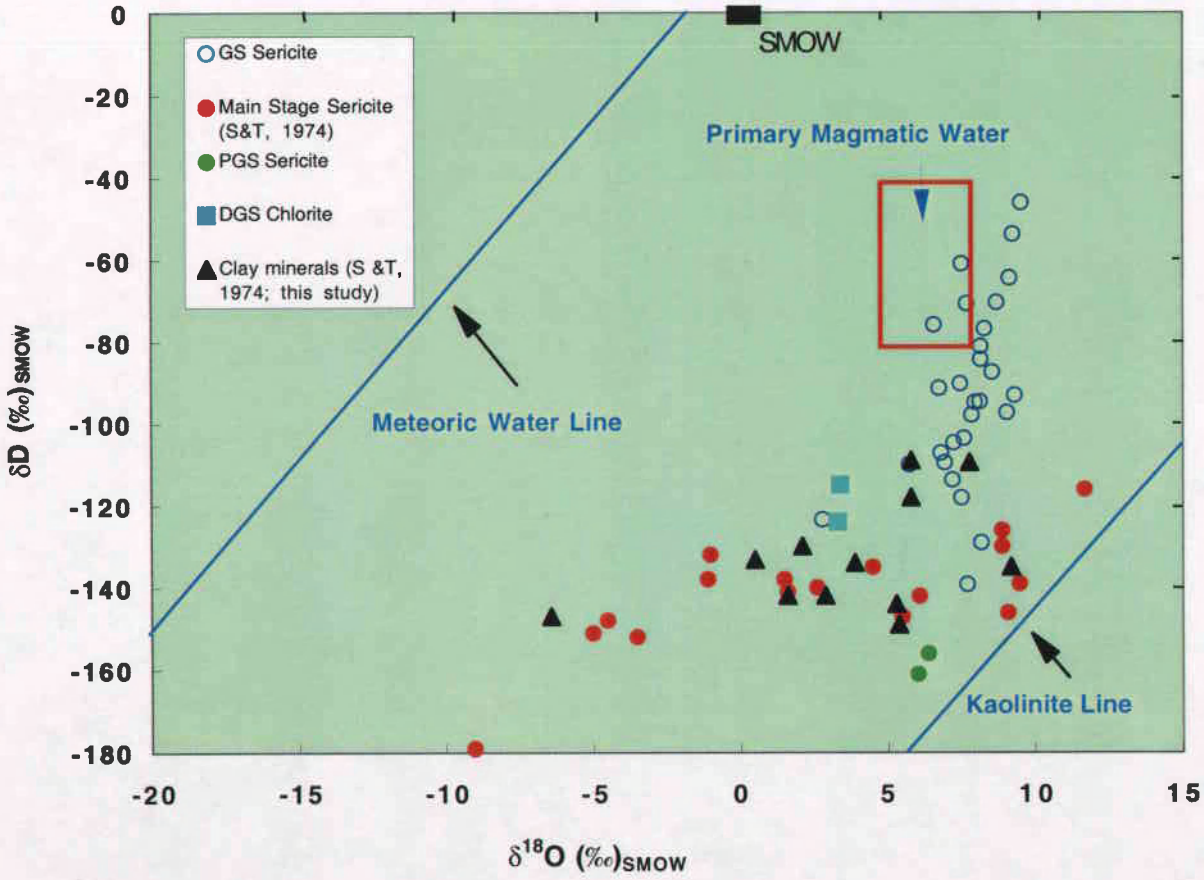

Fig. 13. $\delta^{18}O$ versus δD plot of hydrothermal sericite from gray sericitic alteration. Sericite and chlorite from pale green sericitic and dark green sericitic respectively (this study) and sericite and clay minerals from Main Stage mineralization (Sheppard and Taylor, 1971 & 1974) are also plotted for comparison.

Table 4. Oxygen and Hydrogen Isotopic Data from Gray Sericitic Alteration Assemblages of Porphyry Copper Deposits at Butte, Montana

Sample #	Drill Hole #	Mineral analyzed	Measured isotopic values $\delta^{18}O$ (‰, SMOW)	Measured isotopic values δD (‰, SMOW)	Estimated H2O (wt %)	Calculated values of fluids $\delta^{18}O$ (‰, SMOW)	Calculated values of fluids δD (‰, SMOW)
Pervasive Gray Sericitic Alteration (GS)							
10969-2627	1	Sericite (1)	7.6 ± 1.0	- 105	3.1	6.2	- 84
		Sericite (2)	8.2 ± 0.9	- 100	3.3*	6.8	- 79
		Quartz	10.7 ± 0.3			6.2	
10969-5452	1	Sericite (1)	8.0			6.6	
		Sericite (2)	8.6	- 77	3.7*	7.2	- 54
		Quartz	11.2			6.7	
10969-5618	1	Sericite (1)	8.7			7.3	- 74
		Sericite (2)	9.4	- 97	3.6*	8.0	
		Quartz	10.9			6.4	
10969-6448	1	Sericite (1)	7.0 ± 0.6			5.6	- 86
		Sericite (2)	7.0	-107	3.3*	5.6	
		Quartz	10.4			5.9	
11052-5532	1A	Sericite	9.1	- 64	2.9*	7.7	- 42
		Quartz	11.0			6.5	
11052-6639	1A	Sericite (2)	6.8± 0.0	- 91	3.4*	5.3	- 70
		Quartz	9.8			5.3	
11052-7037	1A	Sericite (1)	6.9	- 109	2.7	5.5	- 86
		Sericite (2)	7.2	- 114	3.0*	5.8	- 93
		Quartz	10.1 ± 0.2			5.6	
11052-7285	1A	Sericite (1)	8.2 ± 0.0	- 81	2.1	6.7	- 58
		Sericite (2)	8.2			6.8	
		Quartz	10.9 ± 0.1			6.4	
11052-7369	1A	Sericite (1)	7.4			5.9	- 118
		Sericite (2)	8.1	- 139 ± 4	3.0 ± 0.0	6.6	
		Quartz	9.1			4.6	
11052-7522	1A	Sericite	7.5 ± 0.1	- 90 ± 3	3.4 ± 0.2	6.1	- 69
		Quartz	10.0 ± 0.2			5.5	
11170-1767	7	Sericite (1)	9.4 ± 0.0	- 93	3.7	8.0	- 71
		Sericite (2)	9.2			7.8	
		Quartz	11.8			7.2	
11170-1790	7	Sericite	9.5	- 46 ± 2	3.1 ± 0.1	8.1	- 25
		Quartz	11.1 ± 0.1			6.6	
11170-2421	7	Sericite	8.2	- 84	4.1	7.6	- 63
11170-2423	7	Sericite	7.5	-118	3.2	6.1	- 97
		Quartz	11.3			6.8	
Non-Pervasive Quartz Sericite Alteration with argillic superimposed on plagioclase outside sericite envelope							
10969-1187	1	Sericite	6.4	-76	5.4*	5.2	- 55
		Quartz	10.4			5.8	
10969-1227	1	Sericite	8.2	- 95	2.8*	6.7	- 73
		Quartz	11.2 ± 0.1			6.7	
10969-2251	1	Sericite	7.9	- 98	4.1*	6.4	- 77
		Quartz	10.6			6.1	
11052-2851	1A	Sericite (1)	7.7	- 129	3.2*	6.3	
		Sericite (2)	8.7			7.3	- 107
		Quartz	10.5			6.0	
11148-888	3	Sericite	6.4 ± 0.9	-110	3.2	5.0	- 89
		Quartz	10.7			6.2	

TABLE 4 (Continued)

11148-1140	3	Sericite	7.6	- 104	3.1	6.2	- 81
		Quartz	10.9			6.4	
11170-864.5	7	Sericite (1)	9.5 ± 0.5	- 54 ± 0	3.5 ± 0.0	8.1	
		Sericite (2)	9.3			7.9	- 33
		Quartz	11.5			7.1	
11170-4871.5	7	Sericite (1)	7.2	- 61	3.7	5.8	
		Sericite (2)	8.5 ± 0.9			7.0	- 40
		Quartz	10.6 ± 0.2			6.1	
11170-4936	7	Sericite (1)	8.7 ± 0.2	- 70	3.7	7.3	
		Sericite (2)	9.3			7.9	- 49
		Quartz	10.9 ± 0.3			6.4	
11170-5333	7	Biotite	5.7				
		Sericite (2)	7.7	- 71	3.2*	6.3	- 49
11166-5885.5	5	Sericite	8.5	- 87	3.2*	7.1	- 66
		Quartz	9.6			5.1	
11185-1595	11	Sericite	8.0	- 95	3.5*	6.6	- 74
		Quartz	10.5			6.0	
11170-882	7	Sericite (1)	8.0				

Notes

1. Sericite (1): pseudomophycally sericite after biotite;
2. Sericite (2): fine-grained hydrothermal sericite;
3. Quartz: all quartz are from quartz-pyrite veins;
4. * Measured water content from mixture of hydrothermal sericite and quartz. Percentage of these minerals was not determined.
5. 1000ln α biotite-H2O= 0.41 $(10^6/T^2)$ - 3.10, (T: 500-800 °C)
   ----- Bottinga and Javoy (1973) and Javoy (1977)--Oxygen
6. 1000ln α quartz-H2O = 2.05 $(10^6/T^2)$ - 1.14, (T: 500-800 °C)
   ----- Matsuhisa et al. (1979)--Oxygen
7. 1000ln α illnite/muscvite-H2O =2.39 $(10^6/T^2)$ – 3.76, (T: 0-700 °C)
   ------ Sheppard and Gilg (1996)---Oxygen
8. 1000ln α mica-H2O = $-22.4(10^6/T^2) + 28.2 + (2X_{Al}-4X_{Mg}-68X_{Fe})$, (T: 450-850 °C)
   ----- Suzuoki and Epstein (1976)—Hydrogen
9. 1000ln α mica-H2O = $-22.4(10^6/T^2)$ + 28.2 + C (where C=32.2) (T: 450-850 °C)
   ----- Suzuoki and Epstein (1976)—Hydrogen

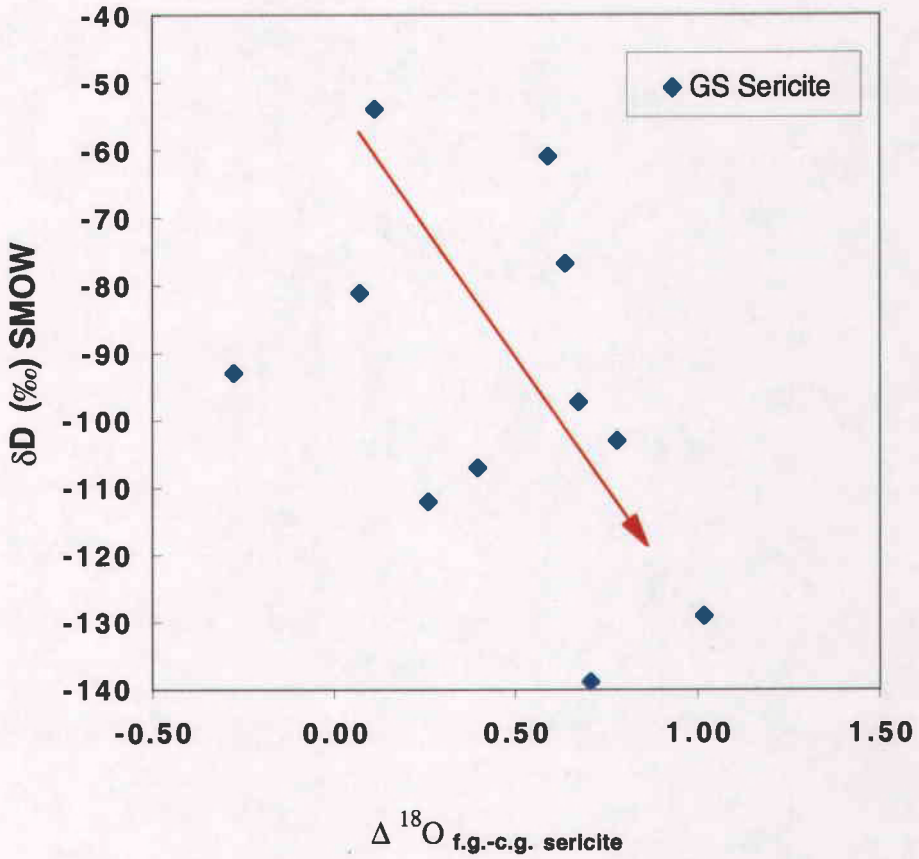

Fig. 14a. Relationship between observed fractionation of $^{18}O/^{16}O$ between coexisting fine-grained and coarse-grained sericite ($\Delta^{18}O_{\text{f.g. ser.-c.g. ser.}}$) versus δD values of gray sericites.

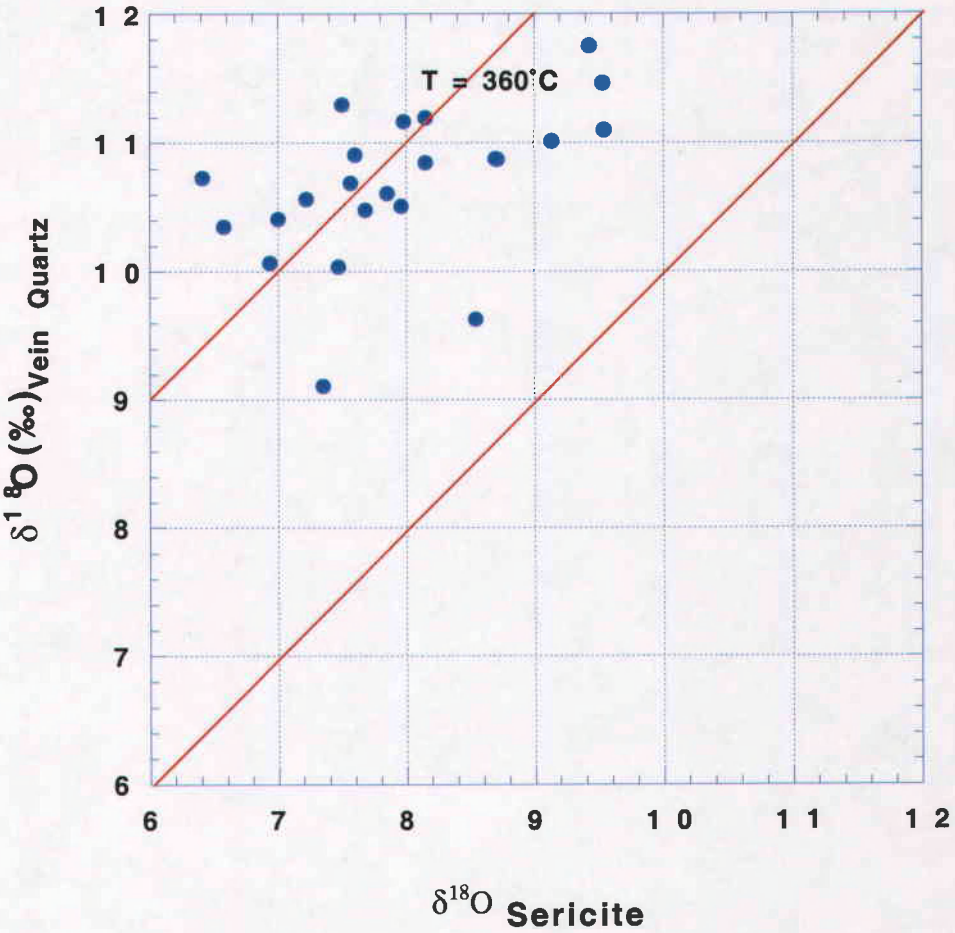

Fig. 14b. Oxygen isotopic composition of Sericite-Quartz pairs from GS alteration, showing apparent equilibrum temperatures of the GS alteration.

of Matsuhisa et al. (1979) for quartz-water and Friedman and O'Neil (1977) for sericite-water. It is noteworthy that the heaviest $\delta^{18}O$ values of sericite (9.4 - 9.5 ‰) and quartz (11.1-11.8 ‰) at Butte come from the upper part of drill hole #7 (samples 11170-864.5, 11170-1767, and 11170-1790), immediately below the center of strong Main Stage sericitic alteration centered near the Berkeley pit (Fig. 1).

Hydrogen isotope data: Hydrogen isotopic compositions were also obtained from the twenty-eight sericite separates from the gray-sericitic altered wall rock (Table 4). For the two samples (11069-2627 and 11152-7037), pairs of sericite pseudomorphic after biotite and fine-grained sericite that replaced feldspar and hydrothermal biotite have been analyzed to check for hydrogen isotopic equilibrium. Observed hydrogen isotopic compositions of these two pairs are rather close within the analytical error (-105 and -100 ‰ for 11069-2627; -109 and -114 ‰ for 11152-7037), indicating the equilibrium was established.

Several samples of non-pervasive sericite alteration with argillic alteration of plagioclase outside the sericitic envelopes and samples with Main Stage white sericite alteration selvages were chosen to study the effect of later fluids on the isotopic compositions of the earlier sericites. Hydrogen isotopic compositions of these sericites are highly variable from -46 to -139 per mil as shown in Figure 13. The heaviest δD values of sericite at Butte district are the three samples 11170-1790 (δD= -46 ‰), 11170-864.5 (δD= -54 ‰), and 11052-5532 (δD= -64 ‰), which also have heavier $\delta^{18}O$ values (9.1-9.5 ‰). The δD values are heavier than both fresh rocks of Butte Quartz Monzonite and K-silicate biotite. On the other hand, two samples 11052-7369 (δD= -139 ‰) and 11052-2851(δD= -129 ‰) from deep drill hole 1A, and sample 11170-2423 (δD= -118 ‰) yield much lighter hydrogen isotopic compositions than most of the sericites, which have δD values ranging from -70 to -109 per mil. One of the isotopically lighter samples (11052-2851) shows evidence of alteration by younger

Main Stage fluids because there exist narrow white sericite selvages adjacent to the pyrite-quartz veinlets. Thus, δD values of sericite form a linear trend on a $\delta^{18}O$ versus δD plot from -46 to -139 per mil (Fig. 13).

Hand specimens of the first group of gray-sericitic samples listed in Table 4 show little effect of younger alteration. However, the second group of samples have either argillic outer-envelopes, or signs of Main Stage overprinting such as containing veinlets and/or disseminated ore minerals (e.g., chalcocite, enargite, and bornite) that characterize the Main Stage. It is interesting to note there is little correlation between the hydrogen isotopic compositions of the sericite and the petrographic characteristics of the samples in terms of the presence or absence of the Main Stage minerals or clays. However, current understanding of the late Main Stage and clay alteration effects on the earlier sericite is limited because (1) all available samples are from core, and little is known about the surrounding area, and (2) in pervasively sericitically altered rock, later fluids left few alteration effects since there was not any plagioclase to be converted into clays. As shown in Figure 15, these sericites do not display any correlation between their hydrogen isotope compositions and their chemical compositions.

Discussion: Evolution of Isotopic Composition of Hydrothermal Fluids

Butte Quartz Monzonite

The four fresh samples of Butte Quartz Monzonite were selected based on the presence of the primary hornblende and other igneous minerals and they contained onlytrace amounts of epidote, chlorite, and clay. However, these samples were collected close to the Main Stage veins within the Butte mining district except sample Bu214 (epidote-bearing), which is from southern lip of Elk Park, at the edge of the district (Fig. 1). Hydrogen isotope compositions of hornblende from these "fresh" Butte Quartz

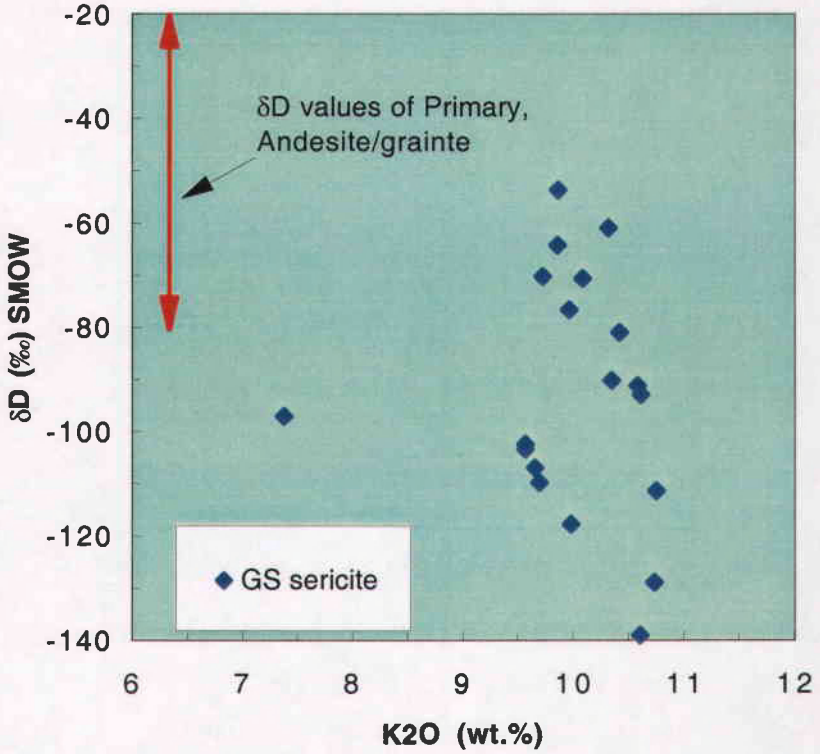

Fig. 15a. Relationship of K_2O content and δD values of sericite from gray sericitic alteration.

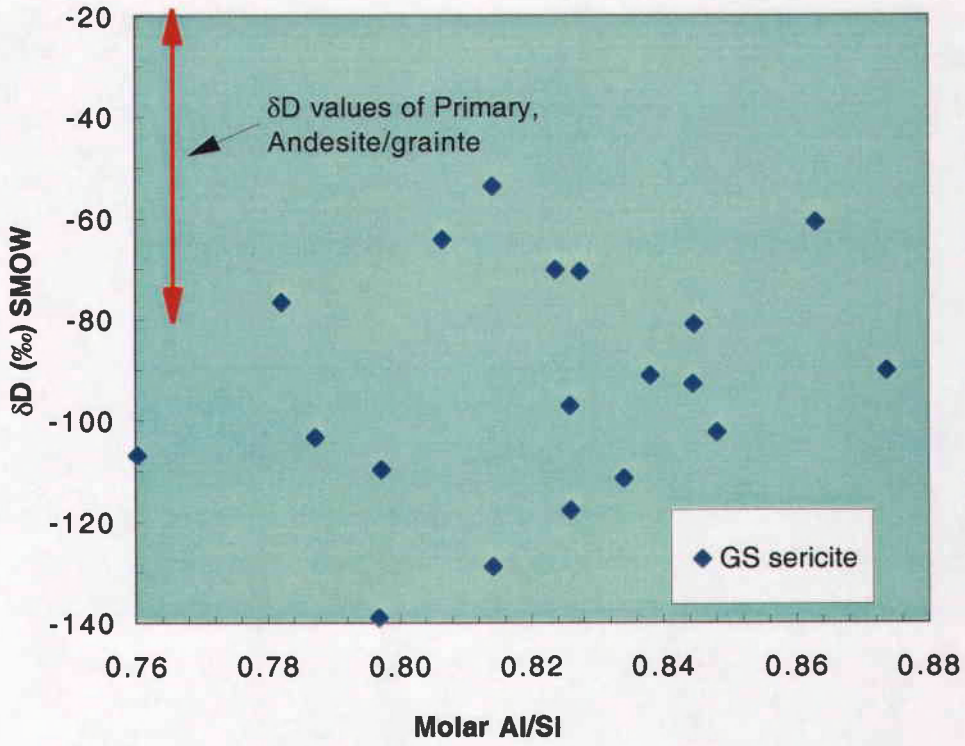

Fig. 15b. Plot of hydrogen isotopic compositions versus chemical variations of Al/Si of sericite from the gray sericitic altered samples.

Monzonite samples are extremely variable and range from typical magmatic values of -68 per mil at Elk Park to D-depleted values of -110 to -149 per mil from the mining district (Fig. 9). This D-depletion strongly suggests meteoric water involvement.

It should be pointed out that both samples Bu211 and Bu96001 were collected at the same location within a few meters from one another by two researchers about one year apart, but the δD values of hornblende and biotite of these two samples differ by 40 to 45 per mil, respectively. The large δD variation of these two adjacent samples of typical Butte Quartz Monzonite can not be explained by D-depletion due to magma degassing as proposed elsewhere (Nabelek and O'Neil, 1986) and at Butte (Hedenquist and Richards, 1998). An alternative interpretation is that there exists a heterogeneous isotopic exchange with late, low temperature fluids. This interpretation seems to be supported by the field observations that each of these two Butte Quartz Monzonite samples was only 3-4 cm away from a late stage pyrite-quartz veinlet with a narrow sericite selvage (~1cm wide). Calculated equilibrium temperatures based on the oxygen isotopic fractionation of the coexisting hornblende and biotite in these two samples also suggest an isotopic re-equilibration of the mineral pairs at low temperatures. As shown in Figure 16, the observed oxygen isotopic fractionation between hornblende and biotite pairs for 3 samples suggest a ~300 °C equilibrium temperature, but sample Bu 211 suggests a much higher equilibrium temperature (> 1000 °C).

The deuterium-hydrogen fractionation between hornblende and biotite (Fig. 9) allows calculation of possible equilibrium temperatures of these co-existing pairs. It is interesting to note that the $\Delta_{hbl\text{-}biot}$ in these Butte Quartz Monzonite samples are quite uniform (from 9 to 20 ‰), and suggest possible equilibrium temperatures of 550 to 600°C based on the equilibrium fractionation equations of Suzuoki and Epstein (1976) and Graham et al. (1984) at 450-850°C for biotite-H_2O, and at 350-805°C for hornblende-H_2O. However, Lambert and Epstein (1980) suggested possible "S-

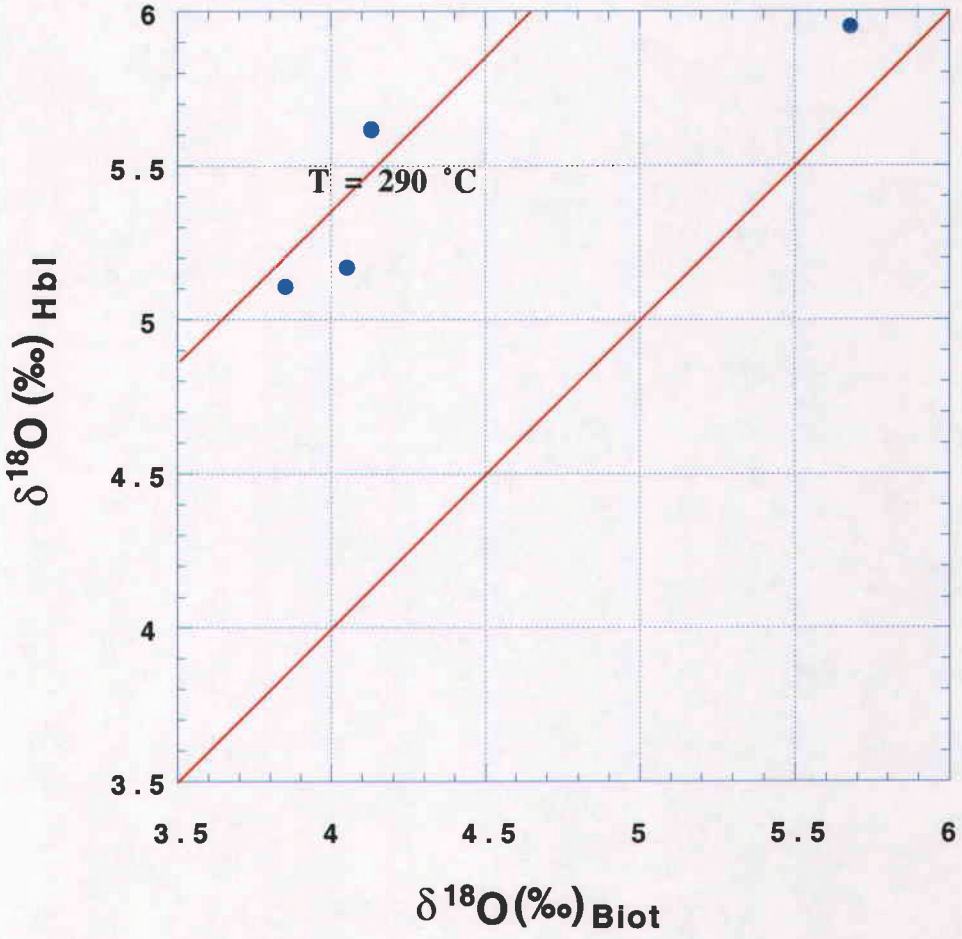

Fig. 16. $\delta^{18}O$ values of the co-existing hornblende and biotite pairs from BQM, showing apparent equilibrum temperatures.

shaped" reversal of the equilibrium hydrogen isotope fractionation curve for biotite-H_2O near the critical point of water (373°C, 220 bar). If this fractionation reversal of biotite did exist, then the same fractionation (Δ) value between the co-existing hornblende and biotite pairs could correspond to two different equilibrium temperatures: one is > 400°C, the other is < 400°C. The small $\Delta_{hbl\text{-}biot}$ of the Butte Quartz Monzonite samples could also suggest lower equilibrium temperatures (< 400°C) than the above calculations (550 to 600°C). Therefore, the Butte Quartz Monzonite samples with lighter δD values could be re-equilibrated at low temperatures (< 400°C) with late meteoric dominated fluids.

Calculated isotopic compositions of waters in equilibrium with these Butte Quartz Monzonite samples at 700°C are consistent with magmatic water compositions for both samples Bu214 ($\delta^{18}O$= 7.0 ‰, δD=-53 ‰) and Bu211 ($\delta^{18}O$=8.3 ‰, δD=-89 ‰), which is in good agreement with previous study by Sheppard and Taylor (1974). However, waters in equilibrium with samples Bu96001 ($\delta^{18}O$=7.3 ‰, δD=-126 ‰) and Bu96014 ($\delta^{18}O$=6.9 ‰, δD=-124 ‰) have hydrogen isotopic compositions that can not be magmatic water alone (Table 3). Since sample Bu214 was collected at the edge of the hydrothermal activity center, it might represent the "true" isotopic composition of the residual water in melt during the crystallization of Butte Quartz Monzonite. However the 20 per mil fractionation of deuterium-hydrogen between the co-existing hornblende and biotite of this sample is much larger than the experimental value of 4.6 per mil at 700°C under the equilibrium conditions (Suzuoki and Epstein, 1976; Graham et al., 1984). If isotopic equilibrium had been established between the two minerals during crystallization of the Butte Quartz Monzonite, this rather large fractionation may suggest some effect of late fluids.

The interpretation that both the large D/H isotope variations and the relatively uniform $\delta^{18}O$ values in these Butte Quartz Monzonite samples are due to their isotopic exchange with small amount of low temperature, late meteoric fluids may not seem

convincing at first, but it is supported by the greater diffusion rates of hydrogen relative to oxygen in the hornblende and biotite minerals. At 200-250°C, hydrogen diffuses about four and ten times faster than oxygen in biotite and hornblende, respectively (Cole and Ohmoto, 1986). Because of the large mass difference between the oxygen and hydrogen atoms, a water/rock ratio of 1 for hydrogen is about a water/rock ratio of 1/40 for oxygen. Thus the net effect for oxygen exchange in biotite is 1/160 (1/40*1/4) and in hornblende 1/400 (1/40*1/10) relative to hydrogen exchange, or in other words, there should be significantly less oxygen exchange than hydrogen in these minerals. Therefore, it is most likely that the deuterium-hydrogen in the hornblende and biotite at Butte (Fig. 6a) might have re-equilibrated with late fluids, but the oxygen has not. This interpretation may also be applied to the observed large D/H isotope variations and the relative uniform $\delta^{18}O$ values in K-silicate alteration samples presented below.

K-silicate alteration

Petrologic study of the early K-silicate alteration assemblages have provided formation temperatures of 600±50°C based on the assemblage of K-feldspar-ablite-muscovite-andalusite (Brimhall, 1977). This temperature range is consistent with both the sulfate-sulfide isotope geothermometry (Zhang et al., 1999) and fluid inclusion studies on the Early Dark Micaceous and quartz-molybdenite veinlets by Roberts (1975) and Rusk et al. (1999). The major fluid inclusion assemblage contains about 6 weight percent NaCl equivalent, a density of 0.65 g/cm^3, and sometimes high copper concentration in the K-silicate veinlets. These inclusions have homogenization temperatures of 365±25°C and yield mineralization temperatures of ~600°C at a pressure of 1.7 to 2.0 kb (or 6-8 km depth) (Dilles et al., 1999). Both high salinity (>35 wt. % NaCl) and high vapor-rich (60-90 vol. % vapor) fluid inclusions are also found in K-silicate veins, but they are only abundant in the underground area of the Steward mine,

not in the Continental area, which is the deepest portion of the K-silicate alteration at Butte. Bodnar (1995) suggested that Robert's (1975) data indicated that the magmatic supercritical fluids were separated from deep porphyry intrusions and had a salinity of about 2-10 weight percent NaCl equivalent. These fluids were than trapped in fluid inclusions at pressures > 1.7 kb within the porphyry deposits in both the Continental area and the deep Anaconda-Pittsmont domes.

The isotopic compositions of fluids that were in equilibrium with minerals at selected temperatures were calculated using published oxygen and hydrogen isotope fractionation factors (Fig. 17, Tables 3 & 4). The $\delta^{18}O$ values of K-silicate water calculated at 550 °C have a relatively narrow range of 6.8 to 8.1 per mil, except one isotopically lighter value of 5.2 per mil calculated from equilibrium with the K-feldspar in sample 11172-4166. The $\delta^{18}O$ value of water is about 2 per mil lighter than the water calculated from the co-existing biotite. The small $\delta^{18}O$ variation of these K-silicate alteration minerals suggests that the K-silicate hydrothermal fluids originated from a magmatic water with a uniform oxygen isotopic composition, and these minerals have not re-equilibrated with younger, low-temperature fluids.

Calculated δD values of waters in equilibrium with K-silicate minerals fall into two groups: -47 to -64 per mil, and -83 to -98 per mil (Fig. 17 and Table 3). These heavier values may represent the isotopic compositions of the original supercritical fluids, derived from the magma, and are similar to or slightly lighter than waters (-35 to -50 ‰) calculated from K-silicate alteration biotite by Sheppard and Taylor (1974). Possible explanations for these D-depleted samples (δDwater = -83 to -98 ‰) are either that these represent "late" K-silicate fluids that were D-depleted via extension of earlier magma-vapor D/H fractionation (Taylor and Westral, 1976), or that these samples may have been affected by low-temperature, meteoric fluids at a relatively low water/rock ratio.

In sample 11172-4166, relict igneous biotite is about 24 per mil heavier in δD value

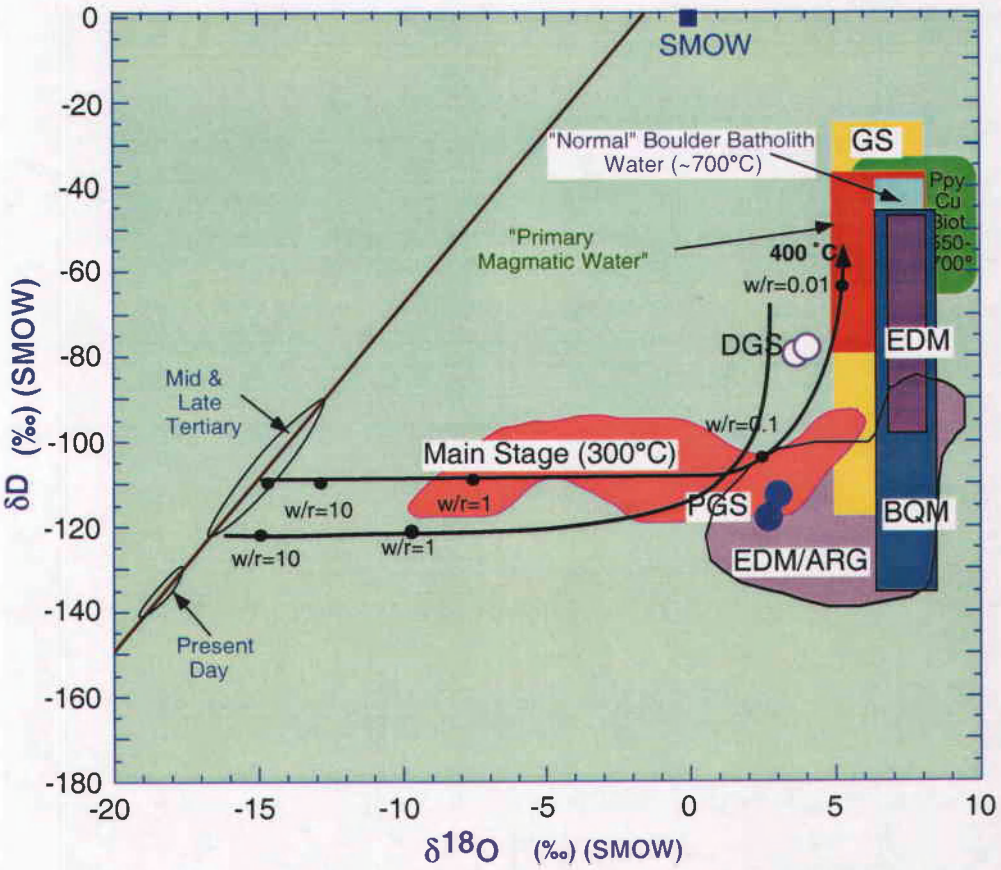

Fig. 17. Calculated δD versus $\delta^{18}O$ of water to be in equilibrium at indicated temperatures with the hydrothermal minerals (isotope compositions in Figures 7&15) from the Butte district. Main Stage data are from Sheppard and Taylor (1974). Also plotted for comparison are current and fossil meteoric waters (left), SMOW, primary magmatic waters, and calculated waters in equilibrium with Boulder Batholith and porphyry copper biotites.

than that of the hydrothermal biotite replacing hornblende (Table 3). This hand specimen also shows some greenish alteration of feldspars (see Appendix C). The combination of the lighter δD value of fine-grained biotite relative to coarse relict igneous biotite with the low $\delta^{18}O$ value of co-existing K-feldspar and the greenish feldspar alteration suggest that late, low-temperature, D- and ^{18}O-depleted waters reacted quickly with minerals such as feldspar and fine-grained biotite, resulting in partial exchange of the isotopic compositions. This evidence and data discussed below on clay-altered K-silicate biotites lands support to the hypothesis that D-depleted K-silicate biotites (-83 to -98 ‰) were the result of low-temperature alteration by meteoric waters.

The isotopic compositions of the fluids in equilibrium with biotite from argillically altered K-silicate samples were also calculated at 550°C. The $\delta^{18}O$ values of fluids range from 0.5 to 9.4 per mil from biotite, and from 2.2 to 8.6 per mil calculated from K-feldspar, which suggest that the co-existing biotite and K-feldspar in these samples have both exchanged their oxygen isotopic compositions with the late Main Stage fluids. However, as listed in Table 5, the co-existing biotite and K-feldspar yield much higher apparent equilibrium temperatures than that of the Main Stage fluids (~250°C). These unreasonably high temperatures suggest that the co-existing biotite and K-feldspar pairs were not in isotopic equilibrium. Cole & Ohmoto (1986) reported that the oxygen diffusion rate in K-feldspar is much faster than that of biotite in equilibrium with water at same temperatures. Therefore, K-feldspar may have re-equilibrated with the Main Stage fluids, but the isotopic exchange between the biotite and the late fluids may not have reached equilibrium.

The hydrogen isotopic compositions of water in equilibrium with biotite from argillically altered samples vary from -84 to -132 ‰ (Fig. 17). The larger range of $\delta^{18}O$ values and D-depletion of these biotites compared to those in the K-silicate samples indicate that these samples are not in isotopic equilibrium with the high temperature K-

Table 5 Calculated Apparent Equilibrium Temperatures from K-feldspar-Biotite, Quartz-Biotite, and Quartz-K-feldspar Pairs from Fresh Rock and K-silicate Alteration Samples

Sample	$\delta^{18}O$ (‰)$_{SMOW}$ Biotite	$\delta^{18}O$ (‰)$_{SMOW}$ K-feldspar	$\delta^{18}O$ (‰)$_{SMOW}$ Quartz	$\Delta_{Ksp\text{-}bi}$	T (°C)	$\Delta_{Qtz\text{-}bi}$	T (°C)	$\Delta_{Qtz\text{-}Ksp}$	T (°C)
Fresh Butte Quartz Monzonite									
Bu214	4.1	7.6	8.6	3.5	449	4.5	537	1.0	450
Bu211	5.7	7.9	8.7	2.2	836	3.0	1014	0.8	494
Bu96014	3.9	7.4	8.7	3.5	449	4.8	482	1.3	396
Bu96001	4.1	7.9	8.9	3.7	424	4.8	490	1.0	450
K-Silicate alteration									
11172-2200	5.2	8.2		3.0	541				
11172-2934	4.9	8.2	9.6	3.3	482	4.7	499	1.4	381
11172-3920	4.5	8.3	8.9	3.8	413	4.4	554	0.6	547
11172-4005	5.2	7.8		2.6	622				
11172-4166	4.7	6.4	9.5	1.6	1003	4.8	487	3.1	218
Bu96017	5.6	8.9		3.3	482				
Bu96018	4.7	8.2		3.6	441				
K-silicate with argillic alteration									
Bu96004	6.9	8.4		1.5	1136				
Bu96006	3	6.1		3.1	510				
Bu96007	-0.5	3.3		3.8	413				
Bu96009	3.5	7.5		4.0	388				
Bu96015	6.2	9.6		3.4	471				
11135-4966	6.1	8.1		2.0	814				
11148-4790.5	-0.4	2.5		2.9	555				
11148-4219.5	4.9	8.7		3.8	418				
11171-4911	5.6	8.9		3.3	482				
11172-1865	5.8	8.8		3.0	532				

Fractionation equations uesd for calculations as in Table 3

silicate fluids. The depletion in both ^{18}O and D of the fluids indicates a meteoric water signature.

The calculated isotopic compositions of fluids from biotite, K-feldspar, and clay at 150 °C for these argillically altered samples are listed in Table 6. The two kaolinite-rich clay samples from 11148-4790.5 and 11148-4219.5 yield water compositions of -5.1 and 0.2 per mil for $\delta^{18}O$ and -101 and -116 per mil for δD, respectively, by using the Sheppard and Gilg (1996) isotope fractionation equations. The three analyses of clay minerals and co-existing K-feldspar give similar $\delta^{18}O$ values of fluids, suggesting that these K-feldspars have re-equilibrated with the low temperature, white argillic (kaolinite-forming) fluids. Provided the calculated $\delta^{18}O$ values from clay accurately represent the isotopic compositions of the late fluids, calculated fluid compositions at 250°C derived from biotite are much heavier in $\delta^{18}O$. This relation is consistent with the observation that these biotites have $\delta^{18}O$ values similar to magmatic biotites, and therefore, they have only partly exchanged oxygen with late, low-temperature fluids.

The fluid composition calculated from a montmorillonite sample (Bu96004) has a $\delta^{18}O$ value of -2.4 per mil and a δD value of -97 ‰ using the fractionation equations of Sheppard and Gilg (1996) for oxygen and Capuano (1992) for hydrogen at 150 °C. However, fluid compositions calculated from biotite in the green argillic altered zone were much ^{18}O-enriched relative to the montmorillonite (Table 3). Clay analyses from previous studies at Butte, including kaolinite (n=4), montmorillonite (n=2), and dickite(n=1) were also re-calculated at selected temperatures for fluid isotopic compositions, respectively (Fig. 13).

In general, fluids that formed white argillic alteration have $\delta^{18}O$ values of -8.2 to -2.9 ‰ and δD values of -129 to -98 ‰, and the fluids for green argillic alteration yield similar $\delta^{18}O$ and δD values ($\delta^{18}O$ = -8.6 to -2.4‰; δD =-130 to -97 ‰) to the white argillic fluids. It is interesting to note that the biotite (and K-feldspar) coexisting with

Table 6 $\delta^{18}O$ Composition of Water Calculated to be in Equilibrium With Minerals from Argillically Altered K-silicate Samples at 150°C

Sample	Mineral	$\delta^{18}O$ (‰)$_{SMOW}$ mineral	T(°C)	1000In a minl-H2O	$\delta^{18}O$ (‰)$_{SMOW}$ H2O
Bu96004	Mont.-rich	7.8	150	10.2	-2.4
	Biotite	6.9	150	-0.8	7.7
	K-feldspar	8.4	150	10.8	-2.4
Bu96006	Biotite	3.0	150	-0.8	3.8
	K-feldspar	6.1	150	10.8	-4.7
Bu96007	Biotite	-0.5	150	-0.8	0.3
	K-feldspar	3.3	150	10.8	-7.5
Bu96009	Biotite	3.5	150	-0.8	4.3
	K-feldspar	7.5	150	10.8	-3.3
Bu96015	Biotite	6.2	150	-0.8	7.0
	K-feldspar	9.6	150	10.8	-1.3
Bu96016	Biotite	-2.0	150	-0.8	-1.2
11148-4219.5	Biotite	4.9	150	-0.8	5.7
	K-feldspar	8.7	150	10.8	-2.2
	Kaolinite	5.8	150	8.7	-2.9
11148-4790.5	Biotite	-0.4	150	-0.8	0.4
	K-feldspar	2.5	150	10.8	-8.3
	Kaolinite	0.4	150	8.7	-8.2
11135-3481	Biotite	0.1	150	-0.8	0.9
11135-3586	Biotite	-1.7	150	-0.8	-0.9
11135-4966	Biotite	6.1	150	-0.8	6.9
	K-feldspar	8.1	150	10.8	-2.7
11171-4911	Biotite	5.6	150	-0.8	6.5
	K-feldspar	8.9	150	10.8	-1.9
11172-1865	Biotite	5.8	150	-0.8	6.6
	K-feldspar	8.8	150	10.8	-2.1

Note:
K-feldspar-H2O: Matsuhisa et al. (1979)--- 400-500°C
Biotite-H2O: Bottinga and Javoy (1973) and Javoy (1977) ---500-800°C
Mont-H2O: Sheppard & Gilg. (1996) 15-300°C
Kaolinite-H2O: Sheppard & Gilg (1996) --- <150-300 °C

montmorillonite in the green argillic alteration are ^{18}O-enriched, and the $\delta^{18}O$ values of fluids calculated from the coexisting clay and biotite in green argillic alteration zones shift in opposite directions. In contrast, in the white argillic alteration zone, all alteration minerals (biotite, K-feldspar, and clay) show consistent ^{18}O-depletion.

The most D-depleted samples in this study are the "fresh" Butte Quartz Monzonite (samples Bu96001 and Bu96014) and the K-silicate assemblages with strong white and green argillic alteration of plagioclase superimposed (Fig. 6b). Calculated fluid compositions from kaolinite in these samples are similar to the waters in equilibrium with biotite in the most D-depleted fresh Butte Quartz Monzonite samples and K-silicate samples superimposed by argillic alteration (Fig. 17). These data suggest that the remnant biotite from K-silicate alteration had reached isotopic equilibrium in deuterium-hydrogen with the argillic fluids.

In addition, two sericite samples from the pale green sericitic alteration and two chlorite samples from the dark green sericitic alteration have also been analyzed for oxygen and hydrogen isotopic compositions and they are included in Table 3. The PGS sericites yield similar isotopic compositions to that of biotite from the K-silicate samples with argillic alteration overprint. Whereas the two chlorites are D-enriched relative to the Butte K-silicate biotite and PGS sericite and show a signature of magmatic water (Fig. 17). One possible explanation of the DGS chlorites is that their heavier δD values are caused by re-equilibration with late gray sericitic fluid since these two samples were collected near the pervasive gray sericitic dome (Fig. 2b). However, it is difficult to draw any conclusive interpretation by the limited data on these two K-silicate alteration subtypes.

Apparent equilibrium temperatures have also been calculated based on temperature dependence of oxygen isotopic fractionation between coexisting phases (Table 5). The fresh rock biotite-K-feldspar pairs yield apparent equilibrium temperatures of 420 to

450°C, excluding sample Bu211 (840°C). The quartz-biotite pairs give 60-90°C higher apparent equilibrium temperatures than the biotite-K-feldspar pairs, with the exception of sample Bu211 (1010°C). However, the four quartz-K-feldspar pairs yield rather consistent temperatures of 450±50°C. The exceptionally high temperatures calculated from both the biotite-K-feldspar pair and the quartz-biotite pair of sample Bu211 suggests that the $\delta^{18}O$ value of the biotite in this sample might have been shifted to a higher value, but not the K-feldspar and quartz.

The biotite-K-feldspar pairs in K-silicate alteration indicate equilibrium temperatures of 410 to 620°C (Table 5), which are close to the 550-600°C inferred from fluid inclusion studies of quartz in the Early Dark Micaceous veins by Roberts (1975) and our S-isotope studies (Zhang et al., 1999). However, sample 11172-4166 yields calculated temperatures of 1000°C, which is unreasonably high. Similar temperatures (490-550°C) are calculated from three quartz-biotite pairs including the 490°C obtained from sample 11172-4166. While the other two quartz-K-feldspar pairs yielded temperatures of 380°C and 540°C, respectively, sample 11172-4166 yielded an unreasonably low calculated temperature of 220°C. The significant differences in the three apparent equilibrium temperatures of 1000°C, 490°C, and 220°C from the biotite-K-feldspar, quartz-biotite, and quartz-K-feldspar pairs of sample 11172-4166 suggest that both the biotite-K-feldspar and quartz-K-feldspar pairs may not be in equilibrium. It may further suggest that the $\delta^{18}O$ value of the K-feldspar in this sample might have been shifted to a lower value (Table 5).

The coexisting biotite-K-feldspar pairs from argillically altered K-silicate samples give calculated equilibrium temperatures of 390 to 560 °C (plus two unreasonably high temperatures of 810 and 1140 °C). These apparent equilibrium temperatures are similar to those from K-silicate samples. However, $\delta^{18}O$ in most of these minerals differs from that of typical K-silicate biotite and K-feldspar, which suggests that the argillic alteration

has changed the mineral isotopic compositions and, therefore, these temperature estimates are probably less meaningful. Three samples (11148-4219.5, 11171-4911, and 11172-1865) have $\delta^{18}O$ values of biotite and K-feldspar similar to that of K-silicate and yield 420 to 530°C equilibrium temperatures. Thus the $\delta^{18}O$ of these three samples was likely not reset by argillic fluids, although plagioclase in sample 11148-4219.5 had been strongly replaced by kaolinite and montmorillonite.

Gray-sericitic alteration

The quartz-sericite geothermometry yields isotopic equilibrium temperatures ranging from 300 to 850°C calculated from the 23 mineral pairs with a mean value of 480 ± 140°C (Table 7). Calculated equilibrium temperatures are unreasonably high (≥ 580°C) in samples 11052-5532, 11052-7369, 11170-1790, and 11166-5885.5, and are in disagreement with phase equilibria and fluid inclusion results, especially the last two samples (Table 7). The homogenization temperature obtained from the fluid inclusions of the quartz-pyrite veinlet of sample 11170-1790 is ~400°C, and the fluid was trapped near critical curve, corresponding to 200-250 bars pressure (Bodnar, personal commun., 1997). Sample 11166-5885.5 yields a homogenization temperature of ~360°C (S. Geiger, personal commun., 1998). However, this sample contains Main Stage ore minerals in the veinlets; plagioclase in the outer alteration envelope was replaced by montmorillonite, and in addition, the $\delta^{18}O$ value of quartz (9.6 ‰) is rather low relative to other gray-sericitic samples.

The calculated $\delta^{18}O$ values of the gray-sericitic fluids from sericite fall within a relatively narrow range (5-8 ‰), but the δD values estimated from sericites in these samples range widely from -25 to -118 per mil (Fig. 17). These data show a continuous range of δD values from the most D-enriched to the most D-depleted. There is no apparent systematic difference in isotopic compositions between samples with argillic

Table 7 Calculated Temperatures Apparent Equilibrium from Quartz-Sericite Pairs in Sericitic Alteration

Sample	$\delta^{18}O$ (‰)$_{SMOW}$ Sericite	$\delta^{18}O$ (‰)$_{SMOW}$ Vein Quartz	$\Delta_{Qz\text{-}Ser}$	T (°C)
Pervasive Gray Sericitic Alteration				
10969-2627	7.9	10.7	2.8	439
10969-5452	8.3	11.2	2.9	422
10969-5618	9.1	10.9	1.8	609
10969-6448	7.0	10.4	3.4	368
11052-5532	9.1	11.0	1.9	589
11052-7037	7.1	10.1	3.0	405
11052-7285	8.2	10.9	2.7	450
11052-7369	7.8	9.1	1.3	758
11170-1767	9.3	11.8	2.5	468
11170-1790	9.5	11.1	1.6	668
11170-2423	7.5	11.3	3.8	334
11052-7522	7.5	10.0	2.5	468
Non-Pervasive Sericitic Alteration				
10969-1187	6.4	10.4	4.0	318
10969-1227	8.2	11.2	3.0	405
10969-2251	7.9	10.6	2.8	439
11052-2851	8.2	10.5	2.3	511
11166-5885.5	8.5	9.6	1.1	853
11170-4871.5	7.9	10.6	2.7	450
11170-4936	9.0	10.9	2.2	530
11148-888	6.4	10.7	4.3	297
11148-1140	7.6	10.9	3.3	378
11170-864.5	9.4	11.5	2.1	540
11185-1595	8.0	10.5	2.5	468

alteration and those without argillic alteration. This isotopic anomaly suggest that argillic alteration has little effect on the isotopic compositions of these sericite samples. For example, sample 11170-864.5 with a strong argillic outer alteration selvage is among the most isotopically D-enriched samples in the Butte district, whereas sample 11052-7369, without any evidence of late alteration, has the most depleted δD values of sericites. Alternatively, many gray-sericitic samples display pervasive sericitic alteration of plagioclase, and consequently, the effect of younger argillic fluids may not be evidenced because the fluids had not altered sericite to clay.

Another striking characteristic of the gray-sericitic sericites is that they are enriched in both ^{18}O and D relative to the Main Stage sericites (Fig. 13). These sericite data clearly indicate different origins for the two hydrothermal alteration events. A magmatic water component for gray-sericitic alteration is strongly suggested by the rather heavy δD compositions (this study), whereas meteoric water was indicated by the uniform low δD values (-140 ± 15‰) and large $\delta^{18}O$ variations (-9 to +12 ‰) of the Main Stage sericites (Sheppard and Taylor, 1974). In general, the most D-rich samples are of sericites the sericite from the upper part of the pervasive gray-sericitic alteration zone (mostly from DDH 7) as shown in Figure 3. Moving away from this core, isotopic compositions of the sericites are generally depleted and have much larger variations of δD than $\delta^{18}O$.

Three possible mechanisms that could cause this apparent pattern of spatial isotopic variation are magma degassing, water-rock reaction, and fluid mixing and they are briefly discussed in the following.

(1) magma degassing: It is well known that magma degassing could cause significant D/H isotopic shifts due to Rayleigh fractionation and the $\Delta_{magma\text{-}water}$ = -20 per mil (Taylor et al., 1983; Nabelek et al., 1983). By this hypothesis, as suggested by Hedenquist and Richards (1998), the ascending originally supercritical fluid

separates into a hypersaline fluid (brine) that forms K-silicate alteration and a vapor phase that forms the advanced argillic alteration. The gray-sericitic alteration forms from later magmatic fluids that were released from magma, which cooled rapidly during the ascent and thus did not intersect the solvus (Figure 18). Therefore, this fluid could have a low salinity and be magmatic in origin, but with a large δD range. The δD values of the fluids depend on the stage of magma degassing, or the amount of water remaining in the melt. After 60% of the water was released from the magma, the δD values of the later released fluids are significantly D-depleted. Therefore, the heaviest isotopic compositions of the sericite at Butte may suggest the isotopic composition of 0-60% fluid exsolved from the magma, and the lightest isotopic compositions of the sericite suggest the last stage of fluid degassed from the magma. The majority of sericite data suggest fluids with hydrogen isotopic compositions of -50 to -97 ‰ that may represent the composition of the fluid with 65%-80% of water exsolved from magma (see Figure 8 in Hedenquist and Richards, 1998).

(2) water-rock reaction: The Main Stage sericites and sericites from gray-sericitic alteration could be interpreted as a single progressive reaction path of meteoric water with Butte Quartz Monzonite at different water/rock reaction ratios at 400°C (Figure 17). The sericites of gray-sericitic alteration may have formed initially from pure magmatic water with isotopic compositions of 8 per mil for $\delta^{18}O$ and -25 per mil for δD. Afterwards, the gray-sericitic altered rocks may have been altered by later Main Stage fluids or meteoric water with $\delta^{18}O$= -16 per mil and δD=-120 per mil. This reaction may have caused the isotopic variations shown in Figure 17. Water/rock ratios of less than 0.1 can significantly shift the deuterium-hydrogen isotopic composition, but cause little change of the oxygen isotopic compositions of sericite. This interpretation could easily explain the large D/H variations between samples that are very close to one another depending on the proximity of samples to late, Main Stage vein channels. For

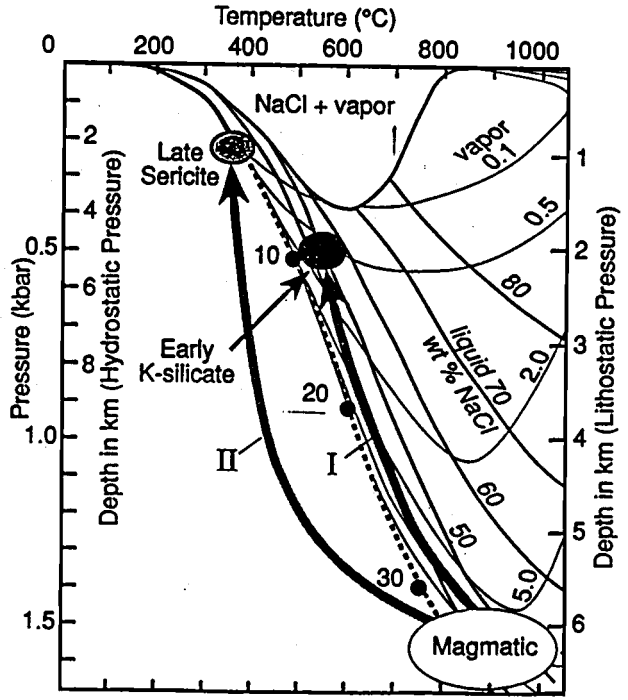

Figure 18a: PTX diagram for the system water-NaCl, showing two possible pathways of ascent of magmatic fluid. Immediately after saturation of a melt, fluid ascends rapidly along path I which results in intersection of the solvus and separation into hypersaline liquid and low-salinity vapor. Later fluids may be exsolved at a slower rate, such that they cool more extensively during ascent and do not intersect the solvus, as shown in path II. Thus water responsible for sericite alteration may have a relatively low salinity yet still be magmatic in origin. (From Shinohara and Hedenquist, 1997).

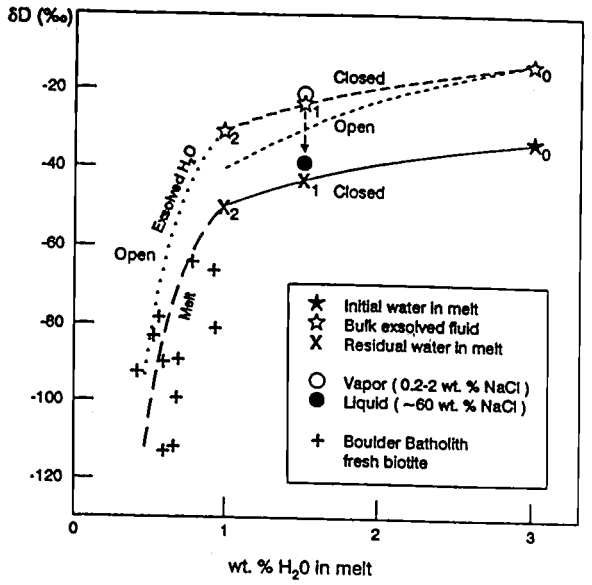

Figure 18b: Evolution of the hydrogen isotope compositions of water remaining dissolved in a melt and the exsolved supercritical fluid, and of the vapor and liquid phases after phase separation. The δD values of igneous phenocrysts commonly reflect the last stage of (open system) degassing of an intrusion. The distribution of δD values of fresh igneous biotite from the Boulder Batholith likely reflects degassing, and not the initial composition of the water dissolved in the melt. (From Taylor, 1986)

example, two samples pairs 11170-2421 (δD=-84 ‰) and 11170-2423 (-118 ‰), 11170-1767 (δD=-93‰) and 11170-1790 (δD=-46‰) are located within one and seven meters, respectively, but they are not in D/H isotopic equilibrium, although they exhibit pervasive gray-sericitic alteration.

(3) Fluid mixing: The isotopic compositions of the gray-sericitic samples show a narrow mixing trend with a small variation in $\delta^{18}O$ (+4.6 to +8.1 ‰), but a wide range of δD values from -118 to -25 per mil. This pattern could be simply explained by mixing of a pure magmatic fluid ($\delta^{18}O$=8 ‰, δD ≥ -20 ‰) with an exchanged, ^{18}O-enriched meteoric fluid that has an isotopic composition of +6 per mil for $\delta^{18}O$ and -120 per mil for δD. Nonetheless there is no evidence for such two hypothesized fluids at Butte.

A Synthetic Model of the Hydrothermal History at Butte

The early stable isotope studies on hydrothermal minerals from porphyry copper deposits by Sheppard et al. (1971) identified hydrothermal fluids of magmatic origin for K-silicate alteration, and a large component of meteoric water for certain late-stage sericite or clay-rich alteration types. The meteoric component is best identified by the δD values, because $\delta^{18}O$ composition of hydrothermal fluids is commonly ^{18}O-enriched by water-rock isotopic exchange. Based on earlier and recent isotope works on this type of deposit, Hedenquist and Richards (1998) proposed a model that the ascending original supercritical fluid was separated into hypersaline fluid (brine) that formed K-silicate alteration and vapor phase that formed the advanced argillic alteration. The gray-sericitic alteration was formed by later magmatic fluids that cooled rapidly during ascent and did not intersect the solvus. Therefore, this fluid should have low salinity and be magmatic in origin.

Unlike other porphyry systems (Fig. 19), at Butte, a large range of δD values has been obtained from the biotite from the K-silicate alteration samples, sericite from the gray-sericitic alteration samples, and even hydrous minerals from the host rock of Butte quartz monzonite (this study; Sheppard and Taylor, 1974), which strongly indicate meteoric water involvement. The key question is whether or not this large range reflects a signature of direct mixing of magmatic water with meteoric water at the time of hydrothermal alteration or that these samples have been isotopically reset by the widespread, younger fluids related to the Main Stage alteration, which has a uniform, low δD value of about -120 per mil.

Four of seven selected K-silicate samples yield fluid isotopic compositions of about 7.0 ‰ for $\delta^{18}O$, and -47 to -64 ‰ for δD which indicate that the Butte K-silicate fluid has a magmatic origin. However, these δD values are minimum because the Main Stage fluids would have reduced δD values. On the other hand, the most D-enriched fluid in Butte was found to be related to the gray-sericitic alteration. This is difficult to explain by a single hydrothermal fluid exsolving from the magma that made the porphyry dikes, producing both the K-silicate alteration and the distinctly later gray-sericitic alteration, because progressive magmatic degassing of a single magma body would have produced successively lighter δD in magmatic water. The heavier δD values of the gray-sericitic fluid relative to that of the K-silicate fluid suggest that the late gray-sericitic fluid came from a new magma intrusion.

Two events hypothesis

In view of the preceding explanation, our data favor the hypothesis that the K-silicate and gray-sericitic mineralization were produced in two distinct hydrothermal stage from different parent magmatic fluids; the K-silicate related to quartz porphyry dikes, whereas gray-sericitic alteration is related to younger rhyolite dikes, or even a

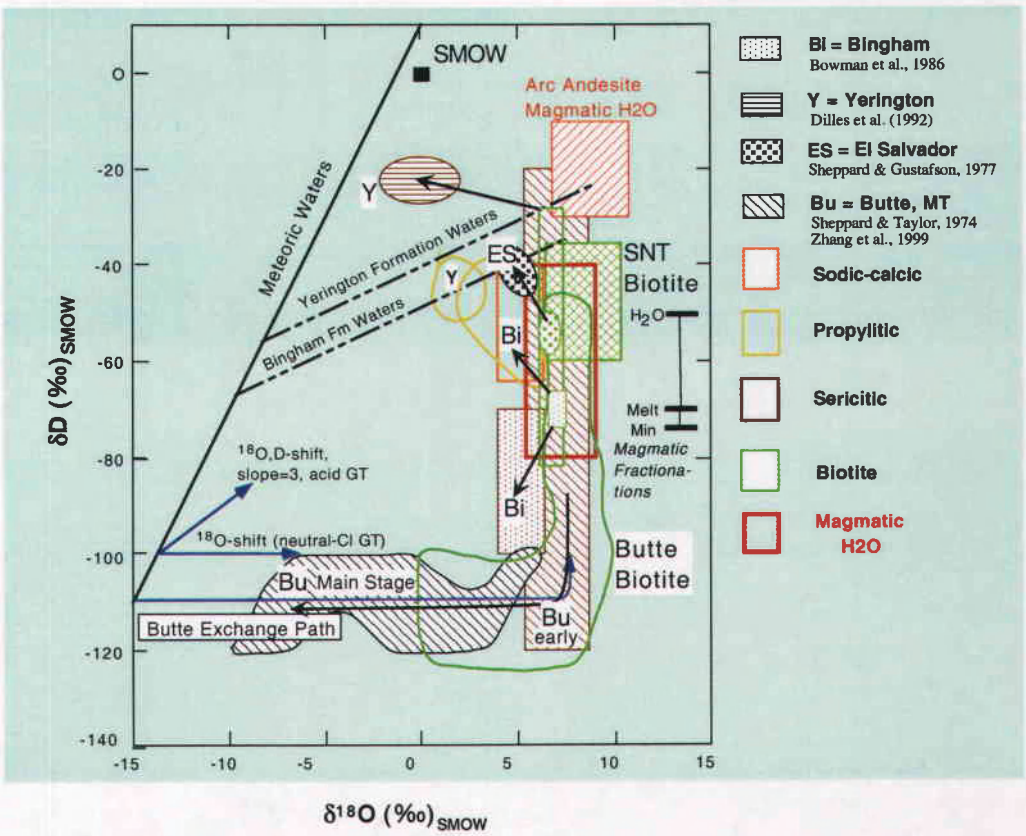

Fig. 19. Summary of isotopic compositions of porphyry Cu waters of Bingham, Yerington, El Salvador, and Butte. Data are from Bowman et al. (1986), Dilles et al. (1992), Sheppard & Gustafon (1977), Sheppard & Taylor (1974), and this study. Meteroric water lines, SMOW, and primary magmatic waters are also shown for comparison.

deeper granite cupola that is not currently exposed (Fig. 20). The two magmatic intrusive events may be as much as 12 Ma apart based on current age data (Martin et al., 1999; Snee et al., 1999).

Our two-event hypothesis is supported by current available data from fluid inclusion and hornblende barometry (Roberts, 1975; Rusk et al., 1999; Dilles et al., 1999; Bodnar, personal commun., 1997), which suggest a large difference in formation-pressure between the deeper K-silicate alteration, which was formed at 7-9 km depth (1.7 -2 kb lithostatic pressure) at 600°C, and the shallower gray-sericitic alteration at 2-3 km depth (~250 bar hydrostatic pressure) at 400°C. This large difference in formation-depth between the two mineralization events cannot be accommodated by hydrothermal fluids that were associated with the emplacement of quartz-porphyry dikes during a short period. However, the hypothesis of two separate hydrothermal events about 12 Ma apart can easily overcome this difficulty in explaining the large pressure difference. It could be caused by the uplift of the Butte area during the 12 Ma period between these two events; most of the alteration formation have been removed at the surface if the erosion rate was quite high.

A water/rock ratio of 2:1 is derived based on oxygen isotopic analyses of the GS sericite. The $\delta^{18}O$ of these sericites has a mean value of 8.0 per mil (Table 4). At 400°C, the $^{18}O/^{16}O$ fractionation between sericite and water is 1.4 per mil (Sheppard and Gilg, 1996). Therefore, the $\delta^{18}O_{water}$ should be 6.6 per mil (8.0 - 1.4), which is also the final water oxygen isotopic composition ($\delta_f{}^{18}O_{w)}$. Based on the assumption of a magmatic origin, the initial water oxygen isotopic composition ($\delta_i{}^{18}O_{water}$) of the GS fluid was about 7 per mil , and the initial rock oxygen isotopic composition ($\delta_i{}^{18}O_{rock}$) of 7.2 per mil was derived from oxygen isotopic data of K-feldspar of BQM and EDM (Table 3). Thus the water/rock ratio for the GS alteration can be obtained from the equation below:

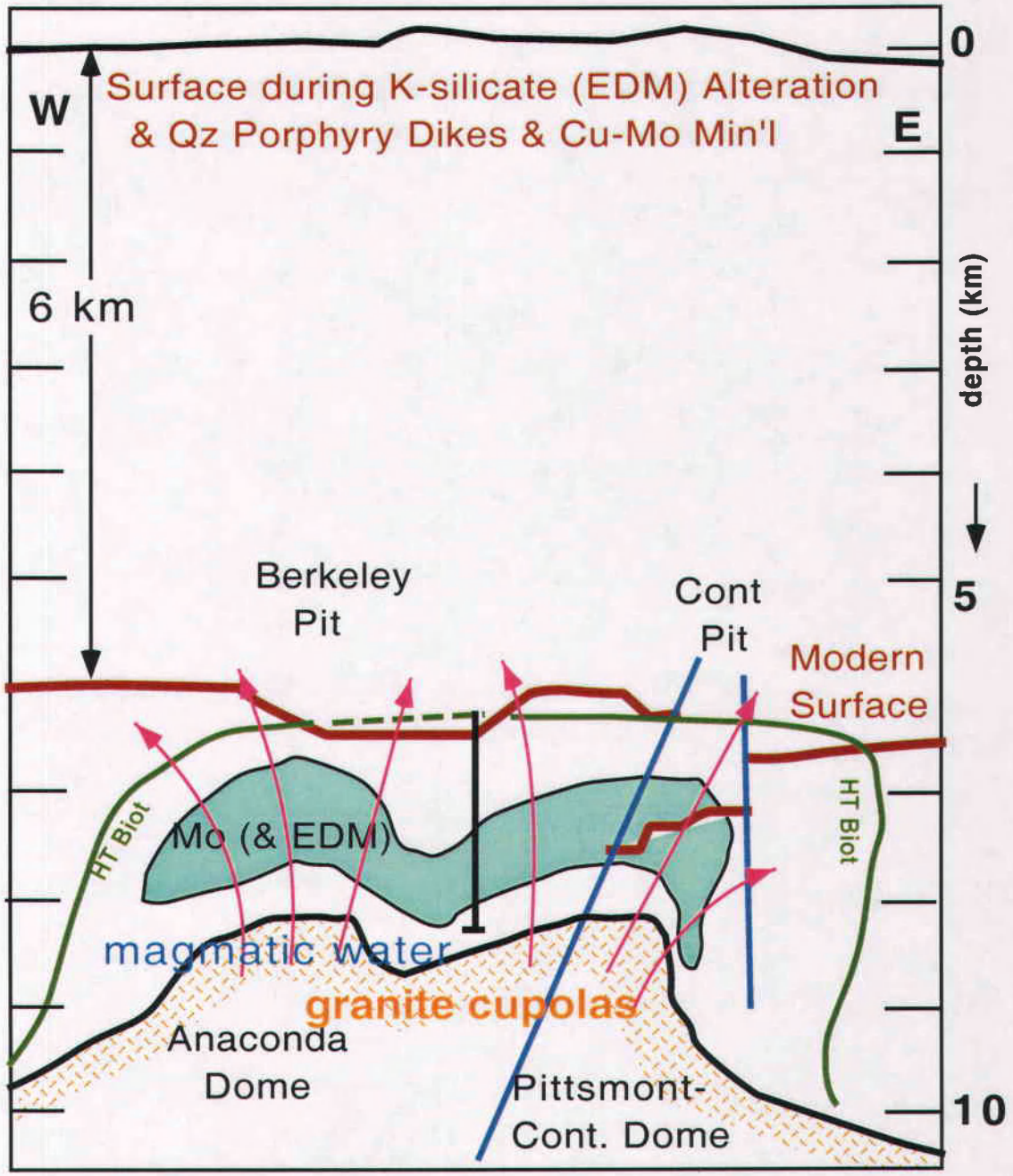

Fig. 20a. Sketch of a synthetic model showing hydrothermal fluid pathways at K-silicate mineralization stage at Butte.

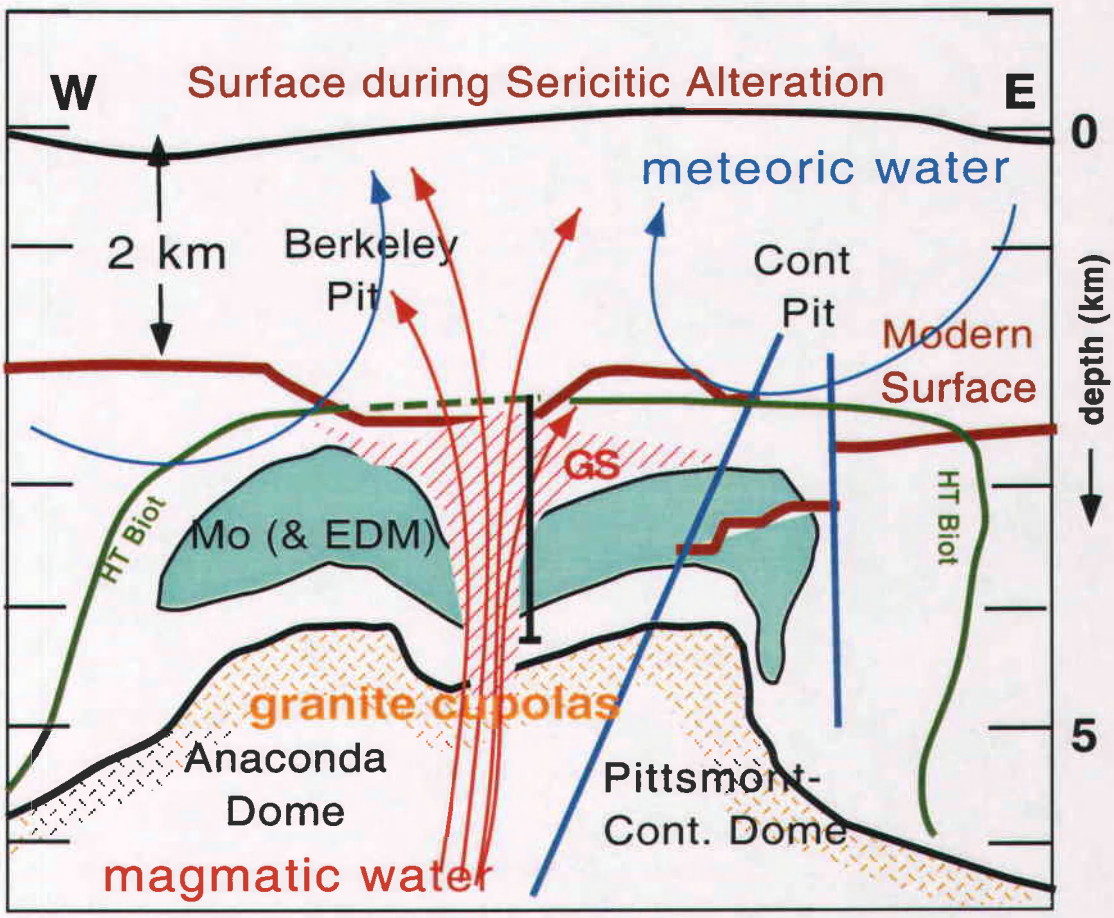

Fig. 20b. Sketch of a synthetic model showing hydrothermal fluid pathways at the Gray-Sericitic mineralization stage at Butte.

$$\frac{W}{r} = \frac{\delta_f{}^{18}O_w - \delta_i{}^{18}O_r + \Delta}{\delta_i{}^{18}O_w - \delta_f{}^{18}O_w} = \frac{6.6-7.2+1.4}{7.0-6.6} = 2.0$$

Provided the estimated volume of the pervasive GS alteration rock of 1 km^3, and the density of the sericitic altered rock is about 2.9 t/m^3, the total mass of the GS altered rock should be 2.9 $x10^{11}$ tons. Therefore, the total water which was involved in the GS alteration should be $2x2.9x10^9=5.8x10^9$ ton or 5.8 km^3 in volume (assume ρ_{water} = 1 t/m^3 at room temperature and pressure). Further, if we assume the 2-3 wt.% or 5 vol.% water present in a granite magma, then the total mass of the granite should be 5.8/2.5% $=2.3x10^{11}$ tons, that is, the total volume of magma needed to produce the GS alteration is $2.3x10^{11}/2.7$ = 85 km^3. The estimated size of this intrusion is not unreasonable; unfortunately, there are no factual observations to validate this estimate.

Hypogene leaching mechanism

The mechanism of "hypogene leaching", first proposed by Brimhall (1979), may be responsible for the mobilization of pre-Main Stage metals into Main Stage veins. Based on the isotopic data on the gray-sericitic alteration from this study and the Main Stage data from Sheppard and Taylor (1974), we favor the following explanation of these two mineralization events.

The sericites of gray-sericitic alteration may have formed initially by a magmatic water with isotopic compositions of 8 per mil for $\delta^{18}O$ and -25 per mil for δD. The gray-sericitic fluids could have altered the earlier K-silicate altered rock, and remobilized metals, such as Cu, Pb, Zn into the ore fluid (Brimhall, 1979, 1980; Brimhall and Ghiorso, 1984). Afterwards, this ore-bearing fluid mixed with a shallow meteoric water with $\delta^{18}O$= -16 per mil and δD=-120 per mil, which was circulating from east to west at Butte and formed low pH fluids that were responsible for the late Main Stage

mineralization and sericitic and argillic alterations. Fluid inclusion data suggest a temperature range of 340°C to 150°C for these Main Stage alterations.

This following calculation supports the hypogene leaching hypothesis of remobilization of ores from earlier K-silicate altered rock to form the Main Stage veins by late gray-sericitic fluids. Assuming gray-sericitic fluids altered 1 km^3 of rock that had been previously altered by K-silicate alteration and that this rock originally had a density of about 2.6 t/m^3 and contained average 0.5 weight percent copper, then the total copper in the 1 km^3 volume K-silicate alteration rock would be 13 Mt (e.g., 0.5 wt. % * $1x10^9$ * 2.6 t/m^3). This number corresponds closely to the copper production of 10.7 MT at Butte during the mining interval from 1880 to 1991, in which most of the ores were from the Main Stage veins (Long, 1995).

Conclusions

We have completed systematic analyses of oxygen and hydrogen isotopic compositions of fifty-four selected samples to investigate the origin of the pre-Main Stage ore fluids within the Butte district, Montana. Among them, four samples were selected from the fresh Butte Quartz Monzonite host rock, seven samples from K-silicate alteration, sixteen samples from K-silicate alteration with later argillic alteration overprint, and twenty-six samples from gray-sericitic alteration. Analyses of these samples lead to the following major conclusions.

The widespread, Main Stage or younger argillic alteration have partly to totally reset the isotopic compositions of minerals in the fresh Butte Quartz Monzonite host rock, the early high temperature K-silicate alteration assemblages, and locally quartz-sericite alteration assemblages. These isotopic exchanges are best identified by the depletion of δD values from -100 to -165 per mil.

The least altered Butte Quartz Monzonite samples from the edge of the Butte district

yield similar isotopic compositions to the felsic magmatic water ($\delta^{18}O$ = 7-8 ‰, and δD=-45 to -60‰). The light δD values of the Butte Quartz Monzonite samples near the mining district suggest that these Butte Quartz Monzonite had partly re-equilibrated with meteoric fluids at low temperatures.

The most D-rich fluids associated with K-silicate alteration related to the porphyry Cu-Mo mineralization were the original supercritical fluids with salinity of 6 weight percent NaCl equivalent and isotopic compositions of 7 per mil for $\delta^{18}O$, and -47 to -64 per mil for δD.

The large variation of oxygen isotopic composition and the D-depletion in the argillically altered K-silicate samples resulted from isotopic exchange of biotite with the younger, low-temperature, meteoric-dominated argillic fluids, as initially proposed by Sheppard and Taylor (1974). These argillically altered K-silicate samples can be further divided into two distinct groups based on their $\delta^{18}O$ values of biotite: (a) $\delta^{18}O$ similar to or slightly enriched relative to typical K-silicate alteration samples and (b) ^{18}O-depleted relative to typical K-silicate alteration samples. The two groups correspond to two argillic alteration types; samples in group (a) are from white argillic overprinted zones, whereas samples in group (b) were superimposed by green argillic alteration.

Calculated isotopic compositions of fluids suggest that: (a) the gray-sericitic alteration was produced by nearly pure magmatic water with δD values of ~-35 per mil; (b) the wide range of δD values of the gray-sericitic sericite may be either due to a mixture of magmatic water derived from felsic magmas (Taylor, 1992) with local, exchanged ^{18}O-enrichment meteoric water, or due to water-rock reactions such as the isotopic exchange of gray-sericitic minerals with later young fluids.

Acknowledgments

This project was supported by the National Science Foundation grants: EAR-9600054 (Dilles and Field) and EAR-9704280 (Reed). We thank Montana Resources and the Montana Bureau of Mines and Geology for giving us access to deep drill hole core samples and Anaconda sample collection for mapping and sampling. We especially thank Lester Zeihen for his persistent and successful efforts to preserve the Anaconda sample collection. We thank Lawrence Snee at USGS in Denver, Colorado for his collaboration in providing of ^{40}Ar-^{39}Ar isotopic age determinations. We also thank Robert Houston and Brain Rusk for their contributions on the Butte geology mapping and fluid inclusion works. Finally, we benefited from discussions with Jeffrey W. Hedenquist.

References

Bigeleiser, J, Perlman, M. L., Prosser, H. C., 1952, Conversion of hydrogen materials to hydrogen for isotopic analysis: Analytical Chemistry, v. 24, p. 1356-1357.

Bodnar, R. J, 1995, Fluid-inclusion evidence for a magmatic source of metals in porphyry copper deposits: in Thompson, J.F.H., ed., Magma, fluids, and ore deposits: Mineralogical Association of Canada Short Course, v. 23, p. 139-152.

Bottinga, Y., and Javoy, M., 1973, Comments on oxygen isotope geothermometry: Earth and Planetary Science Letters, v. 20, p. 250-265.

Brimhall, G. H. , Jr., 1972, Early fracture-controlled disseminated mineralization at Butte, Montana: Unpub. Ph.D. dissert., Univ. California, Berkeley, 103 p.

Brimhall, G. H. , Jr., 1977, Mineralogy, texture, and chemistry of early wall rock alteration in the deep underground mines and Continental area, Butte district, Montana: Econ. Geol., v. 72, p. 37-59.

Brimhall, G. H. , Jr., 1979, Lithologic determination of mass-transfer mechanism of multiple-stage porphyry copper mineralization at Butte, Montana: vein formation by hypogene leaching and enrichment of potassium silicate protore: Econ. Geol., v. 74, p. 556-589.

Brimhall, G. H. , Jr., 1980, Deep hypogene oxidation of porphyry copper potassium-silicate protore at Butte, Montana: a theoretical evaluation of the copper mobilization hypothesis: Econ. Geol., v. 75, p. 384-409.

Burnham, C. W., 1997, Magma and hydrothermal fluids, in Barnes, H.L., ed., Geochemistry of Hydrothermal Ore Deposits (3rd ed.): New York, John Wiley &Sons, Inc., p. 71-136.

Burnham, C. W., and Ohmoto, H., 1980, Late-stage processes of felsic magmatism: Mining Geology Special Issue, No. 8, p. 1-11.

Capuano, R. M., 1992, The temperature dependence of hydrogen isotope fractionation between clay minerals and water: Evidence from a geopressured system: Geochimica et Cosmochimica Acta, v. 56, p. 2547-2554.

Cline, J. S., 1995, Genesis of porphyry copper deposits: the behavior of water, chloride, and copper in crystallizing melts, in Pierce, F. W., and Bolm, J. G., eds., Porphyry copper deposits of the American Cordillera: Arizona Geological Society Digest, v. 20, p. 69-82.

Cole, D. R., and Ohmoto, H., 1986, Kinetics of isotopic exchange at elevated temperatures and pressures: Stable Isotopes in High Temperature Geological Processes, in Valley, J. W., Taylor, H. P., Jr., and O'Neil, J. R., eds., Reviews in Mineralogy: Mineralogical Society of America, v. 16, p. 41-90.

Cooper, J. R., 1973, Geological map of the Twin Buttes quadrangle, southwest of Tucson, Arizona: U.S. Geological Survey Misc. Geol. Inv. Map 745.

Dilles, J. H., Solomon, G. C., Taylor, H. P., and Einaudi, M. T., 1992, Oxygen and hydrogen isotope characteristics of hydrothermal alteration at the Ann-Mason porphyry copper deposit, Yerington, Nevada: Econ. Geol., v. 87, p. 44-63.

Dilles, J. H., Reed, M. H., Roberts, S., Zhang, L., and Houston, R., 1999, Early magmatic-hydrothermal features related to porphyry copper mineralization at Butte, Montana (abs): Geological Society of America Abstracts Programs, v. 31, no 7, p. A-380.

Field, C. W., Rye, R. O., Dymond, J. R., Whelan, J. F., and Senechal, R. G., 1983, Metalliferous sediments of the East Pacific, in Shanks, W. C., III, ed., Cameron Volume on Unconventional Mineral deposits: New York, Society of Mining Engineers of A.I.M.E., p. 133-156.

Garlick, G. D., and Epstein, S., 1966, The isotopic composition of oxygen and carbon in hydrothermal minerals from Butte, Montana: Econ. Geol., v. 62, p. 1325-1335.

Geissman, J. W., Kelly, W. C., Van der Voo, R., and Brimhall, G. H. , Jr., 1980, Paleomagnetic documentation of the early, high temperature zone of mineralization at Butte, Montana: Econ. Geol., v. 75, p. 1210-1219.

Geissman, J. W., Kelly, W. C., Van der Voo, R., and Brimhall, G. H. , Jr., 1980, Paleomagnetism, rock magnetism and aspects of structural deformation of the Butte mining district, Butte, Montana: Jour. Geology, v. 88, p. 129-159.

Gilluly, J., 1946, The Ajo mining district, Arizona: U.S. Geological Survey Prof. Paper 209, 112 p.

Graham, C. M., Harmon, R. S., and Sheppard, S. M. F., 1984, Experimental hydrogen isotope studies--hydrogen isotope exchange between amphibole and water: American Mineralogist, v. 69, p. 128-138.

Guilbert, J. M. and Park, C. F., Jr., 1985, The geology of ore deposits: W. H. Freeman and Company, New York, 984 p.

Hedenquist, J. W., Arribas, A., Jr., and Reynolds, J. R., 1998, Evolution of an intrusion-centered hydrothermal system: Far Southeast-Lepanto porphyry and epithermal Cu-Au deposits, Philippines: Econ. Geol., v. 93, p. 373-404.

Hedenquist, J. W., and Richards, J. P., 1998, The influence of geochemical techniques on the development of genetic models for porphyry copper deposits, in Richards, J. P., and Larson, P. B. (eds.), Techniques in Hydrothermal Ore Deposits Geology: Reviews in Economic Geology, v. 10, p. 235-256.

Houston, R., 1999, The Butte district, Montana – new field data and reassessment of post-mineral structural tilting (abs): Geological Society of America Abstracts Programs, v. 31, no 7, p. A-382.

Javoy, M., 1977, Stable isotopes and geothermometry: Journal of the Geological Society of London, v. 133, p. 609-636.

Knopf, A., 1957, The Boulder batholith of Montana: Am. Jour. Sci., v. 255, p. 81-103.

Lambert, S. J., and Epstein, S., 1980, Stable isotope investigations of an active geothermal system in Valles Caldera, Jemez mountains, New Mexico: Joun. Volc. Geothermal Res., v. 8, p. 111-129.

Martin, M. W., Dilles, J. H., and Proffett, J. M., 1999, U-Pb geochronologic constraints for the Butte porphyry system (abs): Geological Society of America Abstracts Programs, v. 31, no 7, p. A-380.

Matsuhisa, Y., Goldsmith, J. R., and Clayton, R. N., 1979, Oxygen isotopic fractionation in the system quartz-albite-anorthite-water: Geochimica et Cosmochimica Acta, v. 43, p. 1131-1140.

Meyer, C., 1950, Hydrothermal wall-rock alteration at Butte, Montana: Ph.D. thesis, Harvard University.

Meyer, C., 1965, An early potassic type of wall-rock alteration at Butte, Montana: Amer. Mineral., v. 50, p. 1717-1722.

Meyer, C., and Hemley, J. J., 1967, Wall rock alteration, in Geochemistry of Hydrothermal Ore Deposits; H. L. Barnes (ed.): New York, Holt, Rinehart, and Winston, p. 166-235.

Meyer, C., Shea, E. P., Goddard, C. C., and staff, 1968, Ore deposit at Butte, Montana: Ore Deposits of the United States 1933/1967, the Graton-Sales Volume 2, ed., Ridge, J.D., p. 1373-1416.

Nebelek, P. I., O'Neil, J. R., and Papike, J. J., 1983, Vapor phase exsolution as a controlling factor in hydrogen isotope variation in granitic rocks: the Notch Peak granite stock, Utah: Earth Planetary Science Letters, v. 66, p. 137-150.

O'Neil, J. R., 1986, Theoretical and experimental aspects of isotopic fractionation: Stable Isotopes in High Temperature Geological Processes, Reviews in Mineralogy, v. 16, p. 1-40.

O'Neil, J. R., and Kharaka, Y. K., 1976, Hydrogen and oxygen isotope exchange reactions between clay minerals and water: Geochimica et Cosmochimica Acta, v. 40, p. 241-246.

Page, R. H., 1979, Alteration-mineralization history of the Butte, Montana ore deposit, and transmission electron microscopy of phyllosilicate alteration phases: Unpub. Ph.D. dissert., Univ. of California, Berkeley, 234 p.

Proffett, J. M., Jr., 1974, Structure of the Butte district, Montana: Guidebook for the Butte Field Meeting of Society of Economic Geologists, Sec. G, p. G-1-G12.

Proffett, J. M., Jr., 1979, Ore deposits of the western United States: a summary: Nevada Bureau Mines Geology Report 33 (IAGOD 5th Quadrennial Symposium Proceedings), v. 11, p. 13-32.

Proffett, J. M., Jr., and Dilles, H. J., 1984, Early Mesozoic sedimentary and volcanic rocks of the Yerington region, Nevada, and their regional context (U. S. Geological Survey-Nevada Bureau of Mines conterpiece project; U. S. Geological Survey Bulletin).

Reed, M. H., 1979a, Pyrite-quartz-sericite mineralization of Late pre-Main Stage age, Butte, Montana: Anaconda Company Report, 20 p., 7 plates.

Reed, M. H., 1979b, Butte district early stage geology: Anaconda Company Report, 40 p. 24 plates and figures.

Reed, M. H., 1980, Distribution of Mineralization at Butte: Anaconda Company Report, 40 p., 17 plates and figures.

Reyes, G. A., 1990, Petrology of Philippine geothermal systems and the application of alteration mineralogy to their assessment: Jour. of Volcanology and Geothermal Research, v. 43, p. 279-309.

Roberts, S. A., 1975, Early hydrothermal alteration and mineralization in the Butte district, Montana: Unpub. Ph.D. dissert., Harvard Univ., 157 p.

Roedder, E., 1971, Fluid inclusion studies on the porphyry-type deposits at Bringham, Utah, Butte, Montana and Climax, Colorado: Econ. Geol., v. 66, p. 98-120.

Rusk, B., Reed, M. H., and Dilles, J. H., 1999, Fluid inclusions in barren quartz and quartz-molybdenite veins in the porphyry Cu-Mo deposits, Butte, Montana (abs): Geological Society of America Abstracts Programs, v. 31, no 7, p. A-381.

Sales, R.H., 1914, Ore deposits at Butte, Montana: American Institute of Mining, Metallurgical, And Petroleum Engineers Transactions, v. 46, p. 3-106.

Sales, R.H., and Meyer, C., 1948, Wall rock alteration, Butte, Montana: American Institute of Mining, Metallurgical, And Petroleum Engineers Transactions, v. 178, p. 9-35.

Savin, S. M., and Epstein, S., 1970, The oxygen and hydrogen isotope geochemistry of clay minerals: Geochem. Cosmochim. Acta, v. 34, p. 25-42.

Sharp, Z.D., 1990, A laser-based microanalytical method for in situ determination of oxygen isotopic ratios of silicates and oxides: Geochem. Cosmochim. Acta, v. 54, p. 1354-1357.

Sheppard, S. M. F., Nielsen, R. L., and Taylor, H. P., Jr., 1969, Oxygen and hydrogen isotope ratios of clay minerals from porphyry copper deposits: Econ. Geol., v. 64, p. 755-777.

Sheppard, S. M. F., and Taylor, H. P., Jr., 1974, Hydrogen and oxygen isotope evidence for the origin of water in the Boulder Batholith and the Butte ore deposits, Montana: Econ. Geol., v. 69, p. 926-946.

Sheppard, S. M. F., and Gilg, H. A., 1996, Stable isotope geochemistry of clay minerals: Clay Minerals, v. 31, p. 1-24.

Shieh, Y. N., and Taylor, H. P., Jr., 1969, Oxygen and hydrogen isotope studies of contact metamorphism in the Santa Rosa range, Nevada and other areas: Contrib. Mineral. Petrol., v. 20, p. 306-356.

Stormer, J. C., and Carmichael, I. S. E., 1971, Fluorine-hydroxyl exchange in apatite and biotite: A potential igneous geothermometer: Contrib. Mineral. Petrol., v. 31, p. 121-131.

Suzuoki, T., and Epstein, s., 1976, Hydrogen isotope fractionation between OH-bearing minerals and waters: Geochem. Cosmochim. Acta, v. 40, p. 1229-1240.

Smedes, H. W., 1973, Regional setting and general geology of the Boulder batholith, Montana: Guidebook for the Butte Field Meeting of the Society of Economic Geologists, Sec. A, p. A-1-A-6.

Snee, L., Miggins, D., Reed, M. H., Dilles, J. H., and Zhang, L., 1999, Thermal history of the Butte porphyry system, Montana (abs): Geological Society of America Abstracts Programs, v. 31, no 7, p. A-380.

Taylor, H. P., Jr., and Epstein, S., 1962, Relationship between O18/O16 ratios in coexisting minerals of igneous and metamorphic rocks; Part I: Principles and experimental results: Geol. Soc. Amer. Bull., v. 73, p. 461-480.

Taylor, H. P., Jr., 1967, Oxygen isotope studies of hydrothermal mineral deposits, in H. L. Barnes, ed., Geochemistry of Hydrothermal Ore Deposits: New York, Holt, Rinehart and Winston, 670 p.

Taylor, H. P., Jr., 1979, Oxygen and hydrogen isotope relationships in hydrothermal mineral deposits, in Barnes, H. L., ed., Geochemistry of hydrothermal ore deposits: Third Edition: John Wiley and Sons, New York, p. 229-302.

Taylor, B. E., Eichelberger, J. C., and Westrich, H. R., 1983, Hydrogen isotopic evidence of rhyolitic magma degassing during shallow intrusion and eruption: Nature, v. 306, p. 541-545.

Tilling, R. I., Klepper, M. R., and Obradovich, J. D., 1968, K-Ar ages and time span of emplacement of the Boulder batholith, Montana: Am. Jour. Sci., v. 266, p. 671-689.

Wadsworth, W. B., 1968, The Cornelia pluton, Ajo, Arizona: Econ. Geol., v. 63, p. 101-115.

Zhang, L., Field, C. W., Dilles, J. H., and Reed, M. H., 1999, Sulfur isotope record of deep porphyry Cu-Mo mineralizationbarrenthe, Butte, Montana (abs): Geological Society of America Abstracts Programs, v. 31, no 7, p. A-381.

Chapter 3

Sulfur Isotope Record of Deep Porphyry Cu-Mo Mineralization, Butte District, Montana

Lihua Zhang, Cyrus W. Field, and John H. Dilles

Department of Geosciences, Oregon State University, Corvallis, Oregon 97331-5506

Mark H. Reed

Department of Geological Sciences, University of Oregon, Eugene OR 97403

In preparation for submission to

Economic Geology

Abstract

Typical porphyry-type Cu-Mo mineralization predates and largely underlies the well-known, throughgoing, Main Stage polymetallic veins of Butte. Sulfur-bearing minerals of this early pre-Main Stage hydrothermal event recovered from deep drill core include anhydrite, chalcopyrite, pyrite, and molybdenite in veinlets bordered by K-silicate alteration and pyrite from slightly younger quartz-pyrite veinlets with gray-sericitic alteration selvages. The range of $\delta^{34}S$ per mil values for minerals of the K-silicate assemblage are 9.8 to 12.9 per mil in anhydrite (20), 3.0 to 4.7 per mil in molybdenite (6), 0.5 to 3.4 per mil in pyrite (12), and 0.4 to 3.0 per mil in chalcopyrite (10). Mineral fractionation are entirely consistent with an approach to isotopic equilibrium, and calculated temperature ranges for mostly coexisting anhydrite-sulfide pairs are 543 to 632 °C (anh-mb; 6), 534 to 639 °C (anh-py; 10), and 482 to 576 °C (anh-cp; 8). These temperatures are broadly consistent with those of fluid inclusion studies past (Roberts, 1975) and present. The $\delta^{34}S$ values for pyrite (25) in veinlets of the GS assemblage range from 1.7 to 4.3 per mil. The K-silicate and gray-sericitic sulfide data are similar to those of Main Stage sulfides (Lange and Cheney, 1971; Lange and Krouse, 1984) and suggest a conventionally "magmatic" value of about 2 per mil for Butte sulfide-sulfur. However, total sulfur ($\delta^{34}S_{\Sigma S}$ ‰) of the early K-silicate assemblage may be as heavy as 10 per mil, suggesting a possible crustal component to this relatively oxidized system; an inference supported by alteration assemblages, the presence of anhydrite, high modal sulfate to sulfide mineral ratios (Brimhall, 1977), and isotopic effects related to fractionation in a SO_4^{2-}-rich hydrothermal fluid.

Introduction

The Butte Mining District of southwest Montana is preeminent not only as a major U.S. producer of hydrothermal Cu-Pb-Zn-Mn-Ag ores for nearly 130 years, but also as the prominent residence of rogues and heros involved in notorious mineral litigation near the close of the Nineteenth Century. In addition, for ninety years or more, it has been the location of numerous industry, government, and university investigations directed to applied and basic ore deposit research. Several of the latter include the application of stable isotopes to questions relating to ore genesis, and those of sulfur represent an early and recurring subject of these investigations. Most previous sulfur isotope research has been concerned almost exclusively with the large, throughgoing veins related to the well-known Main Stage mineralization. In contrast, our present study is directed to an earlier, deeper, and higher temperature pre-Main Stage type of porphyry Cu-Mo mineralization. The sulfur-bearing minerals analyzed are those contained in thin quartz-sulfate-sulfide veinlets associated with the Early Dark Micaceous, K-silicate alteration, and slightly younger quartz-pyrite veinlets associated with the gray-sericitic alteration selvages, respectively. Samples were selected from diamond drill core obtained by the Anaconda Company in 1979-1981 as part of a deep exploration program at Butte.

The principal objectives of this investigation were to: (1) determine whether or not the $\delta^{34}S$ composition of early Pre-Main Stage mineralization is similar to that of the later Main Stage event; (2) establish the extent to which isotopic equilibrium may have prevailed between different sulfur-bearing minerals and, thus, the apparent reliability of isotopic temperatures derived therefrom; and (3) attempt to estimate the isotopic composition of total sulfur ($\delta^{34}S_{\Sigma S}$ ‰) in the Butte hydrothermal system and thereby gain better insight as to the likely source(s) of this sulfur. Interpretations of our data have benefited greatly from previous isotopic studies of Main Stage mineralization, from

subsequent geologic studies of pre-Main Stage mineralization, and continued improvements in the understanding of sulfur isotope fractionation derived from both experiment and theory.

Geologic Setting

Mineral deposits of the Butte District are located near the southern end of the Late Cretaceous Boulder Batholith. They are hosted by the Butte Quartz Monzonite, the dominant intrusive phase of the batholith. Detailed petrographic studies and field descriptions of the Butte Quartz Monzonite indicate a relatively uniform mineralogy dominated in order of diminishing abundance by plagioclase feldspar, quartz, potassium feldspar, biotite, and hornblende with accessory magnetite, sphene, ilmenite, apatite, and zircon (Weed, 1912, 1914; Meyer, 1950; Lepper and others, 1957; Becraft and others, 1963; Ruppel, 1963; Smedes, 1966; Tilling, 1964; Robson, 1972; Kurz, 1973; Roberts, 1975). Trace amounts of sulfide, but never sulfate, are sparingly present in unaltered Butte Quartz Monzonite.

Pre-Main Stage mineralization at Butte is defined collectively by the types and zonations of metals and of ore, gangue, and alteration minerals. It consists of typical porphyry-type, fracture-controlled, Cu-Mo mineralization that predates and largely underlies the throughgoing Main Stage polymetallic veins for which the district is famous. This mineralization occupies two centers, a western Anaconda Dome and an eastern Pittsmont Dome, that trend about N80° W and straddle a swarm of quartz porphyry dikes as shown in Figures 1 and 2a. Although the Pittsmont Dome is the larger of the two, both contain identical types of alteration and vein assemblages related to Cu-Mo mineralization (Reed, 1979). The shapes of these two domes are defined by zones of anomalously high concentrations of molybdenum and copper, magnetite veinlets, and potassium silicate alteration (Fig. 2), which collectively represent the

earliest phase of pre-Main Stage hydrothermal mineralization at Butte. The associated high-temperature potassium silicate alteration is characterized by pervasively biotitized hornblende (Roberts, 1975) and Early Dark Micaceous veinlets described by Meyer (1965) that contain Cu-Fe sulfides (about 0.5 to 0.8 wt.% Cu), anhydrite, biotite, potassium feldspar, quartz, and other silicates that formed at 550 to 600° C (Brimhall, 1977). Pervasively biotitized Butte Quartz Monzonite is characterized by the total replacement of magmatic hornblende by hydrothermal biotite, destruction of sphene to a mixture of Fe-Ti oxides, quartz, and anhydrite (Roberts, 1975), partial conversion of plagioclase to potassium feldspar, and the introduction of disseminated sulfides (chalcopyrite, pyrite, molybdenite, and bornite), and anhydrite. According to Roberts (1975) and Brimhall (1977), modal analyses indicate that altered Butte Quartz Monzonite contains up to five percent anhydrite and about two percent sulfides. Alteration grades outward and upward from the K-silicate zone into a contemporaneous to slightly younger succession of pale green sericite, dark green sericite-chlorite, and more distal propylitic epidote-chlorite assemblages of pre-Main Stage alteration (Page, 1979; Reed, 1979). Main Stage veins that cut pre-Main Stage mineralization are abundant and well-developed in the north and west parts of the Anaconda Dome. However, these veins are much smaller and fewer in number in the Pittsmont Dome area to the east.

Between the Anaconda and Pittsmont Domes, and partly overlying the latter, is a large bulb-like mass of pervasively sericitized rock (Figs. 2a&b) that is characterized by a stockwork of quartz-pyrite veinlets with sericitic alteration selvages. As these veinlets cut both earlier chalcopyrite- and molybdenite-bearing veinlets, they thereby constitute yet a third distinct episode of pre-Main Stage mineralization. This zone of pervasive gray-sericitic alteration grades laterally outward and upward as a halo of moderately to weakly sericitized rock that envelopes most of the Anaconda and Pittsmont Domes that

served as the principal loci of Cu-Mo mineralization. Again, cross-cutting relationships show that the quartz-pyrite veinlets and gray sericitic alteration are younger than the other EDM, pale green sericite, dark green sericite-chlorite, quartz-molybdenite, and probably propylitic epidote-chlorite veinlets and assemblages of pre-Main Stage alteration and mineralization, but it is older than Main Stage veins. Only trace amounts of chalcopyrite are present in the gray-sericitic zone as is consistent with low concentrations of copper (about 0.05 to 0.20 wt. %) and the near-absence of large Main Stage veins. Pyrite is the dominant sulfur-bearing mineral, and sulfate was not observed, although the very common cavities in quartz-pyrite veinlets may be where anhydrite was leached.

The younger Main Stage mineralization at Butte produced the famous giant fissure veins that contain the high-grade ores of copper, zinc, lead, silver, and manganese. These large Main Stage veins are bordered by an outward succession of alteration halos dominated by "white" sericite, and followed by kaolinite and finally smectitic forms of argillic alteration (Sales and Meyer, 1948; Meyer et al., 1968; Meyer and Hemley, 1967). These veins were best developed in the central and west parts of the district where they were superimposed on the early pre-Main Stage porphyry Cu-Mo mineralization (Fig. 1). Trace amounts of sulfate (alunite) have been reported in veins from the central zone at Butte (Meyer et al., 1968). A pervasive smectitic form of "green argillic" alteration after plagioclase feldspar developed throughout much of the central and peripheral parts of the district. The timing of the argillic alteration in the district may range from Main Stage (Sales and Meyer, 1948) to distinctly younger.

The north-trending and west-dipping Continental fault passes through the east part of the district (see Figs. 1 and 2a &b). Because this normal fault has as much as 1,067 to 1,372 meters of vertical displacement, rocks exposed to the east in the Continental Pit area represent a deep part of the Pittsmont Dome and, thus, Butte porphyry Cu-Mo

system. Exposures in this area provide the best samples for studies of pre-Main Stage mineralization because, unlike most others in the district, it has been least affected by the later Main Stage hydrothermal fluids.

Samples, Procedures, and Conventions

Sulfur-bearing minerals analyzed in this study were separated from samples of core obtained from eight deep diamond drill holes that represent a vertical interval that exceeds 1,500 meters. Sample selection emphasized those containing veinlets associated with K-silicate or gray-sericitic types of alteration. The former provided two or more coexisting or associated sulfur-bearing phases such as anhydrite, chalcopyrite, molybdenite, and (or) pyrite from a single sample, whereas the latter was simply a means of monitoring the isotopic behavior of the single and the most ubiquitous sulfide phase, namely pyrite. The anhydrite-bearing veinlets were observed and collected only from the Pittsmont Dome in drill hole 11172 and over the interval from 1743 to 4245 feet (530 to 1294 m). However, we also include data for similar anhydrite-pyrite veinlets in samples previously collected from the Anaconda Dome and graphically summarized in part by Field and others (1983).

Sulfur isotope analyses have been performed on 19 sulfate (anhydrite) and 60 sulfide (molybdenite, 6; pyrite, 40; chalcopyrite, 13; enargite, 1). These sulfur-bearing mineral concentrates were extracted from 47 samples of the deep drill core. Mineral separations were made after slabbing of core samples by hand-picking and heavy liquid methods of concentration. The purity of most mineral concentrates with respect to other sulfur-bearing contaminants normally exceeded 98 percent, although some contamination (up to 15 percent) was encounted with several pyrite-chalcopyrite and molybdenite-chalcopyrite assemblages that were finely crystalline and intimately admixed.

Sulfur isotope analyses were performed on sulfur dioxide gases extracted by conventional methods from the sulfur-bearing minerals. The sulfur in anhydrite was first reduced to hydrogen sulfide in a boiling solution of hydrochloric-hydriodic-hypophosphorous acid and collected as silver sulfide (Thode et al., 1961). Silver sulfide and the other sulfide minerals were mixed with cupric oxide and oxidized under vacuum at 1025 to 1100°C to sulfur dioxide gas for isotopic analysis according to methods described by Ohmoto and Rye (1979), Ohmoto and Goldhaber (1997) and references cited therein. Recoveries of sulfur normally exceeded 90 and 95 percent for sulfate and sulfide minerals, respectively. Isotopic analyses of the sulfur dioxide gases were performed under the direction of Professor Kevin L. Shelton in the Stable Isotope Laboratory of the Department of Geological Sciences, University of Missouri-Columbia. In addition, a trace amount of magmatic sulfur from an unaltered sample of Butte quartz monzonite was extracted by means of the Kiba reagent, as described by Sasaki and others (1979) and Sakai and others (1982), and isotopically analyzed at facilities of the Geological Survey of Japan.

The sulfur isotope data are presented in terms of conventional del values in per mil ($\delta^{34}S$ ‰) given by the equation

$$\delta^{34}S \text{ ‰} = (R_x/R_s - 1)(10^3), \quad (1)$$

where R_x and R_s are the measured and assumed $^{34}S/^{32}S$ ratios of sample and standard, respectively. Positive or negative del values represent per mil (parts per thousand) enrichment or depletion, respectively, of ^{34}S in the sample relative to the standard: troilite sulfide from the Cañon Diablo meteorite that is zero per mil by definition. The del values may be used to calculate the isotopic separation between two sulfur-bearing compounds (A and B, as minerals, gases, or aqueous species) either from the fractionation factor (α) given by the relationship

$$\alpha_{A\text{-}B} = (1000 + \delta_A \text{ ‰}) / (1000 + \delta_B \text{ ‰}) \quad (2)$$

or from the delta value (Δ) given by the equation

$$\Delta_{A\text{-}B} = \delta_A \text{‰} - \delta_B \text{‰} \cong 1000 \ln \alpha_{A\text{-}B}. \quad (3)$$

This isotopic separation, or fractionation, is caused by differences in the bond strengths of sulfur in different compounds. Because the effect varies inversely with temperature, the fractionation factor (α) or related delta value (Δ) may be used as a geothermometer provided it has been previously determined over a range of temperatures for the appropriate compounds, preferably by experiment or less reliably from theory or empirical relationships.

The total analytical error based on repeated extraction and isotopic analyses of selected samples and a laboratory standard (Bingham pyrite) is less than 0.2 per mil for sulfides and about 0.3 per mil for sulfates. The isotopic data for concentrates contaminated by another sulfide have been adjusted by means of algebraic equations using the raw analytical data and percentage estimates of mineral contamination as visually inferred.

Sulfur Isotope Data Past and Present

The first sulfur isotope analyses from the Butte District were reported by Jensen (1959) as part of a larger reconnaissance investigation of hydrothermal and magmatic sulfides from largely North American localities. He noted that unlike the broad isotopic variability for many of these deposits, that for 19 sulfide concentrates from Main Stage mineralization at Butte exhibited a relatively narrow range of $\delta^{34}S$ values near 0 per mil. This isotopic homogeneity was consistent with a single reservoir or common source for Main Stage hydrothermal fluids, as originally proposed by Sales (1912) on the basis of geologic inferences. Ames (1962) later reanalyzed a number of these samples using improved laboratory procedures and detected a weak apparent gradient of increasing

$\delta^{34}S$ values possibly related to thermal metamorphism of Main Stage sulfides as described by Sales and Meyer (1951) in Butte Quartz Monzonite immediately adjacent to post-ore rhyolite dikes. Field (1966) contributed two additional analyses for Main Stage sulfides from the Berkeley Pit at Butte in a tabular and graphical summary of available sulfur isotope data for porphyry-type deposits of the Western U.S. The total isotopic variation of 106 sulfides from 11 deposits was relatively narrow and ranged from -6.3 to +4.1 per mil, and the isotopic composition of 21 sulfides from Butte ranged from –3.6 to +4.1 per mil.

Lange and Cheney (1971) performed an extensive district-wide sulfur isotope investigation of Butte based on 123 concentrates of different sulfide minerals extracted from samples of the Deep Level, Central, Intermediate, and Peripheral Zones. Although most were representative of Main Stage mineralization, one pyrite and four molybdenite concentrates belonged to the earlier pre-Main Stage. Significant among their conclusions was the documentation of primary fractionation between different sulfide minerals: a theoretical concept initially proposed by Sakai (1968) and subsequently considered more fully by Bachinski (1969) using a wider array of mineral thermochemical data and, in part, the Butte isotopic data of Jensen (1959) and Ames (1962). Lange and Cheney (1971) noted isotopic similarity between sulfides of the east-west striking and northwest striking vein systems that was consistent with the geologic evidence supporting near-contemporaneity of Main Stage mineralization and the previously inferred isotopic homogeneity of the Butte hydrothermal system. They also observed an outward increase in the $\delta^{34}S$ per mil values of the sulfides, especially pyrite, which they ascribed to increasing pH rather than to decreasing temperature as the fluids moved upward and outward from the Central Zone. With these data, the range of $\delta^{34}S$ values for 144 sulfide concentrates from the Butte District was increased slightly from –3.7 to +4.8 per mil and with a mean of about +0.4 per mil.

Field and others (1983) published the results of a preliminary sulfur isotope survey of $\delta^{34}S$ values for associated sulfate-sulfide mineral assemblages in porphyry-type deposits. Their data included three samples of pre-Main Stage anhydrite-pyrite veinlets from the 4200 level of the Steward Mine at Butte. The anhydrites were found to be appreciably enriched in $\delta^{34}S$ (+14.1 to +18.2 ‰) relative to coexisting pyrites (+2.7 to +3.0 ‰), as is consistent with fractionation theory, and the mineral pairs provided reasonable isotopic temperatures approximating the range of 400° to 500°C based on available fractionation factors.

Lange and Krouse (1984) undertook a detailed isotopic study of 69 sulfide concentrates of mostly pyrite collected from a restricted area of a single N-W vein and adjacent wall rock within the Intermediate Zone on the 3200 level of the Steward Mine. Although the $\delta^{34}S$ values of all sulfides were within the previously established range for the district, those for 58 concentrates of vein, veinlet, and disseminated textural forms of pyrite exhibited a particularly narrow spread from +1.3 to +3.9 per mil. Within this narrow range, the authors found that pyrite disseminated in wall rock was slightly depleted in ^{34}S relative to nearby vein pyrite, and that this depletion apparently was progressive with increasing distance from the vein. Although they considered fractionation effects related to diffusion or changing pH-Eh conditions of the hydrothermal fluid to account for the observed isotopic gradients, their favored mechanism was that of mixing through the over-printing of relatively ^{34}S-enriched Main Stage vein mineralization on an earlier and relatively ^{34}S-depleted pre-Main Stage disseminated mineralization.

As previously noted, our work is concerned almost exclusively with pre-Main Stage mineralization, although we will refer to previous investigations where appropriate. A single analysis of whole-rock magmatic sulfur on a sample of unaltered Butte Quartz Monzonite provided a $\delta^{34}S$ value of -0.4 per mil. The mineralogical source of the sulfur

is uncertain because of the small concentration (14 ppm S) in the sample. Perhaps it is present as sulfate-sulfur as a trace to minor constituent of apatite, as described by Streck and Dilles (1998) and by Sha and Chappell (1999), or as likely as sulfide-sulfur that is sparingly dispersed as magmatic sulfides that are a common component of most igneous rocks according to Newhouse (1936), Sakai and others (1982), Field and others (1984), and Borrok and others (1999). The remainder of our data are based on sulfur-bearing mineral concentrates separated from samples collected from deep drill core. Quartz veinlets containing the sulfides molybdenite and (or) pyrite and (or) chalcopyrite associated with K-silicate alteration were obtained from drill holes DDH 2 and 10 that penetrated the Pittsmont Dome on the east side of the district (Figs. 1 and 2a &b). Anhydrite was found only in DDH 10, and abundantly associated with these sulfides. However, also included in our discussion of these sulfate-sulfide assemblages are three anhydrite-pyrite pairs from quartz veinlets with the Early Dark Micaceous alteration, from the western Anaconda Dome in the central part of the district (4200 Level of Steward Mine). The data for these samples have been graphically summarized previously (Field and others, 1983), but they have neither been discussed in detail nor in the context of Butte geology and mineralization.

Finally, we also present data primarily for the sulfide pyrite contained in drill holes DDH 1, 1a, 3, 5, 7, and 11. The pyrite is present with quartz in veinlets and as dissemination in wall rock and is associated with an enormous hydrothermal plume of gray-sericitic alteration in the bottom of and below the southeast part of the Berkeley Pit between the Pittsmont and Anaconda Domes (Figs. 2a &b). Cursory sample descriptions and $\delta^{34}S$ per mil values are given in Table 8 for sulfate and sulfide minerals of the Early K-silicate assemblage and in Table 9 for pyrites of the various gray-sericitic assemblages. This work has increased the data base for Butte hydrothermal sulfates (all anhydrite) from three to 22 $\delta^{34}S$ values, which now range from +9.8 to +18.2 per mil

Table 8. Sulfur Isotope Data for Sulfate and Sulfides Minerals of the pre-Main Stage K-silicate Alteration Assemblage at Butte, Montana

Sample	Description	$\delta^{34}S$ ‰ Sulfide	$\delta^{34}S$ ‰ Anh
11172-1743	BQM; Anh veinlet and K-silicate alteration, no Py & Ccp		11.6
11172-2262.5	BQM; Qtz-Py-Anh veinlet with inner sericite alteration selvage and outer SBb selvage , Ccp replaces biotite	Py 3.4	11.2
11172-2264.5	BQM; Qtz-Py-Anh veinlet with inner sericite alteration selvage and outer SBb selvage, Ccp replaces biotite	Py 2.8	12.2
11172-2276.5	BQM; Qtz-Bi-Anh veinlet with an EDM selvage. Py (Ccp) replaces Bi	Py 3.4	11.9
11172-2424.4	Aplite; Qtz-Py-Anh veinlet with sericite alteration halo	Py 2.4	12.3
11172-2460.5	BQM; Qtz-Anh (4:1) & Qtz-Py (20:1) veinlets, no Ccp	Py 0.5	9.8
11172-2749	Biotite breccia; Irregular green biotite veinlet with abundant anh and Mo, very little Py and Ccp	Mo 4.1	12.1
11172-2948	BQM; Qtz-Anh-Mo veinlet, a little Py and Ccp	Mo 4.0	12.5
11172-3158	BQM; Qtz-Anh-Mo-Ccp veinlet, a little Py in the K-silicate alteration selvage	Mo 4.7 Ccp 2.0	12.7
11172-3252.5	BQM; pure Anh veinlet, a little disseminated Py and Ccp in the K-silicate alteration selvage	Py 2.9	12.3
11172-3429.5	BQM; Qtz-Kspar-Anh-Ccp veinlet	Ccp 0.7	12.7
11172-3505.5	Green biotite (and Muscvite) veinlets with K-feldspar and Anh		12.9
11172-3871	BQM; Qtz-Anh-Mo veinlet, minor Py and Ccp in the K-silicate zone	Mo 4.4 Py 3.4	12.3
11172-3874	BQM; Qtz-Py-Ccp & Qtz-Py-Ccp-Anh veinlets, Some Anh and disseminated Py and Ccp in the K-silicate alteration zone	Py 3.4 Ccp 2.3	12.7
11172-3886.5	BQM; Qtz-Anh-Mo veinlet, minor Py and Ccp in the K-silicate alteration zone	Mo 3.0 Ccp 1.6	12.6
11172-3907.5	BQM; Qtz-Py-Ccp-Anh & Qtz-Bi-Py-Anh veinlets, a little Anh and disseminated Py in the K-silicate alteration zone	Py 2.9 Ccp 1.5	12.8
11172-3920	BQM; Qtz-Ccp-Anh veinlet	Ccp 1.3	11.8
11172-4208	>5cm Anh-Mo veinlet with a little Py and Ccp	Ccp 2.3	12.6
11172-4245	Aplite & BQM(?); Whole rock is made of feldspar, quartz, and Anh, a little Mo, Ccp; no Py	Mo 4.1 Ccp 3.0	12.6
11135-3481	BQM; EDM veinlet with EDM alteration selvage disseminated Py and Ccp in the alteration selvage	Py 3.1 Ccp 2.1	
11135-3586	Biotite breccia; biotite crackles, EDM veinlets with EDM selvages disseminated Py and Ccp in the alteration selvage	Py 1.6 Ccp 0.4	
10772-31	BQM; Qtz-Py-Ccp veinlet with PGS alteration selvage disseminated Py and Ccp in the alteration selvage	Py 1.7 Ccp 0.5	
10778-4	BQM; Qtz-Py-Ccp veinlet with PGS alteration selvage disseminated Py and Ccp in the alteration selvage	Py 1.9 Ccp -0.1	
10759-336	Qtz-Py-Ccp veinlet with DGS alteration selvage disseminated Py and Ccp in the alteration selvage	Py 0.6 Ccp 1.0	
10854-643	Qtz-Py veinlet with DGS alteration selvage	Py 0.4	

Abbreviations as in Table 2 & 3; BQM: Butte Quartz Monzonite;
Note: value in parenthese (20:1) gives modal volumetric ratio of two minerals

Table 9. Sulfur Isotope Data for Pyrite in Quartz-Pyrite Veinlets of the Grey Sericite Assemblage at Butte, Montana

Sample	Description	$\delta^{34}S$ ‰ (Py)
10969-1227	Qtz-Py (3:2) veinlet with successive alteration envelops of grey sericite (1cm wide), SBr (1cm), and white clay.	2.7
10969-2251	Py-Qtz veinlets with minor Mo in grey sericite alteration; clay occurs in feldspar sites	2.3
10969-2627	Py-Qtz-Ccp (4:1:tr) veinlet with grey sericite selvage.	2.3
11052-2851	PyQtz veinlet cut by barren Qtz & Qtz-Py-Mo veinlets with white sericite selvage (4 mm wide) and grey sericite selvage.	2.7
10969-5452	Py-Qtz veinlet with minor hematite? with grey sericite selvage.	2.4
10969-5618	Abundantly vuggy Py-Qz veinlets with GPGS and SBr alteration selvages	2.2
10969-6448	Barren Qtz veinlets cut by Qtz-Py veinlets with grey sericite selvages	2.4
11052-5532	Vuggy PyQtz veinlets in GPGS(?) alteration	3.4
11052-6639	Barren Qtz veinlet & vuggy PyQtz veinlets with GPGS alteration	2.0
11052-7037	Barren Qtz & vuggy Py-Qtz & Qtz-Mo (one sided Mo)-vuggy Py veinlets with GPGS alteration	2.8
11052-7083	Barren Qtz veinlets with apparent advanced argillic alteration (topaz & CaF2 noted in drill log by Page?)	4.3
11052-7285	Barren Qtz & Py-Qtz veinlets with GPGS alteration	2.6
11052-7369	Py-Qtz veinlet with grey sericite and light green sericite selvages; and Qtz-Mo veinlet reopened by Py-Qtz veinlets	3.8
11052-7522	Barren Qtz veinlets in Aplite with late vuggy Py-Qtz veinlets with sericite alteration	2.6
11148-888	Py-Qtz (9:1) veinlet with 3 cm wide grey sericite and SBr alteration selvages, and weak argillic alteration (?)	3.0
11148-1140	Py-Qtz veinlet with grey sericite and SBr selvages;	2.7
11166-5885.5	Qtz veinlet with tr. Mo, vuggy Py, and vuggy Qtz-Py veinlets with sericite alteration	2.9
11170-864.5	Vuggy Py-Qtz (9:1) veinlet with grey sericite and weak argillic selvages.	3.5
11170-1767	Py-Qtz (7:3) veinlets with grey sericite alteration	2.8
11170-1790	Py-Qtz veinlets with grey sericite alteration	3.7
11170-2423	Py-Qtz (4:1) veinlets with grey sericite alteration	2.1
11170-4871.5	Late Py-Qtz (9:1) veinlets with grey sericite selvage (2 cm wide) cutting barren Qtz veinlet	2.2
11170-4936	Vuggy Py-Qtz (7:3) veinlet with inner light green sericite and outer grey sericite selvages cutting Qtz-Mo veinlet	1.7
11170-5333	Vuggy Py-Qtz-hematite(?) veinlet with 6 mm wide inner grey sericite and outer SBr selvages	1.9
11185-1595	Py-Qtz (1:9) with trace Bn and En & Py-Qtz(2:8) veinlets with grey sericite, SBr selvages, and green argillic alteration	3.1

Abbreviations as in Table 2; GPGS: Greyish pale green sericite

Note: Value in parentheses (1:9) gives volumetric ratio of preceding minerals

with a mean of +12.9 per mil. The data base for Butte sulfides now consists of 276 analyses that range from –3.7 to +4.8 per mil, unchanged from the earlier study by Lange and Cheney (1971), but the mean value has now increased to about +1.4 per mil caused by the preponderance of pyrite analyses undertaken by Lange and Krouse (1984) and this investigation.

A graphical summary of all sulfur isotope analyses available to date is portrayed in Figure 21. The data are listed vertically from bottom to top with respect to minerals contained in specific zones and they are given in general paragenetic order from oldest to youngest, in decreasing order of depth, and in probable diminishing order of temperature and pressure of mineral deposition. Included with the K-silicate assemblage are the $\delta^{34}S$ values of four molybdenites and one pyrite previously reported by Lange and Cheney (1971). The principal feature depicted by the illustration is the narrow distribution of $\delta^{34}S$ values for sulfides about the 0 per mil value for meteoritic sulfur and the obvious ^{34}S enrichment of the sulfates relative to all sulfides. Less evident is the subtle ^{34}S enrichment of molybdenite with respect to pyrite and of these two sulfides with respect to all others. These and other features and related interpretations will be considered in the sections that follow.

Discussion of the Data

A more detailed portrayal of the sulfur isotope data for pre-Main Stage mineralization is provided in Figures 22 and 23, which represent the majority of $\delta^{34}S$ values obtained for minerals common to the K-silicate and gray-sericitic assemblages, respectively. Sampling was purposefully selective and directed towards those diamond drill holes that were likely to provide the most information. For example, DDH 10 near the south end of the Continental Pit was sampled extensively because alteration of the Butte Quartz Monzonite host was restricted almost entirely to the K-silicate assemblage,

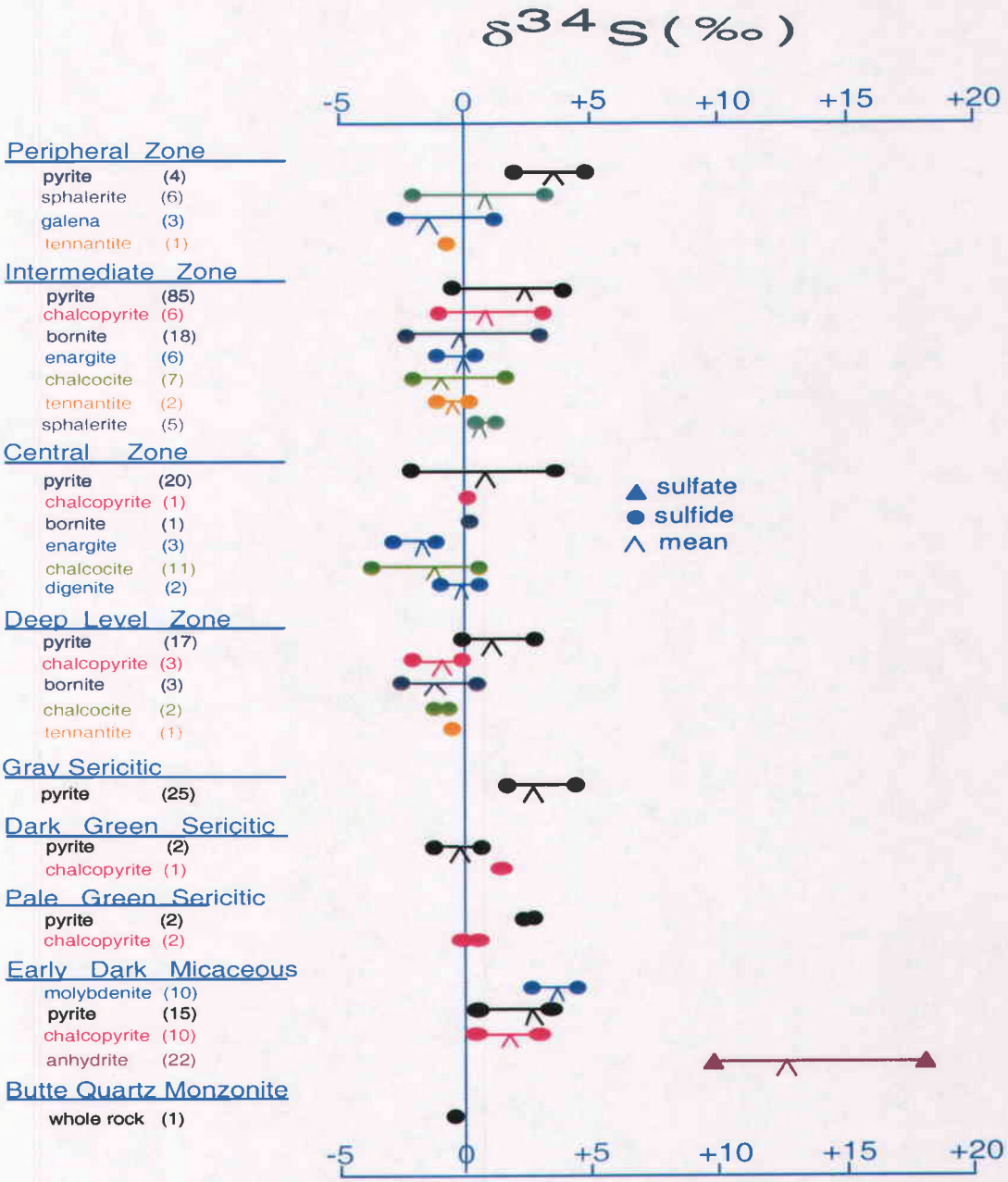

Figure 21. Summary of sulfur isotopic compositions from Butte district.

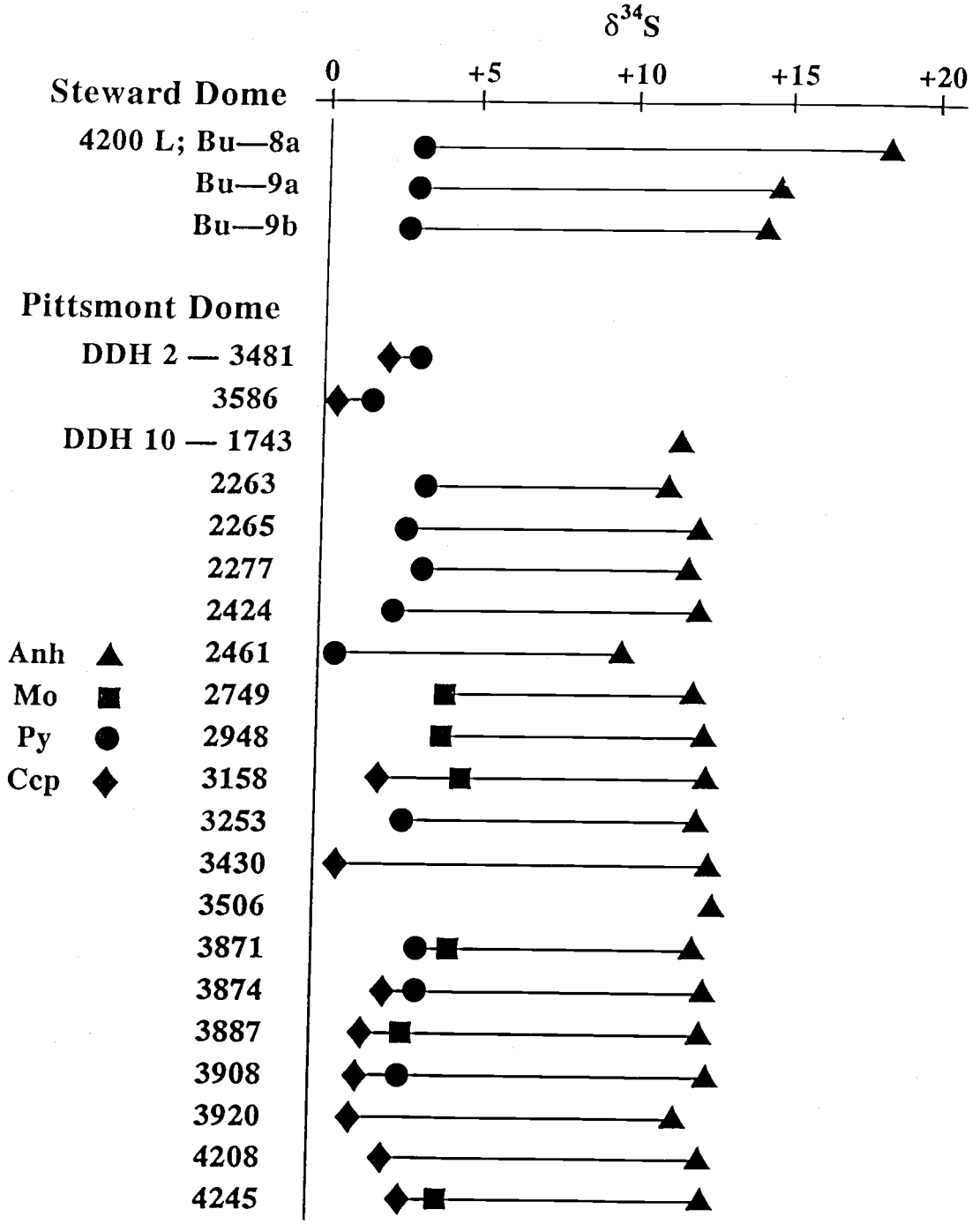

Figure 22. Sulfur isotope compositions of sulfates and sulfides from pre-Main Stage K-silicate alteration assemblage.

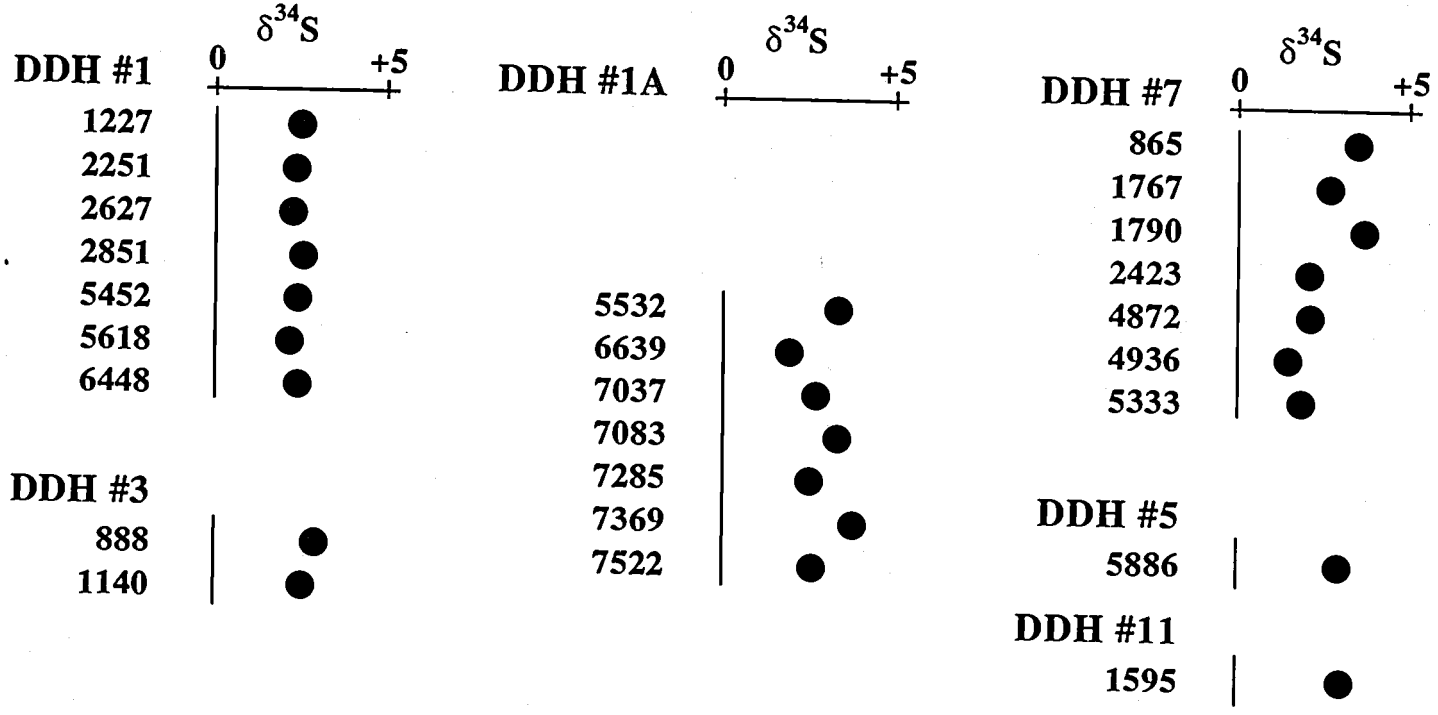

Figure 23. Sulfur isotope compositions of pyrite from gray sericite veinlets.

mineralization was represented by a characteristic suite of porphyry-type sulfides in association with the sulfate anhydrite, and with both alteration and mineralization extending over a significant vertical interval (about 760 m) and depth as a consequence of later structural displacement upward of about 1,500 meters along the nearby Continental Fault to the west (Figs. 1 and 2b). Similarly, DDH 1 and its subsurface deflection (DDH 1A) at depth provided a lengthy vertical (about 1,591 m) and sub-horizontal (about 607 m) intersection through the central gray-sericitic plume of hydrothermal alteration. Accordingly, rock samples from each of these drill holes, and the mineral components therein, are considered to be representative of a hydrothermal environment in which the chemical and physical conditions did not vary appreciably. Perhaps of equal or more importance, the "container" or host Butte Quartz Monzonite, was initially of homogeneous composition and with subsequent changes a function of the imposed hydrothermal environment. As a general approximation, sulfur-bearing minerals of the K-silicate assemblage (DDH 2 and 10, and Anaconda Dome; Fig. 22) were deposited in a hydrothermal system having a higher pH, and temperature and lower oxygen and sulfur fugacity than those of the gray-sericitic assemblage (DDH 1, 1A, 3, 5, 7, and 11; Fig. 23).

The 30 sulfide concentrates representative of the K-silicate assemblage from the Pittsmont and Anaconda Domes exhibit a particularly narrow range of $\delta^{34}S$ values (from +0.4 to +4.7 ‰; see Table. 8 and Fig. 22). Additionally, the ranges for individual sulfide mineral species are more restricted: molybdenite (6, from +3.0 to +4.7 ‰); pyrite (14, from +0.5 to +3.4 ‰); and chalcopyrite (10, +0.4 to +3.0 ‰). The data reported by Lange and Cheney (1971) for one pyrite and four molybdenite concentrates of the Early Dark Micaceous assemblage are within or near these ranges (pyrite, +1.7 ‰, and molybdenite, +2.6 to +3.4 ‰). The $\delta^{34}S$ values of four pyrite concentrates extracted from four samples from the dark green sericite and pale green sericite

assemblage (Table. 8) range from +0.4 to +1.9 per mil, and thus, fully brackets that of pyrite (+0.5 to +3.4 ‰) in the K-silicate assemblage. However, there remains some uncertainty as to the paragenetic position of these sericitic alteration subtypes to the mineralization sequence at Butte, and three of the four samples contain chalcopyrite (-0.1 to +1.0 ‰). These sericitic alteration subtypes may perhaps represent a transitional event between the principal pre-Main Stage assemblages (Reed, 1979).

The $\delta^{34}S$ values for 22 anhydrite concentrates associated with the K-silicate assemblage range from +9.8 to +18.2 per mil and all are significantly enriched in ^{34}S relative to their associated sulfides (Table. 8 and Fig. 22). Nonetheless, anhydrite from the Anaconda Dome (3, from +14.1 to +18.2 ‰) display a moderately higher ^{34}S enrichment and a slightly larger range than their counterparts from the Pittsmont Dome (19, from +9.8 to +12.9 ‰, but 18, from +11.6 to +12.9 ‰).

Pyrite is abundantly and almost exclusively the only sulfide and sulfur-bearing mineral found associated with the gray-sericitic assemblage, which is best developed in the large hydrothermal plume situated between the Pittsmont and Anaconda Domes (Figs. 2a &b). The $\delta^{34}S$ values for 25 concentrates taken from samples of drill core (DDH 1, 1A, 7) from within this plume and from its eastern flank (DDH 3, 5, 11) are listed in Table 9 and graphically portrayed in Figure 23. Again, the values from this suite range narrowly from +1.7 to +4.3 per mil, and they overlap and extend the ^{34}S-enriched end of the range for pyrite (+0.5 to +3.4 ‰) of the K-silicate assemblage.

Isotopic Equilibrium and Temperature Estimates

Previously, it was noted that the $\delta^{34}S$ values of the anhydrites were invariably heavier than those of associated or coexisting sulfides (see Table. 8 and Fig. 22). Moreover, and although there is some overlap in the ranges of $\delta^{34}S$ values between groups of specific sulfide minerals, without exception in samples that contain sulfide

mineral pairs, molybdenite is enriched in ^{34}S relative to associated pyrite and pyrite in turn is similarly enriched in ^{34}S relative to associated chalcopyrite. In addition, two of three samples representing subtypes of the gray-sericitic assemblage also contain ^{34}S-enriched pyrite relative to associated chalcopyrite. These isotopic trends are not fortuitous as they have been observed elsewhere, including at other porphyry Cu-Mo deposits, and they are consistent with isotope equilibrium theory and sulfur isotope fractionation trends determined from theoretical, experimental, and empirical relationships that have been investigated and summarized by Ohmoto and Rye (1979), Ohmoto and Lasaga (1982), Ohmoto and Goldhaber (1997), and references cited therein. These investigations, with reference to minerals relevant to this study, have documented that sulfates are most enriched in ^{34}S and that progressive ^{34}S depletion follows in the mineralogical order molybdenite, pyrite, sphalerite, chalcopyrite, bornite, covellite, galena, and chalcocite (Ohmoto and Rye, 1979), and as was originally postulated from theory by Sakai (1968) and Bachinski (1969).

Provided it is assumed that the observed isotopic differences between the Butte sulfates and sulfides represent the effects of primary equilibrium isotope exchange reactions at the time of mineral deposition, then isotopic temperature estimates may be determined from delta (Δ) values for various mineral pairs that have been calculated from the $\delta^{34}S$ per mil data in Table 8 using Equation 3. The delta values are then entered into fractionation equations for the appropriate mineral pairs to obtain the temperature estimates. Fractionation equations for sulfate-H_2S and sulfide-H_2S isotopic equilibria given by Ohmoto and Lasaga (1982) and Ohmoto and Rye (1979), respectively, were combined as appropriate to calculate temperature estimates for various sulfate-sulfide mineral pairs contained in samples of the K-silicate assemblage from the Anaconda and Pittsmont Domes. The results are listed in Table 10 for anhydrite-molybdenite (6), anhydrite-pyrite (12), and anhydrite-chalcopyrite pairs (8). Delta values for the 26

sulfate-sulfide pairs range from 7.8 to 15.2, and those for the 23 mineral pairs of the Pittsmont Dome range from 7.8 to 12.0. Although the overall range of calculated temperatures for the Pittsmont Dome is from 480° to 630°C, the range within a specific mineral pair group approximates 100°C or less. There is fair to moderate consistency in temperatures provided by two mineral pairs from the same sample, but nonetheless, it is clear from such comparisons and the means and ranges, that the anhydrite-molybdenite pairs consistently provide the highest temperatures and the anhydrite-chalcopyrite pairs the lowest. The reason for such consistent temperature differences between different mineral pairs, and yet among largely coexisting minerals, is uncertain. Possible, but speculative, explanations might include: (1) subtle paragenetic differences in mineral deposition; (2) systematic analytical errors; (3) small to moderately large errors in the fractionation equations for sulfide-H_2S equilibria; and (4) isotopic disequilibrium and(or) retrograde effects. This problem of relatively small temperature variations between the different anhydrite-sulfide pairs is reexamined below. Regardless of potential shortcomings, the isotopic temperature estimates (about 500° to 650°C) obtained from the three anhydrite-sulfide mineral pair systems are in reasonable agreement with fluid inclusion homogenization temperatures ranging from 350° to 390°C (Roberts,1975) and from 320° to 390°C (Rusk et al., 1999) provided a pressure correction of about 1.7 kilobars is applied to account for depth at the time of mineralization of the K-silicate assemblage.

Temperatures for three anhydrite-pyrite pairs from the Anaconda Dome previously reported graphically by Field et al. (1983) are listed above data for the Pittsmont Dome in Table 10. Delta values for these mineral pairs (11.4 to 15.2 ‰) are larger than those for equivalent mineral pairs from the Pittsmont Dome (7.8 to 9.9 ‰), and the calculated temperatures are proportionately lower and range from 370° to 475°C. There are at least three possible explanations for this apparent temperature difference. First, samples

Table 10. Sulfur Isotopic Temperature Estimates of Sulfate-Sulfide Mineral Pairs Calculated from Delta Values Using the Fractionation Equations of Ohmoto and Rye (1979) and Ohmoto and Lasaga (1982).

	$\Delta_{Anh\text{-}Mo}$	T°C	$\Delta_{Anh\text{-}Py}$	T°C	$\Delta_{Anh\text{-}Ccp}$	T°C
Steward Dome (Mine)						
Bu-8a (4200 L)			15.2	370		
Bu-9a (4200 L)			11.8	460		
Bu-9b (4200 L)			11.4	475		
Mean			**12.8** (3)	**435**		
Range			**11.4-15.2**	**370-475**		
Pittsmont Dome (DDH 10)						
2262.5			7.8	640		
2264.5			9.4	555		
2276.5			8.5	605		
2424.4			9.9	535		
2460.5			9.3	560		
2749.0	8.0	625				
2948.0	8.5	595				
3158.0	8.0	625			10.7	530
3252.5			9.4	555		
3429.5					12.0	480
3871.0	7.9	630	8.9	580		
3874.0			9.3	560	10.4	540
3886.5	9.6	545			11.0	515
3907.5			9.9	535	11.3	505
3920.0					10.5	535
4208.0					10.3	545
4245.0	8.5	595			9.6	575
Mean	**8.4** (6)	**605**	**9.2** (9)	**570**	**10.7** (8)	**530**
Range	**7.9-9.6**	**545-630**	**7.8-9.9**	**535-640**	**9.6-12.0**	**480-575**

collected from the 4200 level of the Steward Mine are from near the top of the Anaconda Dome, whereas those from drill core of DDH 10 represent a deeper and more continuous vertical sampling within the Pittsmont Dome. Thus, the apparent difference in domal depths might favor higher temperatures in the Pittsmont Dome. Second, the 4200 level of the Steward mine is at an altitude of 573 meters and the collar of DDH 10 is at 1,010 meters. Taking into account the sampling interval of from 690 to 1294 meters in the drill hole and as much as 1,500 meters of upward post-mineralization displacement along the Continental Fault, the restored sample interval ranges from about -405 to -1,006 meters (–1,330 to –3,300 ft.) below sea level. Thus, the Pittsmont Dome samples are both topographically and geologically below those of the Anaconda Dome, which might favor higher temperatures in the former. Third, all samples collected from the Anaconda and Pittsmont Domes are intimately associated with the pre-Main Stage K-silicate assemblage. However, the anhydrite-pyrite veinlet from sample Bu-8a of the Anaconda Dome is distinguished by having a quartz-sericite selvage between veinlet and potassium silicate altered Butte Quartz Monzonite host. The quartz-sericite alteration presumably represents a later and lower temperature assemblage than does the K-silicate, and it may not be fortuitous that the anhydrite-pyrite pair from this sample provided the lowest isotopic temperature (370°C, Table. 10) of any from the suite. However, the relationship of this thin (< 2 cm) alteration selvage to either the pre-Main Stage gray-sericitic plume or to the later Main Stage quartz-sericite alteration is unknown, although both are nearby.

The sulfate-sulfide assemblages serve as good evidence for isotopic equilibrium, and especially the isotopic temperature estimates derived therefrom, and it was previously noted that the progressive relative ^{34}S depletion in the sulfide sequence from molybdenite through pyrite to chalcopyrite (Table 8 and Fig. 22) suggests that at least partial equilibrium prevailed between the different sulfide minerals. Moreover, the

sulfide-sulfide mineral pairs could provide additional isotopic temperature estimates, assuming equilibrium, and they might possibly offer insight into the problem of consistently decreasing temperatures calculated from anhydrite-molybdenite, anhydrite-pyrite, and anhydrite–chalcopyrite mineral pairs. Because the sulfide-sulfide pairs from the K-silicate sample suite are relatively few in number (11) and provided some unexpected results, the relevant data for all potentially useful sulfide-sulfide mineral pairs from past and present studies of the Butte District are summarized in Table 11. Data for each sample are listed by sulfide mineral pair, mineral assemblage or zone, sample number, investigator, delta value, and calculated temperature. The list contains 71 sulfide-sulfide pairs for which the $\delta^{34}S$ per mil values have been published, but it excludes several potential mineral pairs involving enargite or tennantite for which reliable fractionation data are unavailable.

A cursory inspection of Table 11 reveals a moderate number (6) of impossible delta values (zero to negative) and a larger number of delta values yielding improbably high (9; >650°C) or low (19; <200°C) temperatures. These problems are prevalent in most of the sulfide-sulfide systems for which there are a sufficient number of samples, and regardless of mineralization zone, but they are particularly evident among all four molybdenite- pyrite pairs (-176° to -77° C), five of six pyrite-sphalerite pairs (4° to 190°C), and the one sphalerite-galena pair (1,078°C). Possible causes of apparent disequilibrium and unreasonable temperatures among these sulfide pairs may be lack of contemporaneity, or problems with or in the application of the sulfide-sulfide fractionation equations. Pyrite has a broad zonal and paragenetic distribution throughout the Butte District, as does sphalerite to a lesser extent, and some pre-Main Stage quartz-molybdenite veinlets have been refractured and mineralized by later Main Stage pyrite. In addition, the molybdenite-pyrite fractionation equation is probably inexact because it has been derived only partly by experimentation (Ohmoto and Rye, 1979), which may

Table 11. Sulfur Isotopic Temperature Estimates of Sulfide-Sulfide Mineral Pairs Calculated from Delta Values Using the Fractionation Equations of Ohmoto and Rye (1979) and Including all Published Analyses of Samples from the Butte District. [assemblage/ mineralization zone (EDM), Early Dark Micaceous; (GS), Gray Sericite; (DLZ), Deep Level Zone; (CZ), Central Zone; (IZ), Intermediate Zone; (PZ), Peripheral Zone; and subscripts (1) Jensen, 1959; (2) Ames, 1962; (3) Lange and Cheney, 1971; (4) Lange and Krouse, 1984; and (5) this study].

Sulfide Pair	Sample	Delta	T°C
Δ Molybdenite-Pyrite:			
EDM	11172-3871.0 (5)	1.0	-50
CZ	4248#9 (3)	5.3	-175
CZ	4382#3 (3)	1.3	-75
IZ	7134#1 (3)	3.5	-155
Δ Molybdenite-Chalcopyrite:			
EDM	11172-3158.0 (5)	2.7	155
EDM	11172-3886.5 (5)	1.4	325
EDM	11172-4245.0 (5)	1.1	400
Δ Pyrite-Chalcopyrite:			
EDM	11172-3874.0 (5)	1.1	365
EDM	11172-3907.5 (5)	1.4	295
EDM	11135-3481.0 (5)	1.0	400
EDM	11135-3586.0 (5)	1.2	340
GS	10759-336.0 (5)	-0.5	diseq
GS	10772-31.0 (5)	1.2	340
GS	10778-4.0 (5)	2.0	200
DLZ	7297#19B (3)	0.3	950
DLZ	7297#20B (3)	2.8	130
DLZ	6350#4 (3)	0.5	675
IZ	D2-Bu129 (1,2)	0.3	950
IZ	71334#19 (3)	2.8	130
IZ	6564#4 (3)	1.9	215
IZ	8911I (4)	2.5	150
Δ Pyrite-Bornite:			
DLZ	6869#2 (3)	1.8	330
DLZ	6869#4 (3)	0.3	1,200

Sulfide Pair	Sample	Delta	T°C
Δ Pyrite-Bornite: (continued)			
DLZ	6869#4 (3)	0.3	1,200
DLZ	7297#19B (3)	2.7	220
CZ	7607 (3)	1.2	465
IZ	7644 (3)	0	diseq
IZ	7645#2 (3)	2.9	200
IZ	7646#2 (3)	1.0	535
IZ	7134#10 (3)	1.0	535
IZ	7134#19 (3)	3.7	145
IZ	6564#3 (3)	2.9	200
IZ	6564#4 (3)	2.6	225
IZ	6337#1 (3)	-1.9	diseq
IZ	6337#2 (3)	3.0	190
IZ	6337#6 (3)	0.8	630
IZ	6585#7 (3)	2.8	210
IZ	B.64.3 (3)	2.9	200
IZ	8911-dv (4)	3.5	160
IZ	8911-g (4)	3.0	190
IZ	8914-b (4)	5.1	85
IZ	8914-c (4)	2.8	210
Δ Pyrite-Chalcocite:			
DLZ	6869#4 (3)	2.2	450
DLZ	7634#1 (3)	2.7	380
CZ	Dl-Bu52 (1)	0.4	1,425
CZ	7606 (3)	5.0	205
CZ	7607 (3)	0.9	855
CZ	7648#1 (3)	-0.6	diseq
CZ	7649 (3)	-0.3	diseq
CZ	7650#1 (3)	4.3	245
CZ	7651#1 (3)	3.2	325
CZ	7051#7 (3)	2.9	355
CZ	7051#7A (3)	3.9	270

TABLE 11 (continued).

Sulfide Pair	Sample	Delta	T°C
Δ Pyrite-Chalcocite: (continued)			
CZ	3090 (3)	-1.0	diseq
IZ	D2-Bu130 (1,2)	0.9	855
IZ	7644 (3)	2.0	485
IZ	7645#2 (3)	4.9	210
IZ	7646#2 (3)	1.6	575
IZ	7134#10 (3)	1.8	525
IZ	6337#2 (3)	4.0	265
IZ	6337#6 (3)	2.7	380
Δ Pyrite-Sphalerite:			
IZ	8910-a (4)	2.7	60
IZ	8911-dv (4)	2.0	115
PZ	X-420 (3)	1.6	160
PZ	7602 (3)	1.4	190
PZ	7641 (3)	1.2	225
PZ	7642 (3)	3.9	4
Δ Pyrite-Galena:			
PZ	7641 (3)	1.6	529
Δ Sphalerite-Galena:			
PZ	7641 (3)	0.4	1,080
Δ Chalcopyrite-Bornite:			
IZ	D2-Bu128 (1,2)	0.2	725
IZ	7134#19 (3)	0.9	200
IZ	6564#4 (3)	0.7	260

explain the consistently low (negative) isotopic temperatures. Moreover, the A factor of this equation (Ohmoto and Rye, 1979; and Ohmoto and Goldhaber, 1997) is exceedingly small (0.05) in contrast to most other common sulfur-bearing mineral pair systems (such as molybdenum-chalcopyrite, 0.5; anhydrite-molybdenite, 6.01), and thus calculated temperatures may also be hugely perturbed by analytical errors.

More "reasonable" isotopic temperature estimates were calculated for some, but not all, of the molybdenite-chalcopyrite pairs (2 of 3; range 325° to 400°C; mean 365°C), pyrite-chalcopyrite pairs (7 of 14; range 215° to 400°C; mean 305°C), pyrite-bornite pairs (12 of 20; range 200° to 630°C; mean 330°C), and pyrite-chalcocite pairs (13 of 19; range 205° to 575° C; mean 385°C). Disregarding the extensive range of temperatures among these selected values, the mean temperature of all 34 reasonable sulfide-sulfide pairs representing both pre-Main Stage and Main Stage mineralization is 350°C, and which is identical to the mean temperature of four pre-Main Stage pyrite-chalcopyrite pairs (range 295° to 400°C).

The sulfides from two of these pairs were previously included as part of the anhydrite-pyrite and anhydrite-chalcopyrite pairs from which substantially higher temperatures were calculated (505° to 565°C; see Table 10). Thus, pre-Main Stage sulfide-sulfide mineral pair temperatures are similar to those of their later Main Stage counterparts, and they are significantly lower by 150°C or more than their related sulfate-sulfide temperatures. These results suggest that the most reliable temperatures are provided by the sulfate-sulfide mineral pairs. Most likely this is because of the large A factors that characterize the fractionation equations involving sulfate-sulfide equilibria (Ohmoto and Rye, 1979; Ohmoto and Goldhaber, 1997), which tend to minimize the potentially adverse effects of analytical error, equation error, minor disequilibrium, and non-contemporaneity. However, these results do not explain the temperature similarity between pre-Main Stage and Main Stage sulfide-sulfide equilibria, and the small but

progressively diminishing temperatures given by anhydrite-molybdenite, -pyrite, and –chalcopyrite mineral pairs. These differences may relate to retrograde equilibrium during the waning stages of hydrothermal activity. Because the strength of the metal-sulfur bonds decrease in the order molybdenite, pyrite, chalcopyrite, etc. (Sakai, 1968; Bachinski, 1969; Ohmoto and Rye, 1979), it follows that molybdenite and pyrite would be the sulfides least likely to undergo isotopic reequilibration with decreasing temperature, whereas it would be increasingly likely for sulfides in the progression sphalerite, chalcopyrite, bornite, galena, and chalcocite. These speculations warrant further study.

Isotopic Composition of Total Sulfur in The Butte Hydrothermal System

Contrary to the assumptions of many previous investigators, the pioneering studies of Sakai (1968) and Ohmoto (1972) demonstrated that the $\delta^{34}S$ per mil values for a suite of sulfide, or sulfate, minerals individually are not necessarily diagnostic of the isotopic composition of total sulfur ($\delta^{34}S_{\Sigma S}$ ‰) in a particular magmatic or hydrothermal deposit. The reason for this assertion is that because in any system containing both oxidized (SO_4^{2-} or SO_2) and reduced (H_2S) aqueous or gaseous species of sulfur, the isotopic composition of either sulfate or sulfide minerals formed therein is dependent not only on the temperature and $\delta^{34}S_{\Sigma S}$ ‰ of the system, but additionally on the mole fraction ratio of oxidized to reduced sulfur species. Moreover, this ratio is further controlled by the acidity (pH) and oxidation state (fO_2) of the system, which in turn may affect the kinds and proportions of the oxidized and reduced sulfur species (Ohmoto, 1972). The discussion that follows present three approaches taken to assess the $\delta^{34}S_{\Sigma S}$ ‰ in the Butte hydrothermal system.

A single sample of unaltered and unmineralized Butte Quartz Monzonite (Bd-1, Table 8) collected about 5 miles southeast of the Butte District was isotopically analyzed

for total sulfur using the Kiba reagent method at the Geological Survey of Japan. The sulfur content of this sample was exceedingly small (14 ppm) and provided an isotopic value of –0.4 per mil. The sulfur is presumed to be of magmatic origin, but the mineralogical source is unknown. It may be either sulfate-sulfur as a trace to minor constituent of apatite as described by Streck and Dilles (1998) and by Sha and Chappell (1999) for granitic rocks of Nevada and Australia, respectively, or sulfide-sulfur that is dispersed at low concentrations as tiny magmatic sulfides in most continental and oceanic igneous rocks according to the studies of Newhouse (1936), Sakai and others (1982), Field and others (1984), and Borrok and others (1999). The isotopic composition of this sulfur (-0.4 ‰) is suggestive of a sulfide source, and it falls within the accepted range (0 ± 3 ‰) for most magmatic sulfide values (Ohmoto and Rye, 1979). A sulfide source is entirely consistent with results of petrographic studies by Brownlow and Kurz (1979) who found up to 0.7 weight percent (average 0.01 wt. %) of disseminated and minute masses of sulfides and up to 0.3 weight percent sulfur (average 0.01 wt. %, or 100 ppm S) in unaltered phases of the Boulder Batholith. The sulfides are predominantly pyrite, although chalcopyrite and pyrrhotite or mackinawite may also be present as inclusions within pyrite and within or along the grain boundaries of oxide and silicate minerals of the host. The isotopic value for this whole rock sulfur analysis (-0.4 ‰) is also within the range of those for Butte sulfides (see Fig. 21). However, data are lacking to estimate the mole fraction ratio of oxidized to reduced sulfur in this sample, and thus, an estimate of $\delta^{34}S_{\Sigma S}$ ‰ cannot be undertaken.

The presence of sulfate (anhydrite) in paragenetically close association with sulfides (molybdenite, pyrite, and chalcopyrite) in quartz veinlets of the K-silicate assemblage provides a better isotopic means of approximating the $\delta^{34}S_{\Sigma S}$ ‰ value of the pre-Main Stage hydrothermal system at Butte. In accordance with fractionation theory and experiment, and as illustrated in Figure 22 for samples of the Pittsmont Dome, the

$\delta^{34}S_{\Sigma S}$ ‰ value for this system must occupy a position between values for the ^{34}S-enriched anhydrites (mean +12.2 ‰) and those for the relatively ^{34}S-depleted sulfides (mean +2.8 ‰). A more precise approximation requires an estimate of the SO_4^{2-}:H_2S mole fraction ratio.

Investigations and references cited by Burnham (1997), Ohmoto and Rye (1979), and Ohmoto (1986) indicate that SO_4^{2-} or SO_3 are likely to be the dominant dissolved sulfur-bearing phases of oxidized felsic magmas, in contrast to H_2S or SH^- that characterize the more reduced state of mafic magmas. With cooling and subsequent exsolution of an aqueous fluid phase from a semicrystalline felsite at submagmatic temperatures (700° or less), sulfur is partitioned as SO_2 into the fluid and undergoes hydrolysis according to the disproportionation reaction

$$4SO_2 + 4H_2O = H_2S + 3H_2SO_4 \quad (4)$$

The oxidized product, sulfuric acid, undergoes the following dissociation

$$H_2SO_4 = H^+ + HSO_4^- = 2H^+ + SO_4^{2-} \quad (5)$$

with hydrogen and bisulfate ions being the stable end products of this reaction at 400° to 650°C. Dilles and Field (1996) applied the SO_4^{2-}-H_2S and SO_2-H_2S fractionation equations of Ohmoto and Lasaga (1982) and Ohmoto and Rye (1979) to whole rock $\delta^{34}S$ per mil values of magmatic sulfides to determine the bulk $\delta^{34}S_{\Sigma S}$ ‰ in the Yerington Batholith, Nevada. The result of this calculation (+8 to +10 ‰) was remarkably similar to that (+8.5 ‰) obtained independently using a modified version of Equations 4 and 5 as follows,

$$\delta^{34}S_{\Sigma S}\text{ ‰} = 0.25\,(\delta^{34}S_{H2S}\text{ ‰}) + 0.75\,(\delta^{34}S_{SO4^{2-}}\text{ ‰}) \quad (6)$$

and substituting the $\delta^{34}S$ per mil values for hydrothermal sulfides and sulfates of the Yerington Mining District for those of H_2S and SO_4^{2-} in Equation 6. Similar calculations using the Butte data are not as consistent. The estimate of bulk $\delta^{34}S_{\Sigma S}$ ‰ using the

single whole rock analysis of magmatic sulfur (-0.4 ‰), as previously described, provides a $\delta^{34}S$ value of +4 to +6 per mil, whereas that obtained using the Pittsmont Dome sulfate and sulfide data in Equation 6 is +9.9 per mil. The cause of this discrepancy is uncertain, but is possibly the result of having an insufficient number of whole rock analyses of magmatic sulfur, or that the single analysis is not of magmatic sulfur. Alternatively, the relatively ^{34}S-depleted value of this sample does represent magmatic sulfur, but from a late batch of degassed SO_2 that had undergone fractionation by means of a Rayleigh distillation process such as proposed by Dilles and Field (1996) for similarly depleted magmatic sulfides in plutonic phases of the Yerington Batholith.

Another approach to estimating both the SO_4^{2-}: H_2S mole fraction ratios and $\delta^{34}S_{\Sigma S}$ ‰ of hydrothermal systems has been described and applied to the El Salvador porphyry Cu-Mo deposit by Field and Gustafson (1976) and to deposits elsewhere by Field and others (1983). A plot of the $\Delta^{34}S_{sulfate\text{-}sulfide}$ values versus the $\delta^{34}S$ per mil values for the sulfate and sulfide minerals of each mineral pair of a sample population may ideally form two linear and converging plots of the data. Because of the temperature dependency of isotopic fractionation, the point of convergence of these two lines extrapolated to infinitely high temperature (> 1,000°C and at $\Delta = 0$) should define the value for $\delta^{34}S_{\Sigma S}$ ‰ and the slopes of these lines should approximate the SO_4^{2-}: H_2S mole fraction ratio (Field and Gustafson, 1976) of the hydrothermal system. The reliability of this approach requires having a representative suite of coexisting (contemporaneous) sulfate-sulfide mineral pairs that were deposited over a range of temperatures, that isotopic equilibrium prevailed at the time of deposition and was retained thereafter, that the SO_4^{2-}:H_2S mole fraction ratio remained relatively constant, and that the $\delta^{34}S_{\Sigma S}$ ‰ composition of the system remained unchanged because of an infinite sulfur reservoir or lack of contamination from an isotopically distinct extraneous source (Field and Gustafson, 1976; Field and others, 1983; and further critical

discussion by Ohmoto, 1986). Isotopic equilibrium between sulfate and sulfide minerals from the Pittsmont Dome suite is favored by the assumed high temperature of the porphyry-type environment, the associated potassium silicate alteration assemblage, and the measured fractionation and calculated temperatures obtained from the isotopic data.

The distributions of delta values for 26 sulfate-sulfide mineral pairs versus the $\delta^{34}S$ per mil values for the sulfate and sulfide members of each pair are plotted on Figure 24 for samples of the K-silicate assemblage from the Pittsmont and Anaconda Domes. The three samples from the Anaconda Dome appear to represent a distinct and nearly separate population as they plot above and (or) to the right of those from the Pittsmont Dome. With the exception of one Pittsmont Dome sample (11172-2460.5; Table 8), the remaining 22 sulfate-sulfide pairs exhibit a fairly linear distribution, and the regression lines calculated for the respective delta-sulfate and delta-sulfide per mil values converge, when extrapolated to the ordinate ($\Delta = 0$), to a value of +10.9 for $\delta^{34}S_{\Sigma S}$ ‰. This value is remarkably similar to that (+9.9 ‰) calculated from Equation 6 using SO_4^{2-} and H_2S mole fractions derived from the disproportionation reaction for SO_2 hydrolysis (Eq. 4) and the mean $\delta^{34}S$ values for both anhydrites and sulfides from the Pittsmont Dome. Additionally, a comparison of the slopes of the two regression lines on Figure 24 to those given by Field and Gustafson (1976, Fig. 21) suggests mole fractions for SO_4^{2-} and H_2S of approximately 0.75 and 0.25, respectively. Not only are these mole fraction estimates in agreement with those dictated by Equation 4 and used in the calculation of $\delta^{34}S_{\Sigma S}$ ‰ with Equation 6, they are consistent with those determined from modal mineral estimates of anhydrite and sulfides by Roberts (1975; about 5 vol.% anhydrite to 2 vol.% sulfide) and Brimhall (1977; SO_4^{2-}:H_2S mole ratio of about 2 to 3). Sample 11172-2460.5, which is isotopically anomalous (Anh = +9.8 and Py = +0.5 ‰) and was omitted from calculations of the regression lines for the Pittsmont Dome samples, is potentially significant. Sulfide is present only in trace amounts and the anhydrite:pyrite

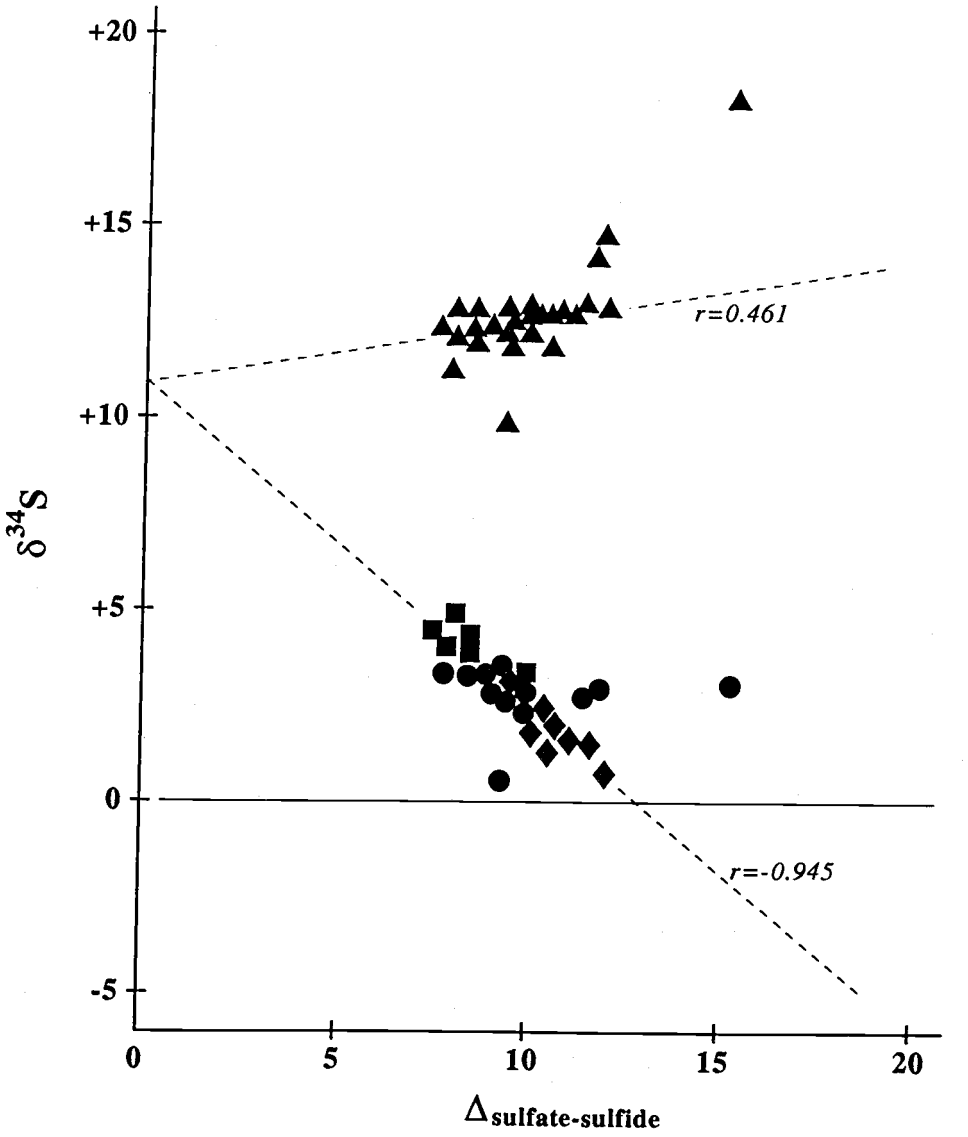

Figure 24. The delta values (Δ) of sulfate-sulfide versus $\delta^{34}S$ values.

ratio exceeds 100. If this mineral ratio is an approximation of the SO_4^{2-}:H_2S mole fraction ratio of the hydrothermal fluid from which these minerals were deposited, then the per mil value of $\delta^{34}S_{\Sigma S}$ must approximate that of the anhydrite (+9.8 ‰). It is difficult to assess this apparent agreement for these independent approximations of $\delta^{34}S_{\Sigma S}$ ‰ and mole fraction ratios. The linearity of regression lines in Figure 24 is largely a consequence of differences related to increasingly larger delta values (and decreasing temperatures), as previously noted, between anhydrite-molybdenite, anhydrite-pyrite, and anhydrite-chalcopyrite mineral pairs, but the overall range of calculated mineralization temperatures (480° to 640°C; Table 10) is not sufficiently large to provide good linear control. The reason for the discrepancy between the values of +9.9 to +10.9, and +9.8 per mil for $\delta^{34}S_{\Sigma S}$, as described above, and that of about +4 to +6 per mil, as calculated from the single analysis of whole rock magmatic sulfur, continues to remain unresolved.

The three anhydrite-pyrite pairs from the Anaconda Dome (Fig. 24) appear to be representative of an isotopically different population because the anhydrite fractions, but not the pyrite, are all ^{34}S-enriched relative to their counterparts from the Pittsmont Dome. Delta values for these pairs are moderately larger and, accordingly, yield lower isotopic temperatures of 370° to 475°C (Table. 10). Sample Bu-8a contains the heaviest anhydrite (+18.2 ‰), has the largest delta value (+15.2 ‰), and provides the lowest temperature (370°C) of any of the Butte sulfate-sulfide mineral pairs. The presence of a thin quartz-sericite alteration selvage adjacent to this quartz-anhydrite-pyrite veinlet, and superimposed on a K-silicate assemblage that characterizes the overall host, is qualitatively consistent with the lower temperature. These data and regression lines, as illustrated by Field and others (1983), suggest a $\delta^{34}S_{\Sigma S}$ ‰ value of about +2 per mil and SO_4^{2-} and H_2S mole fractions of about 0.01 and 0.99, respectively. Although these Anaconda Dome samples are geographically separated from those of the Pittsmont

Dome (Figs. 1 and 2a &b), are geologically higher in the hydrothermal system, exhibit larger ^{34}S enrichment of anhydrite, and similarities to the ^{34}S values of pyrite elsewhere in the district, any reconciliation of the isotopic differences to factors other than probably lower temperatures and possibly lower SO_4^{2-}:H_2S mole fraction ratios is speculative at best, because of the meager amount of data presently available.

Composition of Sulfur in the Gray-Sericitic Assemblage and the Main Stage

Significant quantities of sulfate, as anhydrite, were deposited only during the pre-Main Stage event and in association with the K-silicate assemblage. With the exception of a thin quartz-sericite selvage to the anhydrite-pyrite pair in sample Bu-8a from the 4200 level of the Steward Mine, anhydrite has not been reported with other assemblages or zones of mineralization at Butte. Meyer and others (1968) list alunite as a trace mineral from the Central Zone and barite as a trace mineral widely dispersed throughout the Deep Level, Central, Intermediate, and Peripheral Zones of Main Stage mineralization. Sulfur isotope analyses have not been performed on either of these sulfate minerals. Thus, sulfate data unfortunately are unavailable to assist in bracketing the isotopic composition of sulfur in later stages of Butte mineralization, in contrast to the voluminous amount of existing sulfide data.

Nonetheless, the isotopic data for sulfides can provide some useful constraints on the composition of sulfur in hydrothermal systems, and that for sulfides most relevant to this study are tabulated in Table 12. Listed are the number of analyses and mean and range of $\delta^{34}S$ per mil values for anhydrite and specific sulfide minerals for the assemblages and zones of the Butte District. Although these data are given for all minerals of the K-silicate assemblage that have been analyzed, including those of Lange and Cheney (1971), the minerals important to this discussion are pyrite and chalcopyrite because they are widely distributed throughout most assemblages and zones of the

Table 12. Means and Ranges of $\delta^{34}S$ Per Mil Values for Selected and (or) Widespread Sulfate and Sulfide Minerals of the Butte District and the Calculated Values for Coexisting H_2S at Assumed Temperatures Based on the Fractionation Equations of Ohmoto and Rye (1979) and Ohmoto and Lasaga (1982).

Mineral Assemblage/Zone		N	$\delta^{34}S$ ‰ Mineral Mean	$\delta^{34}S$ ‰ Mineral Range	$\delta^{34}S$ ‰ H2S Mean	$\delta^{34}S$ ‰ H2S Range	T°C
Anhydrite	K-silicate (Pittsmont)	19	+12.2	+9.8 to +12.9	+3.2	+0.8 to +3.9	600
Molybdenite	K-silicate	10	+3.6	+2.6 to +4.7	+3.0	+2.0 to +4.1	600
Pyrite	K-silicate	15	+2.7	+0.5 to +3.4	+2.2	0 to +2.9	600
	GS	25	+2.7	+1.7 to +4.3	+1.8	+0.8 to +3.4	400
	DGS&PGS	4	+1.1	+0.4 to +1.9	+0.2	-0.5 to +1.0	400
	DLZ	17	+1.0	-0.1 to +2.7	+0.1	-1.0 to +1.8	400
	CZ	20	+0.9	-1.8 to +3.6	0	-2.7 to +2.7	400
	IZ	86	+2.4	-0.9 to +3.9	+1.2	-2.1 to +2.7	300
	PZ	4	+3.6	+2.0 to +4.8	+2.4	+0.8 to +3.6	300
Chalcopyrite	K-silicate	10	+1.7	+0.4 to +3.0	+1.8	+0.5 to +3.1	600
	DGS&PGS	3	+0.5	-0.1 to +1.0	+0.6	0 to +1.1	400
	DLZ	3	-0.9	-2.2 to –0.1	-0.8	-2.1 to 0	400
	CZ	1	0		+0.1		400
	IZ	6	+0.8	-1.0 to +3.1	+1.0	-0.8 to +3.3	300
Sphalerite	IZ	5	+0.6	+0.4 to +0.9	+0.3	+0.1 to +0.6	300
	PZ	6	+0.5	-2.0 to +3.2	+0.2	-2.3 to +2.9	300

district. The $\delta^{34}S$ per mil values of the sulfide minerals closely approximate those of their aqueous precursor (H_2S), and the latter can be estimated more precisely using the measured mineral values with the sulfide-H_2S fractionation equations summarized by Ohmoto and Rye (1979) and Ohmoto and Goldhaber (1997). Assuming depositional temperatures of 600°C for the K-silicate assemblage, 400°C for the gray-sericitic assemblage, and 275° for the Deep Level, Central Zones, and Intermediate and Periperhal Zones of the Main Stage, application of these equations to the sulfide $\delta^{34}S$ data of Table 12 provides equivalent values for coexisting H_2S in the hydrothermal fluids. Compared to the sulfide mineral data, these H_2S values differ only slightly by less than 1 per mil and have slightly lower means and similar ranges at slightly lower values. Nonetheless, the most important feature of either data set is the general similarity of the means and ranges of $\delta^{34}S$ per mil values within and between specific sulfide minerals (especially pyrite and chalcopyrite) and their zonal and (or) paragenetic occurrence. They suggest that the isotopic composition of reduced sulfur ($\delta^{34}S$ of H_2S $\cong 1.5 \pm 1.0$ ‰) in the hydrothermal system and resulting sulfide minerals ($\delta^{34}S \cong 2.0 \pm 1.5$ ‰) did not change appreciably with respect to time (pre-Main Stage through Main Stage) or geographic position (between different mineral assemblages and zones).

If the foregoing statement is correct, it is possible to speculate on the composition of $\delta^{34}S_{\Sigma S}$ and the SO_4^{2-}:H_2S mole fraction ratio of the system during later gray-sericitic and Main Stage hydrothermal activity, and in spite of the apparent near-absence of sulfate minerals in these assemblages. A number of quartz-pyrite veinlets associated with the gray-sericitic assemblage exhibit a peculiar vuggy texture that is suggestive of euhedral-like voids formed by the leaching of anhydrite, either at low temperatures by near-surface supergene processes or at intermediate temperatures with dissolution caused by the retrograde solubility of anhydrite at T less than 375 ° to 400 °C (Holland and Malinin, 1979) attendant with the waning stage of hypogene processes.

Moreover, the paucity of alunite and barite with Main Stage mineralization may relate to chemical factors such as the limited availability of K^+, Na^+, and Ba^{2+} in the fluids, and not necessarily to low concentrations of $SO4^{2-}$ or low $SO4^{2-}$:$H2S$ mole fraction ratios. If it is assumed that conditions of $\delta^{34}S_{\Sigma S}$ ($\cong$ +10 ‰) and SO_4^{2-}:H_2S ($\cong$ 3) for the K-silicate assemblage were retained during the transition to lower temperatures of the later gray-sericitic assemblage ($\cong$ 400°C) and Main Stage (400° to 300°C) event, $\delta^{34}S$ values of H_2S and resulting sulfide minerals would diminish by about 5 to 9 per mil and result in negative values (about -2 to –8 ‰) for pyrite and chalcopyrite. Such ^{34}S-depleted values for these sulfides are absent from the available data set.

Alternatively, if the $\delta^{34}S_{\Sigma S}$ value remained the same and the SO_4^{2-}:H_2S ratio decreased to a value ($\cong$ 0.01) representing a less oxidized and sulfide dominant system, $\delta^{34}S$ values of H_2S and associated sulfide minerals would approach the isotopic composition of $\delta^{34}S_{\Sigma S}$ (about +10 ‰) and with little variation. Again, such ^{34}S-enriched sulfides are not in the data set. The more abundant sulfides of pyrite and chalcopyrite do not exhibit such predicted anomalous isotopic compositions and they do not vary appreciably (mostly –1 to +3 ‰) with paragenesis or zones of mineralization (Table 12).

Although speculative, yet another explanation is possible for the isotopic similarity and minimal variation of δ34S per mil values for sulfides of the Butte District. Perhaps the value for $\delta^{34}S_{\Sigma S}$ changed from about +10 per mil during deposition of the K-silicate assemblage to about +2 per mil with deposition of the later gray-sericitic assemblage and sulfides of the Main Stage. The source of this isotopically lighter sulfur might be that of sulfides deposited previously with the K-silicate assemblage through the process of remobilization associated with later hydrothermal leaching that accompanied widespread and pervasive quartz-sericite and argillic alteration of host rocks and earlier pre-Main

Stage mineralization. It was Brimhall (1980) who was first to introduce the concept and multitude of geologic and related evidence in support of remobilization as a viable mechanism for the formation of Main Stage ores at Butte. This hypothetical application of the model requires that either the SO_4^{2-}:H_2S mole fraction ratio was low ($\cong$ 0.2 or less), or that there was little or no isotopic equilibration between the sulfide-sulfur and that of presumably larger quantities of sulfate-sulfur released with dissolution of anhydrite during the remobilization process, to account for the absolute and narrow range of sulfide $\delta^{34}S$ per mil values that seemingly were insensitive, except perhaps locally, to changes in redox state and temperature of the hydrothermal fluids.

Conclusions

Three major observations were obtained from sulfur isotope analyses of forty-seven samples selected from deep drill cores, which include sulfate-sulfide assemblages in veinlets associated with K-silicate alteration selvages, and pyrite in slightly younger quartz-pyrite veinlets associated with gray sericitic alteration selvages.

1) The range of $\delta^{34}S$ per mil values for minerals of the K-silicate assemblage are 9.8 to 12.9 ‰ (anhydrite; 20), 3.0 to 4.7 ‰ (molybdenite; 6), 0.5 to 3.4 ‰ (pyrite; 12), and 0.4 to 3.0 ‰ (chalcopyrite; 10).

2) Mineral fractionation are entirely consistent with an approach to isotopic equilibrium, and calculated temperature ranges for mostly coexisting anhydrite-sulfide pairs are 543 to 632 °C (anh-mb; 6), 534 to 639 °C (anh-py; 10), and 482 to 576 °C (anh-cp; 8). These temperatures are broadly consistent with those of fluid inclusion studies past (Roberts, 1975) and present (Rusk et al, 1999).

3) $\delta^{34}S$ values for pyrite (25) in veinlets of the gray-sericitic assemblage range from 1.7 to 4.3 ‰.

In general, the K-silicate and gray-sericitic sulfide data are similar to those of Main Stage sulfides (Lange and Cheney, 1971; Lange and Krouse, 1984), which suggests a conventionally "magmatic" value of about 2 ‰ for Butte sulfide-sulfur. However, total sulfur ($\delta^{34}S_{\Sigma S}$ ‰) of the early K-silicate assemblage may be as heavy as 10 ‰, suggesting a possible crustal component to this relatively oxidized system; an inference supported by alteration assemblages, the presence of anhydrite, high modal sulfate to sulfide mineral ratios (Brimhall, 1977), and isotopic effects related to fractionation in a SO_4^{2-}-rich hydrothermal fluid.

Acknowledgments

This project was supported by the National Science Foundation grants: EAR-9600054 (Dilles and Field) and EAR-9704280 (Reed). We thank Montana Resources and the Montana Bureau of Mines and Geology for giving us access to deep drill hole core samples and Anaconda sample collection for mapping and sampling. We especially thank Lester Zeihen for his persistent and successful efforts to preserve the Anaconda sample collection. We also thank Robert Houston and Brain Rusk for their contributions on the Butte geology mapping and fluid inclusion works.

References

Ames, R.L., 1962, Sulfur isotopic study of the Tintic Mining Districts, Utah: New Haven, Yale University, Ph.D. dissertation, 163 p.

Bachinski, D.J., 1969, Bond strength and sulfur isotopic fractionation in coexisting sulfides: Economic Geology, v. 64, p. 56-65.

Becraft, G. E., Pickney, D. M., and Rosenblum, S., 1963 , Geology and mineral deposits of Jefferson City quadrangle, Jefferson and Lewis & Clark counties, Montana: U.S. Geological Survey Prof. Paper, 428, p. 101.

Borrok, David, Kesler, S.E., and Vogel, T.A., 1999, Sulfide minerals in intrusive and volcanic rocks of the Bingham-Park City Belt, Utah: Economic Geology, v. 94, p. 1213-1230.

Brimhall, G. H. , Jr., 1977, Mineralogy, texture, and chemistry of early wall rock alteration in the deep underground mines and Continental area, Butte district, Montana: Econ. Geol., v. 72, p. 37-59.

Brimhall, G. H. , Jr., 1979, Lithologic determination of mass-transfer mechanism of multiple-stage porphyry copper mineralization at Butte, Montana: vein formation by hypogene leaching and enrichment of potassium silicate protore: Econ. Geol., v. 74, p. 556-589.

Brimhall, G. H. , Jr., 1980, Deep hypogene oxidation of porphyry copper potassium-silicate protore at Butte, Montana: a theoretical evaluation of the copper mobilization hypothesis: Econ. Geol., v. 75, p. 384-409.

Brownlow, A. H. , and Kurz, S. L., 1979, Occurrence, distribution, and composition of sulfide minerals, Boulder batholith, Montana: Mineralium Deposita, v. 14, p. 175-184.

Burnham, C. W., 1997, Magma and hydrothermal fluids, in Barnes, H.L., ed., Geochemistry of Hydrothermal Ore Deposits (3rd ed.): New York, John Wiley &Sons, Inc., p. 71-136.

Dilles, J. H., and Field, C. W., 1996, Sulfur geochemistry of porphyry copper deposits as a record of magma degassing: Data from the Yerington district, Nevada: Geol. Soc. Amer., v. 28, No 7, p. A. 93.

Field, C.W., 1966, Sulfur isotope abundance data, Bingham District, Utah: Economic Geology, v. 61, p. 850-871.

Field, C.W., Rye, R.O., Dymond, J.R., Whelan, J.F., and Senechal, R.G., 1983, Metalliferous Sediments of the East Pacific, in Shanks, W.C., III, ed., Cameron Volume on Unconventional Mineral deposits: New York, Society of Mining Engineers of the American Institute of Mining, Metallurgical, and Petroleum Engineers, Inc., p. 133-156.

Field, C.W., Sakai, H., and Ueda, A., 1984, Isotopic constraints on the origin of sulfur in oceanic igneous rocks, in Wauschkuhn, A., Kluth, C., and Zimmermann, R.A., eds., Syngenesis and epigenesis in the formation of mineral deposits: Berlin-Heidelberg, Springer-Verlag, p. 573-589.

Holland, H. D., and Malinen, S. D., 1979, The solubility and occurrence of non-ore minerlas, in Barnes, H.L., ed., Geochemistry of Hydrothermal Ore Deposits (2nd ed.): New York, John Wiley &Sons, Inc., p. 461-508.

Jensen, M.L., 1959, Sulfur isotopes and hydrothermal mineral deposits: Economic Geology, v. 54, p. 374-394.

Lange, I.M., and Cheney, E.S., 1971, Sulfur isotope reconnaissance of Butte, Montana: Economic Geology, v. 66, p. 63-74.

Lange, I.M., and Krouse, H.R., 1984, Sulfur isotopic variations in the A2844 vein and wall rock, Butte, Montana: Geochemical Journal (Japan), v. 18, p. 269-280.

Meyer, C., 1965, An early potassic type of wall-rock alteration at Butte, Montana: Amer. Mineral., v. 50, p. 1717-1722.

Meyer, C., and Hemley, J. J., 1967, Wall rock alteration, in Barnes, H. L., ed., Geochemistry of hydrothermal ore deposits: New York, John Wiley & Sons, Inc., p. 166-235.

Meyer, C., Shea, E. P, Goddard, C. C, Jr., and Staff, 1968, Ore deposit at Butte, Montana: Ore Deposits of the United States 1933/1967, the Graton-Sales Volume (Vol. II): New York, American Institute of Mining, Metallurgical, and Petroleum Engineers, Inc., p. 1373-1416.

Newhouse, W.H., 1936, Opaque oxides and sulphides in common igneous rocks: Geological Society of America Bulletin, v. 47, p. 1-52.

Ohmoto, H., 1972, Systematics of sulfur and carbon isotopes in hydrothermal ore deposits: Econ. Geol., v. 67, p. 551-578.

Ohmoto, H., 1986, Stable isotope geochemistry of ore deposits, in Valley, J. W., Taylor, H. P., Jr., and O'Neil, J. R., eds., Stable Isotopes in High Temperature Geological Processes: Mineralogical Society of America, Reviews in Mineralogy, v. 16, p. 491-559.

Ohmoto, H., and Goldhaber, M.B., 1997, Sulfur and carbon isotopes, in Barnes, H.L., ed., Geochemistry of hydrothermal ore deposits (3d ed.): New York, John Wiley & Sons, Inc., p. 517-611.

Ohmoto, H., and Lasaga, A. C., 1982, Kinetics of reactions between aqueous sulfates and sulfides in hydrothermal systems: Geochim. et Cosmochim. Acta, v. 46, p. 1727-1745.

Ohmoto, H., and Rye, R.O., 1979, Isotopes of sulfur and carbon, in Barnes, H.L., ed., Geochemistry of hydrothermal ore deposits (2d ed.): New York, John Wiley & Sons, p. 509-567.

Reed, M. H., 1979, Butte District early stage geology: Anaconda Company Report, 40 p. 24 plates and figures.

Roberts, S. A, 1975, Early hydrothermal alteration and mineralization in Butte district, Montana: Unpub. Ph.D thesis, Harvard University. Cambridge, 173 p.

Robson, J., 1971, An optical study of the mamgatic rocks near Butte, Montana: Unpub. MS thesis, Montana School of Mine, Butte, Montana.

Ruppel, E. T., 1963, Geology of the Basin quadrangle, Jefferson, Lewis & Clark and Powell counties, Montana: U.S. Geological Survey Bull. 1151, 121 p.

Rusk, B., Reed, M. H., and Dilles, J. H., 1999, Fluid inclusions in barren quartz and quartz-molybdenite veins in the porphyry Cu-Mo deposits, Butte, Montana (abs): Geological Society of America Abstracts Programs, v. 31, no 7, p. A-381.

Sakai, Hitoshi, 1968, Isotopic properties of sulfur compounds in hydrothermal processes: Geochemical Journal (Japan), v. 2, p. 29-49.

Sakai, Hitoshi, Casadevall, T.J., and Moore, J.G., 1982, Chemistry and isotope ratios of sulfur in basalts and volcanic gases at Kilauea Volcano, Hawaii: Geochimica et Cosmochimica Acta, v. 46, p. 729-738.

Sales, R.H., 1914, Ore deposits at Butte, Montana: American Institute of Mining, Metallurgical, And Petroleum Engineers Transactions, v. 46, p. 3-106.

Sales, R.H., and Meyer, C., 1948, Wall rock alteration, Butte, Montana: American Institute of Mining, Metallurgical, And Petroleum Engineers Transactions, v. 178, p. 9-35.

Sales, R.H., and Meyer, C., 1951, Effect of post-ore dike intrusion on Butte ore minerals: Economic Geology, v. 46, p. 813-820.

Sasaki, Akira, Arikawa, Yoshiko, and Folinsbee, R.E., 1979, Kiba reagent method of sulfur extraction applied to isotopic work: Bulletin of the Geological Survey of Japan, v. 30, p. 241-245.

Sha, Lian-Kun, and Chappell, B.W., 1999, Apatite chemical compositions, determined by Electron microprobe and laser-ablation inductively coupled plasma mass spectrometry, as a probe into granite petrogenesis: Geochimica et Cosmochimica Acta, v. 63, p. 3861-3881.

Smedes, H. W., 1966, Geology and igneous petrology of the Northern Elkhorn Mountains, Jefferson and Broadwater counties, Montana: U.S. Geological Survey Prof. Paper, no. 510, p. 116.

Streck, M.J., and Dilles, J.H., 1998, Sulfur evolution of oxidized arc magmas as recorded in apatite from a porphyry copper batholith: Geology, v. 26, p. 523-526.

Thode, H.G., Monster, J., and Dunford, H.B., 1961, Sulphur isotope Geochemistry: Geochimica et Cosmochimica Acta, v. 25, p. 159-174.

Tilling, R. I., 1973, The Boulder Batholith, Montana: A product of two contemporaneous but chemically distinct magma series: Geological Society of America Bulletin, v. 84, p. 3879-3900.

Weed, W. H., 1912, Geology and ore deposit of the Butte distict, Montana: U.S. Geological Survey Prof. Paper 74, 262 p.

4. SUMMARY

The goals of this thesis research have been twofold: establish an extensive and systematic data base of stable isotope compositions of the pre-Main Stage minerals and test the hypothesis of the magmatic to meteoric transition during hydrothermal evolution in currently accepted porphyry Cu models.

These goals have been approached separately using oxygen and hydrogen isotopic compositions and sulfur isotope analyses, which are the main thrusts of Chapters II and III, respectively.

Major conclusions that can be drawn from the systematic oxygen and hydrogen isotope analyses of sixty-two samples presented in Chapter II are:

1) The most fresh Butte Quartz Monzonite samples from the edge of the Butte district yield similar isotopic compositions to the felsic magmatic water ($\delta^{18}O$ = 7-8 ‰, and δD=-45 to -60‰). The light δD values of the Butte Quartz Monzonite samples near the mining district suggest that these Butte Quartz Monzonite had partly re-equilibrated with meteoric fluids at low temperatures.

2) The most D-rich fluids associated with K-silicate alteration are similar to felsic magmatic water.

3) The wide range of oxygen isotopic compositions and the D-depletion in the argillically altered K-silicate samples results from isotopic exchange of biotite with the younger, low-temperature, meteoric-dominated Main Stage fluids as initially proposed by Sheppard and Taylor (1974).

4) The gray-sericitic fluids range from pure magmatic water (δD ~ -35 ‰, n=4) to <50% magmatic water (δD ~ -93 ‰, n=9).

These observations provide the first systematic and extensive data base of oxygen and hydrogen isotopic compositions for the pre-Main Stage alterations at Butte district.

Combined with existing isotope data of Main Stage minerazations, these data indeed suport the theory of current porphyry Cu models that the associated hydrothermal fluids evolved from early magmatic origin to later meteoric water. One important finding from our observations is that the widespread, Main Stage or younger argillic alteration have partly to totally reset the isotopic compositions of minerals in the fresh Butte Quartz Monzonite host rock, the early high temperature K-silicate alteration assemblages, and locally quartz-sericite alteraion assemblages.

In Chapter 3, sulfur isotope analyses have been applied to forty-seven samples selected from deep drill core. These include sulfate-sulfide assemblages in veinlets and slightly younger quartz-pyrite veinlets associated with K-silicate and grey sericitic alteration selvages, respectively. Major observations include:

1) The range of $\delta^{34}S$ per mil values for minerals of the K-silicate assemblage are 9.8 to 12.9 ‰ (anhydrite; 20), 3.0 to 4.7 ‰ (molybdenite; 6), 0.5 to 3.4 ‰ (pyrite; 12), and 0.4 to 3.0 ‰ (chalcopyrite; 10).

2) Mineral fractionations are entirely consistent with an approach to isotopic equilibrium, and calculated temperature ranges for mostly coexisting anhydrite-sulfide pairs are 543 to 632 °C (anh-mb; 6), 534 to 639 °C (anh-py; 10), and 482 to 576 °C (anh-cp; 8). These temperatures are broadly consistent with those of fluid inclusion studies past (Roberts, 1975) and present (Rusk et al, 1999).

3) $\delta^{34}S$ values for pyrite (25) in veinlets of the gray-sericitic assemblage range from 1.7 to 4.3 ‰.

The K-silicate and gray-sericitic sulfide data are similar to those of Main Stage sulfides (Lange and Cheney, 1971; Lange and Krouse, 1984) and suggest a conventionally "magmatic" value of about 2 ‰ for Butte sulfide-sulfur. However, total sulfur ($\delta^{34}S_{\Sigma S}$ ‰) of the early K-silicate assemblage may be as heavy as 10 ‰, suggesting a possible crustal component to this relatively oxidized system; an inference

supported by alteration assemblages, the presence of anhydrite, high modal sulfate to sulfide mineral ratios (Brimhall, 1977), and isotopic effects related to fractionation in a SO_4^{2-}-rich hydrothermal fluid.

Bibliography

Ames, R.L., 1962, Sulfur isotopic study of the Tintic Mining Districts, Utah: New Haven, Yale University, Ph.D. dissertation, 163 p.

Bachinski, D.J., 1969, Bond strength and sulfur isotopic fractionation in coexisting sulfides: Economic Geology, v. 64, p. 56-65.

Becraft, G. E., Pickney, D. M., and Rosenblum, S., 1963 , Geology and mineral deposits of Jefferson City quadrangle, Jefferson and Lewis & Clark counties, Montana: U.S. Geological Survey Prof. Paper, 428, p. 101.

Bigeleiser, J, Perlman, M. L., Prosser, H. C., 1952, Conversion of hydrogen materials to hydrogen for isotopic analysis: Analytical Chemistry, v. 24, p. 1356-1357.

Bodnar, R. J, 1995, Fluid-inclusion evidence for a magmatic source of metals in porphyry copper deposits: in Thompson, J.F.H., ed., Magma, fluids, and ore deposits: Mineralogical Association of Canada Short Course, v. 23, p. 139-152.

Borrok, David, Kesler, S.E., and Vogel, T.A., 1999, Sulfide minerals in intrusive and volcanic rocks of the Bingham-Park City Belt, Utah: Economic Geology, v. 94, p. 1213-1230.

Bottinga, Y., and Javoy, M., 1973, Comments on oxygen isotope geothermometry: Earth and Planetary Science Letters, v. 20, p. 250-265.

Brimhall, G. H. , Jr., 1972, Early fracture-controlled disseminated mineralization at Butte, Montana: Unpub. Ph.D. dissert., Univ. California, Berkeley, 103 p.

Brimhall, G. H. , Jr., 1977, Mineralogy, texture, and chemistry of early wall rock alteration in the deep underground mines and Continental area, Butte district, Montana: Econ. Geol., v. 72, p. 37-59.

Brimhall, G. H. , Jr., 1979, Lithologic determination of mass-transfer mechanism of multiple-stage porphyry copper mineralization at Butte, Montana: vein formation by hypogene leaching and enrichment of potassium silicate protore: Econ. Geol., v. 74, p. 556-589.

Brimhall, G. H. , Jr., 1980, Deep hypogene oxidation of porphyry copper potassium-silicate protore at Butte, Montana: a theoretical evaluation of the copper mobilization hypothesis: Econ. Geol., v. 75, p. 384-409.

Brownlow, A. H. , and Kurz, S. L., 1979, Occurrence, distribution, and composition of sulfide minerals, Boulder batholith, Montana: Mineralium Deposita, v. 14, p. 175-184.

Burnham, C. W., 1997, Magma and hydrothermal fluids, in Barnes, H.L., ed., Geochemistry of Hydrothermal Ore Deposits (3rd ed.): New York, John Wiley &Sons, Inc., p. 71-136.

Burnham, C. W., and Ohmoto, H., 1980, Late-stage processes of felsic magmatism: Mining Geology Special Issue, No. 8, p. 1-11.

Capuano, R. M., 1992, The temperature dependence of hydrogen isotope fractionation between clay minerals and water: Evidence from a geopressured system: Geochimica et Cosmochimica Acta, v. 56, p. 2547-2554.

Cline, J. S., 1995, Genesis of porphyry copper deposits: the behavior of water, chloride, and copper in crystallizing melts, in Pierce, F. W., and Bolm, J. G., eds., Porphyry copper deposits of the American Cordillera: Arizona Geological Society Digest, v. 20, p. 69-82.

Cole, D. R., and Ohmoto, H., 1986, Kinetics of isotopic exchange at elevated temperatures and pressures: Stable Isotopes in High Temperature Geological Processes, in Valley, J. W., Taylor, H. P., Jr., and O'Neil, J. R., eds., Reviews in Mineralogy: Mineralogical Society of America, v. 16, p. 41-90.

Cooper, J. R., 1973, Geological map of the Twin Buttes quadrangle, southwest of Tucson, Arizona: U.S. Geological Survey Misc. Geol. Inv. Map 745.

Dilles, J. H., and Field, C. W., 1996, Sulfur geochemistry of porphyry copper deposits as a record of magma degassing: Data from the Yerington district, Nevada: Geol. Soc. Amer., v. 28, No 7, p. A. 93.

Dilles, J. H., Solomon, G. C., Taylor, H. P., and Einaudi, M. T., 1992, Oxygen and hydrogen isotope characteristics of hydrothermal alteration at the Ann-Mason porphyry copper deposit, Yerington, Nevada: Econ. Geol., v. 87, p. 44-63.

Dilles, J. H., Reed, M. H., Roberts, S., Zhang, L., and Houston, R., 1999, Early magmatic-hydrothermal features related to porphyry copper mineralization at Butte, Montana (abs): Geological Society of America Abstracts Programs, v. 31, no 7, p. A-380.

Field, C.W., 1966, Sulfur isotope abundance data, Bingham District, Utah: Economic Geology, v. 61, p. 850-871.

Field, C.W., Rye, R.O., Dymond, J.R., Whelan, J.F., and Senechal, R.G., 1983, Metalliferous Sediments of the East Pacific, in Shanks, W.C., III, ed., Cameron Volume on Unconventional Mineral deposits: New York, Society of Mining Engineers of the American Institute of Mining, Metallurgical, and Petroleum Engineers, Inc., p. 133-156.

Field, C.W., Sakai, H., and Ueda, A., 1984, Isotopic constraints on the origin of sulfur in oceanic igneous rocks, in Wauschkuhn, A., Kluth, C., and Zimmermann, R.A., eds., Syngenesis and epigenesis in the formation of mineral deposits: Berlin-Heidelberg, Springer-Verlag, p. 573-589.

Garlick, G. D., and Epstein, S., 1966, The isotopic composition of oxygen and carbon in hydrothermal minerals from Butte, Montana: Econ. Geol., v. 62, p. 1325-1335.

Geissman, J. W., Kelly, W. C., Van der Voo, R., and Brimhall, G. H. , Jr., 1980, Paleomagnetic documentation of the early, high temperature zone of mineralization at Butte, Montana: Econ. Geol., v. 75, p. 1210-1219.

Geissman, J. W., Kelly, W. C., Van der Voo, R., and Brimhall, G. H. , Jr., 1980, Paleomagnetism, rock magnetism and aspects of structural deformation of the Butte mining district, Butte, Montana: Jour. Geology, v. 88, p. 129-159.

Gilluly, J., 1946, The Ajo mining district, Arizona: U.S. Geological Survey Prof. Paper 209, 112 p.

Graham, C. M., Harmon, R. S., and Sheppard, S. M. F., 1984, Experimental hydrogen isotope studies--hydrogen isotope exchange between amphibole and water: American Mineralogist, v. 69, p. 128-138.

Guilbert, J. M. and Park, C. F., Jr., 1985, The geology of ore deposits: W. H. Freeman and Company, New York, 984 p.

Hedenquist, J. W., Arribas, A., Jr., and Reynolds, J. R., 1998, Evolution of an intrusion-centered hydrothermal system: Far Southeast-Lepanto porphyry and epithermal Cu-Au deposits, Philippines: Econ. Geol., v. 93, p. 373-404.

Hedenquist, J. W., and Richards, J. P., 1998, The influence of geochemical techniques on the development of genetic models for porphyry copper deposits, in Richards, J. P., and Larson, P. B. (eds.), Techniques in Hydrothermal Ore Deposits Geology: Reviews in Economic Geology, v. 10, p. 235-256.

Holland, H. D., and Malinen, S. D., 1979, The solubility and occurrence of non-ore minerlas, in Barnes, H.L., ed., Geochemistry of Hydrothermal Ore Deposits (2nd ed.): New York, John Wiley &Sons, Inc., p. 461-508.

Houston, R., 1999, The Butte district, Montana – new field data and reassessment of post-mineral structural tilting (abs): Geological Society of America Abstracts Programs, v. 31, no 7, p. A-382.

Javoy, M., 1977, Stable isotopes and geothermometry: Journal of the Geological Society of London, v. 133, p. 609-636.

Jensen, M.L., 1959, Sulfur isotopes and hydrothermal mineral deposits: Economic Geology, v. 54, p. 374-394.

Knopf, A., 1957, The Boulder batholith of Montana: Am. Jour. Sci., v. 255, p. 81-103.

Lambert, S. J., and Epstein, S., 1980, Stable isotope investigations of an active geothermal system in Valles Caldera, Jemez mountains, New Mexico: Joun. Volc. Geothermal Res., v. 8, p. 111-129.

Lange, I.M., and Cheney, E.S., 1971, Sulfur isotope reconnaissance of Butte, Montana: Economic Geology, v. 66, p. 63-74.

Lange, I.M., and Krouse, H.R., 1984, Sulfur isotopic variations in the A2844 vein and wall rock, Butte, Montana: Geochemical Journal (Japan), v. 18, p. 269-280.

Martin, M. W., Dilles, J. H., and Proffett, J. M., 1999, U-Pb geochronologic constraints for the Butte porphyry system (abs): Geological Society of America Abstracts Programs, v. 31, no 7, p. A-380.

Matsuhisa, Y., Goldsmith, J. R., and Clayton, R. N., 1979, Oxygen isotopic fractionation in the system quartz-albite-anorthite-water: Geochimica et Cosmochimica Acta, v. 43, p. 1131-1140.

Meyer, C., 1965, An early potassic type of wall-rock alteration at Butte, Montana: Amer. Mineral., v. 50, p. 1717-1722.

Meyer, C., and Hemley, J. J., 1967, Wall rock alteration, in H. L. Barnes, ed., Geochemistry of Hydrothermal Ore Deposits: New York, Holt, Rinehart and Winston, p. 166-235.

Meyer, C., Shea, E. P, Goddard, C. C, Jr., and Staff, 1968, Ore deposit at Butte, Montana: Ore Deposits of the United States 1933/1967, the Graton-Sales Volume (Vol. II): New York, American Institute of Mining, Metallurgical, and Petroleum Engineers, Inc., p. 1373-1416.

Nebelek, P. I., O'Neil, J. R., and Papike, J. J., 1983, Vapor phase exsolution as a controlling factor in hydrogen isotope variation in granitic rocks: the Notch Peak granite stock, Utah: Earth Planetary Science Letters, v. 66, p. 137-150.

Newhouse, W.H., 1936, Opaque oxides and sulphides in common igneous rocks: Geological Society of America Bulletin, v. 47, p. 1-52.

Ohmoto, H., 1972, Systematics of sulfur and carbon isotopes in hydrothermal ore deposits: Econ. Geol., v. 67, p. 551-578.

Ohmoto, H., 1986, Stable isotope geochemistry of ore deposits, in Valley, J. W., Taylor, H. P., Jr., and O'Neil, J. R., eds., Stable Isotopes in High Temperature Geological Processes: Mineralogical Society of America, Reviews in Mineralogy, v. 16, p. 491-559.

Ohmoto, H., and Goldhaber, M.B., 1997, Sulfur and carbon isotopes, in Barnes, H.L., ed., Geochemistry of hydrothermal ore deposits (3d ed.): New York, John Wiley & Sons, Inc., p. 517-611.

Ohmoto, H., and Lasaga, A. C., 1982, Kinetics of reactions between aqueous sulfates and sulfides in hydrothermal systems: Geochim. et Cosmochim. Acta, v. 46, p. 1727-1745.

Ohmoto, H., and Rye, R.O., 1979, Isotopes of sulfur and carbon, in Barnes, H.L., ed., Geochemistry of hydrothermal ore deposits (2d ed.): New York, John Wiley & Sons, p. 509-567.

O'Neil, J. R., 1986, Theoretical and experimental aspects of isotopic fractionation: Stable Isotopes in High Temperature Geological Processes, Reviews in Mineralogy, v. 16, p. 1-40.

O'Neil, J. R., and Kharaka, Y. K., 1976, Hydrogen and oxygen isotope exchange reactions between clay minerals and water: Geochimica et Cosmochimica Acta, v. 40, p. 241-246.

Page, R. H, 1979, Alteration-mineralization history of the Butte, Montana ore deposit, and transmission electron microscopy of phyllosilicate alteration phases. Unpub. Ph.D thesis, University of California at Brokley, 226p.

Proffett, J. M., Jr., 1974, Structure of the Butte district, Montana: Guidebook for the Butte Field Meeting of Society of Economic Geologists, Sec. G, p. G-1-G12.

Proffett, J. M., Jr., 1979, Ore deposits of the western United States: a summary: Nevada Bureau Mines Geology Report 33 (IAGOD 5th Quadrennial Symposium Proceedings), v. 11, p. 13-32.

Proffett, J. M., Jr., and Dilles, H. J., 1984, Early Mesozoic sedimentary and volcanic rocks of the Yerington region, Nevada, and their regional context (U. S. Geological Survey-Nevada Bureau of Mines conterpiece project; U. S. Geological Survey Bulletin).

Reed, M. H., 1979a, Pyrite-quartz-sericite mineralization of Late pre-Main Stage age, Butte, Montana: Anaconda Company Report, 20 p., 7 plates.

Reed, M. H., 1979b, Butte district early stage geology: Anaconda Company Report, 40 p. 24 plates and figures.

Reed, M. H., 1980, Distribution of Mineralization at Butte: Anaconda Company Report, 40 p., 17 plates and figures.

Reyes, G. A., 1990, Petrology of Philippine geothermal systems and the application of alteration mineralogy to their assessment: Jour. of Volcanology and Geothermal Research, v. 43, p. 279-309.

Roberts, S. A, 1975, Early hydrothermal alteration and mineralization in Butte district, Montana: Unpub. Ph.D thesis, Harvard University. Cambridge, 173p.

Robson, J., 1971, An optical study of the mamgatic rocks near Butte, Montana: Unpub. MS thesis, Montana School of Mine, Butte, Montana.

Roedder, E., 1971, Fluid inclusion studies on the porphyry-type deposits at Bringham, Utah, Butte, Montana and Climax, Colorado: Econ. Geol., v. 66, p. 98-120.

Ruppel, E. T., 1963, Geology of the Basin quadrangle, Jefferson, Lewis & Clark and Powell counties, Montana: U.S. Geological Survey Bull. 1151. p. 121.

Rusk, B., Reed, M. H., and Dilles, J. H., 1999, Fluid inclusions in barren quartz and quartz-molybdenite veins in the porphyry Cu-Mo deposits, Butte, Montana (abs): Geological Society of America Abstracts Programs, v. 31, no 7, p. A-381.

Sakai, Hitoshi, 1968, Isotopic properties of sulfur compounds in hydrothermal processes: Geochemical Journal (Japan), v. 2, p. 29-49.

Sakai, Hitoshi, Casadevall, T.J., and Moore, J.G., 1982, Chemistry and isotope ratios of sulfur in basalts and volcanic gases at Kilauea Volcano, Hawaii: Geochimica et Cosmochimica Acta, v. 46, p. 729-738.

Sales, R.H., 1914, Ore deposits at Butte, Montana: American Institute of Mining, Metallurgical, And Petroleum Engineers Transactions, v. 46, p. 3-106.

Sales, R.H., and Meyer, C., 1948, Wall rock alteration, Butte, Montana: American Institute of Mining, Metallurgical, And Petroleum Engineers Transactions, v. 178, p. 9-35.

Sales, R.H., and Meyer, C., 1951, Effect of post-ore dike intrusion on Butte ore minerals: Economic Geology, v. 46, p. 813-820.

Sasaki, Akira, Arikawa, Yoshiko, and Folinsbee, R.E., 1979, Kiba reagent method of sulfur extraction applied to isotopic work: Bulletin of the Geological Survey of Japan, v. 30, p. 241-245.

Savin, S. M., and Epstein, S., 1970, The oxygen and hydrogen isotope geochemistry of clay minerals: Geochem. Cosmochim. Acta, v. 34, p. 25-42.

Sha, Lian-Kun, and Chappell, B.W., 1999, Apatite chemical compositions, determined by Electron microprobe and laser-ablation inductively coupled plasma mass spectrometry, as a probe into granite petrogenesis: Geochimica et Cosmochimica Acta, v. 63, p. 3861-3881.

Sharp, Z. D., 1990, A laser-based microanalytical method for in situ determination of oxygen isotopic ratios of silicates and oxides: Geochem. Cosmochim. Acta, v. 54, p. 1354-1357.

Sheppard, S. M. F., Nielsen, R. L., and Taylor, H. P., Jr., 1969, Oxygen and hydrogen isotope ratios of clay minerals from porphyry copper deposits: Econ. Geol., v. 64, p. 755-777.

Sheppard, S. M. F., and Taylor, H. P., Jr., 1974, Hydrogen and oxygen isotope evidence for the origin of water in the Boulder Batholith and the Butte ore deposits, Montana: Econ. Geol., v. 69, p. 926-946.

Sheppard, S. M. F., and Gilg, H. A., 1996, Stable isotope geochemistry of clay minerals: Clay Minerals, v. 31, p. 1-24.

Shieh, Y. N., and Taylor, H. P., Jr., 1969, Oxygen and hydrogen isotope studies of contact metamorphism in the Santa Rosa range, Nevada and other areas: Contrib. Mineral. Petrol., v. 20, p. 306-356.

Smedes, H. W., 1966, Geology and igneous petrology of the Northern Elkhorn Mountains, Jefferson and Broadwater counties, Montana: U.S. Geological Survey Prof. Paper, no. 510, p. 116.

Smedes, H. W., 1973, Regional setting and general geology of the Boulder batholith, Montana: Guidebook for the Butte Field Meeting of the Society of Economic Geologists, Sec. A, p. A-1-A-6.

Snee, L., Miggins, D., Reed, M. H., Dilles, J. H., and Zhang, L., 1999, Thermal history of the Butte porphyry system, Montana (abs): Geological Society of America Abstracts Programs, v. 31, no 7, p. A-380.

Stormer, J. C., and Carmichael, I. S. E., 1971, Fluorine-hydroxyl exchange in apatite and biotite: A potential igneous geothermometer: Contrib. Mineral. Petrol., v. 31, p. 121-131.

Streck, M.J., and Dilles, J.H., 1998, Sulfur evolution of oxidized arc magmas as recorded in apatite from a porphyry copper batholith: Geology, v. 26, p. 523-526.

Suzuoki, T., and Epstein, s., 1976, Hydrogen isotope fractionation between OH-bearing minerals and waters: Geochem. Cosmochim. Acta, v. 40, p. 1229-1240.

Taylor, H. P., Jr., and Epstein, S., 1962, Relationship between O18/O16 ratios in coexisting minerals of igneous and metamorphic rocks; Part I: Principles and experimental results: Geol. Soc. Amer. Bull., v. 73, p. 461-480.

Taylor, H. P., Jr., 1967, Oxygen isotope studies of hydrothermal mineral deposits, in H. L. Barnes, ed., Geochemistry of Hydrothermal Ore Deposits: New York, Holt, Rinehart and Winston, 670 p.

Taylor, H. P., Jr., 1997, Oxygen and hydrogen isotope relationships in hydrothermal mineral deposits, in Barnes, H.L., ed., Geochemistry of Hydrothermal Ore Deposits (3rd ed.): New York, John Wiley &Sons, Inc., p. 229-302.

Taylor, B. E., Eichelberger, J. C., and Westrich, H. R., 1983, Hydrogen isotopic evidence of rhyolitic magma degassing during shallow intrusion and eruption: Nature, v. 306, p. 541-545.

Thode, H.G., Monster, J., and Dunford, H.B., 1961, Sulphur isotope Geochemistry: Geochimica et Cosmochimica Acta, v. 25, p. 159-174.

Tilling, R. I., 1964, Variation in modes and norms of a "homogenous" pluton of the Boulder Batholith, Montana: U.S. Geological Survey Prof. Paper, no. 501-D, p. D8-D15.

Tilling, R. I., 1973, The Boulder Batholith, Montana: A product of two contemporaneous but chemically distinct magma series: Geological Society of America Bulletin, v. 84, p. 3879-3900.

Tilling, R. I., Klepper, M. R., and Obradovich, J. D., 1968, K-Ar ages and time span of emplacement of the Boulder batholith, Montana: Am. Jour. Sci., v. 266, p. 671-689.

Wadsworth, W. B., 1968, The Cornelia pluton, Ajo, Arizona: Econ. Geol., v. 63, p. 101-115.

Weed, W. H., 1912, Geology and ore deposit of the Butte distict, Montana: U.S. Geological Survey Prof. Paper 74, 262 p.

Zhang, L., Field, C. W., Dilles, J. H., and Reed, M. H., 1999, Sulfur isotope record of deep porphyry Cu-Mo mineralizationbarrenthe, Butte, Montana (abs): Geological Society of America Abstracts Programs, v. 31, no 7, p. A-381.

APPENDICES

Appendix A: Standards Used for Microprobe Analyses

Element	Standard	Mineral
Si	Fluorophlogopite	Biotite, Sericite
	Augite	Hornblende
Al	Labradonite	Biotite, Sericite, Hornblende
Mg	Fluorophlogopite	Biotite, Sericite
	Augite	Hornblende
Fe	Augite/basalt	Biotite, Sericite
	Augite	Hornblende
Ti	Basalt	Biotite, Sericite, Hornblende
Mn	Pyroxman	Biotite, Sericite, Hornblende
K	Fluorophlogopite	Biotite, Sericite
	Sanidine	Hornblende
Na	Anorthoclase	Biotite, Sericite, Hornblende
Ca	Augite	Biotite, Sericite, Hornblende
Rb	Rb glass	Biotite, Sericite
Cs	Pollucite	Biotite, Sericite
Ba	Sanidine	Biotite, Sericite
F	Fluorophlogopite	Biotite, Sericite, Hornblende
Cl	Tugtupite	Biotite, Sericite, Hornblende
Cr	Chromite	Hornblende

Appendix B-a: Average Microprobe Analyses of Hornblende, Biotite and Sericite from Fresh and Altered Rocks

Sample	Bu211	Bu211	Bu214	Bu214	Bu96014	Bu96014
Mineral	Biotite	Hornblende	Biotite	Hornblende	Biotite	Hornblende
	Igneous	Igneous	Igneous	Igneous	Igneous	Igneous
	n=13	n= 8	n=12	n= 17	n=15	n=13
Oxide						
SiO2	35.52	47.46	36.10	49.48	36.51	46.69
Al2O3	13.18	6.55	12.74	4.69	12.92	6.11
TiO2	4.03	1.20	3.90	0.64	4.25	1.16
FeO	17.42	14.53	17.34	14.25	19.74	15.95
MgO	11.78	13.40	12.00	13.92	11.76	12.88
MnO	0.41	0.50	0.46	0.63	0.31	0.53
CaO	0.01	11.50	0.01	11.67	0.00	11.36
K2O	9.53	0.74	9.54	0.48	9.61	0.71
Na2O	0.10	1.19	0.10	0.91	0.13	1.16
Rb2O	0.11		0.10		0.11	
Cs2O	0.01		0.01		0.01	
BaO	0.21		0.13		0.00	
Cr2O3		0.02		0.01		0.01
H2O	3.73	1.78	3.60	1.76	3.70	1.71
SUM	96.03	98.86	96.04	98.43	99.05	98.26
Cation	(calculated per 22 oxygen equivalents for mica and 23 oxygen for hbl)					
Si4+	5.61	7.05	5.69	7.34	5.88	7.03
Al3+ (T)	2.39	0.95	2.31	0.66	2.12	0.97
Al3+ (O)	0.07	0.20	0.05	0.16	0.33	0.12
Ti4+	0.48	0.13	0.46	0.07	0.51	0.13
Fe2+	2.30	1.81	2.29	1.77	2.66	2.01
Mg2+	2.78	2.97	2.82	3.08	2.82	2.89
Mn2+	0.06	0.06	0.06	0.08	0.04	0.07
Na+	0.03	0.34	0.03	0.26	0.04	0.34
K+	1.92	0.14	1.92	0.09	1.97	0.14
Ca2+	0.00	1.83	0.00	1.85	0.00	1.83
Rb+	0.01		0.01		0.01	
Cs+	0.00		0.00		0.00	
Ba2+	0.01		0.01		0.00	
Cr3+		0.00		0.00		0.00
Total	15.66	15.71	15.65	15.61	16.40	15.80
Anion						
F-	0.37	0.20	0.49	0.23	0.43	0.24
Cl-	0.02	0.03	0.03	0.02	0.07	0.04
OH-	3.61	1.77	3.48	1.75	3.50	1.73
Fe/(Fe+Mg)	0.45	0.38	0.45	0.36	0.48	0.41
Al/(Fe+Mg+Al	0.33	0.19	0.32	0.14	0.31	0.18

Note: Total Fe was reported as Fe2+

Sample	Bu96001	Bu96001	Bu96001	Bu96001	Bu96001	Bu96001
Mineral	Biotite	Hornblende	Biotite	Biotite	Sericite	Sericite
	Igneous	Igneous	Relict	HT	EDM-f.g.	PGS-PU
	n=12	n= 18	n=16	n=1	n= 8	n=16
Oxide						
SiO2	36.13	48.22	35.69	39.25	46.74	48.02
Al2O3	13.63	5.81	14.52	19.61	32.60	34.49
TiO2	4.53	0.94	4.03	0.56	0.07	0.22
FeO	18.75	15.08	16.91	11.94	2.55	0.65
MgO	12.10	13.87	13.46	14.40	2.26	1.37
MnO	0.33	0.56	0.38	0.25	0.03	0.02
CaO	0.01	11.87	0.22	0.00	0.00	0.02
K2O	9.63	0.60	8.67	9.92	10.19	10.03
Na2O	0.09	0.95	0.08	0.10	0.18	0.21
Rb2O	0.10		0.10	0.08	0.09	0.10
Cs2O	0.03		0.01	0.00	0.01	0.01
BaO	0.17		0.20	0.00	0.10	0.09
Cr2O3		0.01				
H2O	3.83	1.82	3.75	4.43	4.73	4.00
SUM	99.32	99.72	98.02	100.54	99.54	99.22
Cation	(calculated per 22 oxygen equivalents for mica and 23 oxygen for hbl)					
Si4+	5.79	7.11	5.72	6.63	6.58	5.94
Al3+ (T)	2.21	0.89	2.28	1.37	1.42	2.06
Al3+ (O)	0.37	0.12	0.46	4.24	3.99	1.43
Ti4+	0.55	0.10	0.49	0.02	0.01	0.06
Fe2+	2.51	1.86	2.27	0.07	0.30	1.51
Mg2+	2.89	3.05	3.22	0.28	0.47	3.25
Mn2+	0.04	0.07	0.05	0.00	0.00	0.03
Na+	0.03	0.27	0.02	0.06	0.05	0.03
K+	1.97	0.11	1.77	1.77	1.83	1.91
Ca2+	0.00	1.88	0.04	0.00	0.00	0.00
Rb+	0.01		0.01	0.01	0.01	0.01
Cs+	0.00		0.00	0.00	0.00	0.00
Ba2+	0.01		0.01	0.01	0.01	0.00
Cr3+		0.00				
Total	16.40	15.67	16.34	14.47	14.67	16.23
Anion						
F-	0.37	0.18	0.45	0.11	0.13	0.73
Cl-	0.03	0.02	0.03	0.00	0.00	0.01
OH-	3.60	1.80	3.52	3.89	3.87	3.26
Fe/(Fe+Mg)	0.47	0.38	0.41	0.21	0.39	0.32
Al/(Fe+Mg+Al	0.32	0.17	0.33	0.94	0.87	0.42

Note: Total Fe was reported as Fe2+

Sample	11172-2200	11172-2200	11172-2934	11172-2934	11172-3920
Mineral	Biotite Relict	Biotite HT	Biotite Relict	Biotite HT	Biotite Relict
	n=12	n=10	n=7	n=11	n= 6
Oxide					
SiO2	37.11	37.74	37.45	37.01	36.40
Al2O3	16.18	16.16	15.81	16.27	17.18
TiO2	2.96	2.33	2.57	2.33	2.70
FeO	15.89	15.20	15.51	15.70	17.02
MgO	13.60	14.00	14.27	14.11	12.29
MnO	0.23	0.23	0.24	0.26	0.23
CaO	0.01	0.01	0.06	0.06	0.02
K2O	9.98	9.94	9.81	9.45	9.83
Na2O	0.09	0.08	0.12	0.09	0.11
Rb2O	0.10	0.11	0.11	0.11	0.10
Cs2O	0.02	0.01	0.04	0.02	0.02
BaO	0.00	0.00	0.05	0.00	0.01
Cr2O3					
H2O	3.54	3.48	3.52	3.53	3.66
SUM	99.72	99.30	99.56	98.94	99.56
Cation	(calculated per 22 oxygen equivalents for mica and 23 oxygen for hbl)				
Si4+	5.88	5.97	5.91	5.89	5.79
Al3+ (T)	2.12	2.03	2.09	2.11	2.21
Al3+ (O)	0.90	0.99	0.87	0.94	1.02
Ti4+	0.35	0.28	0.33	0.28	0.32
Fe2+	2.11	2.01	2.08	2.09	2.27
Mg2+	3.21	3.30	3.32	3.35	2.92
Mn2+	0.03	0.03	0.03	0.03	0.03
Na+	0.03	0.03	0.04	0.03	0.03
K+	2.02	2.01	1.98	1.91	2.00
Ca2+	0.00	0.00	0.01	0.01	0.00
Rb+	0.01	0.01	0.01	0.01	0.01
Cs+	0.00	0.00	0.00	0.00	0.00
Ba2+	0.00	0.00	0.00	0.00	0.00
Cr3+					
Total	16.66	16.66	16.67	16.65	16.60
Anion					
F-	0.72	0.78	0.74	0.71	0.59
Cl-	0.02	0.02	0.02	0.02	0.02
OH-	3.26	3.20	3.24	3.27	3.39
Fe/(Fe+Mg)	0.40	0.38	0.39	0.38	0.44
Al/(Fe+Mg+Al	0.36	0.36	0.35	0.36	0.38

Note: Total Fe was reported as Fe2+

Sample	11172-3920	11172-4166	11172-4166	Bu96017	Bu96017
Mineral	Biotite HT	Biotite Relict	Biotite HT	Biotite Relict	Biotite HT
	n=10	n=16	n=13	n= 9	n= 8
Oxide					
SiO2	36.48	36.40	36.15	37.12	36.79
Al2O3	16.93	17.40	17.28	15.84	16.19
TiO2	2.65	3.05	2.29	2.72	2.60
FeO	16.52	16.87	17.18	14.65	16.09
MgO	12.27	11.92	11.96	14.48	13.45
MnO	0.21	0.18	0.21	0.20	0.23
CaO	0.02	0.00	0.01	0.01	0.01
K2O	9.79	9.74	9.77	9.71	9.76
Na2O	0.10	0.12	0.09	0.20	0.15
Rb2O	0.10	0.09	0.10	0.10	0.10
Cs2O	0.02	0.03	0.01	0.01	0.02
BaO	0.00	0.04	0.00	0.17	0.00
Cr2O3					
H2O	3.61	3.65	3.57	3.32	3.41
SUM	98.71	99.51	98.63	98.53	98.81
Cation	(calculated per 22 oxygen equivalents for mica and 23 oxygen for hbl)				
Si4+	5.84	5.79	5.82	5.93	5.89
Al3+ (T)	2.16	2.21	2.18	2.07	2.11
Al3+ (O)	1.04	1.07	1.09	0.91	0.94
Ti4+	0.32	0.36	0.28	0.33	0.31
Fe2+	2.21	2.24	2.31	1.96	2.15
Mg2+	2.93	2.81	2.87	3.45	3.21
Mn2+	0.03	0.03	0.03	0.03	0.03
Na+	0.03	0.04	0.03	0.06	0.05
K+	2.00	1.98	2.01	1.98	1.99
Ca2+	0.00	0.00	0.00	0.00	0.00
Rb+	0.01	0.01	0.01	0.01	0.01
Cs+	0.00	0.00	0.00	0.00	0.00
Ba2+	0.00	0.00	0.00	0.01	0.00
Cr3+					
Total	16.58	16.54	16.63	16.73	16.71
Anion					
F-	0.62	0.61	0.65	0.89	0.80
Cl-	0.02	0.02	0.02	0.02	0.02
OH-	3.36	3.37	3.33	3.09	3.17
Fe/(Fe+Mg)	0.43	0.44	0.45	0.36	0.40
Al/(Fe+Mg+Al	0.38	0.39	0.39	0.36	0.36

Note: Total Fe was reported as Fe2+

Sample	11172-4005	11172-4005	Bu96018	Bu96009	Bu96009
Mineral	Biotite Relict	Biotite HT	Biotite HT	Biotite Relict	Biotite HT
	n= 9	n= 18	n=13	n= 12	n=10
Oxide					
SiO2	36.94	36.61	36.11	37.58	36.94
Al2O3	17.67	17.83	16.96	17.71	18.32
TiO2	2.69	2.65	1.68	2.38	1.76
FeO	14.49	14.86	16.76	15.63	16.43
MgO	13.53	13.14	13.10	13.09	12.44
MnO	0.18	0.20	0.33	0.21	0.23
CaO	0.01	0.01	0.03	0.02	0.01
K2O	9.96	9.71	8.34	9.93	9.85
Na2O	0.13	0.12	0.10	0.14	0.16
Rb2O	0.11	0.10	0.11	0.10	0.10
Cs2O	0.02	0.01	0.01	0.02	0.02
BaO	0.02	0.03	0.00	0.02	0.00
Cr2O3					
H2O	3.63	3.63	3.48	3.52	3.49
SUM	99.37	98.91	97.02	100.35	99.75
Cation	(calculated per 22 oxygen equivalents for mica and 23 oxygen for hbl)				
Si4+	5.82	5.80	5.85	5.89	5.84
Al3+ (T)	2.18	2.20	2.15	2.11	2.16
Al3+ (O)	1.10	1.13	1.10	1.16	1.26
Ti4+	0.32	0.32	0.21	0.28	0.21
Fe2+	1.91	1.97	2.28	2.05	2.17
Mg2+	3.18	3.10	3.16	3.06	2.93
Mn2+	0.02	0.03	0.05	0.03	0.03
Na+	0.04	0.04	0.03	0.04	0.05
K+	2.00	1.96	1.73	1.98	1.99
Ca2+	0.00	0.00	0.01	0.00	0.00
Rb+	0.01	0.01	0.01	0.01	0.01
Cs+	0.00	0.00	0.00	0.00	0.00
Ba2+	0.00	0.00	0.00	0.00	0.00
Cr3+					
Total	16.59	16.56	16.56	16.61	16.66
Anion					
F-	0.66	0.64	0.69	0.77	0.77
Cl-	0.01	0.02	0.03	0.02	0.02
OH-	3.32	3.34	3.28	3.21	3.21
Fe/(Fe+Mg)	0.38	0.39	0.42	0.40	0.43
Al/(Fe+Mg+Al	0.39	0.40	0.37	0.39	0.40

Sample	Bu96009	11171-3367	11172-1865	11172-1865	11135-4966
Mineral	Sericite	Biotite HT	Biotite Relict	Biotite HT	Biotite Relict
	n= 7	n=17	n= 14	n= 6	n= 5
Oxide					
SiO2	46.97	38.41	37.56	37.86	37.40
Al2O3	34.55	15.70	15.86	16.58	15.11
TiO2	0.47	1.98	3.14	2.77	2.76
FeO	2.89	11.88	15.35	15.02	12.66
MgO	0.86	17.37	13.95	13.77	16.38
MnO	0.01	0.11	0.29	0.29	0.13
CaO	0.01	0.00	0.01	0.03	0.01
K2O	10.25	10.03	9.84	9.53	9.90
Na2O	0.51	0.18	0.11	0.10	0.22
Rb2O	0.10	0.11	0.10	0.10	0.11
Cs2O	0.00	0.02	0.01	0.02	0.02
BaO	0.01	0.00	0.02	0.00	0.15
Cr2O3					
H2O	4.76	2.88	3.51	3.55	2.92
SUM	101.39	98.68	99.76	99.63	97.79
Cation	(calculated per 22 oxygen equivalents for mica and 23 oxygen for hbl)				
Si4+	6.51	6.06	5.93	5.95	6.00
Al3+ (T)	1.49	1.94	2.07	2.05	2.00
Al3+ (O)	4.16	0.98	0.88	1.02	0.85
Ti4+	0.05	0.23	0.37	0.33	0.33
Fe2+	0.34	1.57	2.00	1.97	1.70
Mg2+	0.18	4.08	3.30	3.23	3.92
Mn2+	0.00	0.02	0.04	0.04	0.02
Na+	0.14	0.06	0.03	0.03	0.07
K+	1.81	2.02	1.98	1.91	2.02
Ca2+	0.00	0.00	0.00	0.01	0.00
Rb+	0.01	0.01	0.01	0.01	0.01
Cs+	0.00	0.00	0.00	0.00	0.00
Ba2+	0.00	0.00	0.00	0.00	0.01
Cr3+					
Total	14.68	16.97	16.63	16.54	16.93
Anion					
F-	0.17	1.33	0.76	0.74	1.25
Cl-	0.00	0.02	0.02	0.02	0.02
OH-	3.83	2.65	3.22	3.25	2.73
Fe/(Fe+Mg)	0.65	0.28	0.38	0.38	0.30
Al/(Fe+Mg+Al	0.92	0.34	0.36	0.37	0.34

Note: Total Fe was reported as Fe2+

Sample	11135-4966	Bu96016	Bu96016	11148-4219.	11148-4219.
Mineral	Biotite HT	Biotite Relict	Biotite HT	Biotite Relict	Biotite HT
	n= 20	n=10	n=12	n= 16	n= 3
Oxide					
SiO2	37.54	37.05	35.93	38.00	38.21
Al2O3	15.24	16.69	17.35	15.90	16.00
TiO2	2.53	2.60	1.72	2.39	2.40
FeO	12.42	14.76	16.83	12.61	12.47
MgO	16.52	13.57	12.13	15.66	15.16
MnO	0.15	0.15	0.18	0.12	0.15
CaO	0.02	0.00	0.01	0.01	0.01
K2O	9.89	9.67	9.89	9.90	9.91
Na2O	0.23	0.16	0.10	0.19	0.19
Rb2O	0.11	0.11	0.10	0.11	0.13
Cs2O	0.01	0.02	0.02	0.02	0.02
BaO	0.00	0.09	0.00	0.09	0.00
Cr2O3					
H2O	2.95	3.44	3.36	3.07	3.13
SUM	97.61	98.31	97.62	98.08	97.77
Cation	(calculated per 22 oxygen equivalents for mica and 23 oxygen for hbl)				
Si4+	6.01	5.91	5.85	6.04	6.08
Al3+ (T)	1.99	2.09	2.15	1.96	1.92
Al3+ (O)	0.89	1.05	1.17	1.02	1.08
Ti4+	0.31	0.31	0.21	0.29	0.29
Fe2+	1.66	1.97	2.29	1.68	1.66
Mg2+	3.94	3.23	2.94	3.71	3.60
Mn2+	0.02	0.02	0.02	0.02	0.02
Na+	0.07	0.05	0.03	0.06	0.06
K+	2.02	1.97	2.05	2.01	2.01
Ca2+	0.00	0.00	0.00	0.00	0.00
Rb+	0.01	0.01	0.01	0.01	0.01
Cs+	0.00	0.00	0.00	0.00	0.00
Ba2+	0.00	0.01	0.00	0.01	0.00
Cr3+					
Total	16.92	16.62	16.74	16.80	16.73
Anion					
F-	1.23	0.78	0.79	1.14	1.09
Cl-	0.02	0.02	0.02	0.01	0.02
OH-	2.75	3.20	3.18	2.84	2.89
Fe/(Fe+Mg)	0.30	0.38	0.44	0.31	0.32
Al/(Fe+Mg+Al	0.34	0.38	0.39	0.36	0.36

Note: Total Fe was reported as Fe2+

Sample	Bu96004	Bu96004	Bu96004	11148-4790.	11148-4790.
Mineral	Biotite Relict	Biotite HT	Sericite HT	Biotite Relict	Biotite HT
	n= 13	n= 3	n=10	n= 13	n= 17
Oxide					
SiO2	36.06	32.59	48.42	38.56	37.24
Al2O3	14.74	16.17	34.29	16.56	17.20
TiO2	3.47	6.57	0.33	2.83	2.18
FeO	16.79	18.23	0.74	11.26	14.64
MgO	14.18	13.02	1.33	16.62	13.90
MnO	0.32	0.49	0.01	0.13	0.18
CaO	0.03	2.22	0.01	0.00	0.01
K2O	8.19	3.38	10.40	9.72	9.26
Na2O	0.09	0.06	0.23	0.15	0.11
Rb2O	0.10	0.07	0.11	0.10	0.11
Cs2O	0.02	0.01	0.01	0.01	0.02
BaO	0.23	0.02	0.00	0.24	0.11
Cr2O3					
H2O	3.78	3.94	4.79	3.28	3.40
SUM	98.00	96.78	100.67	99.47	98.34
Cation	(calculated per 22 oxygen equivalents for mica and 23 oxygen for hbl)				
Si4+	5.80	5.25	6.67	5.99	5.92
Al3+ (T)	2.20	2.75	1.33	2.01	2.08
Al3+ (O)	0.60	0.33	4.24	1.02	1.14
Ti4+	0.42	0.81	0.03	0.33	0.26
Fe2+	2.26	2.46	0.09	1.46	1.95
Mg2+	3.41	3.14	0.27	3.85	3.29
Mn2+	0.04	0.07	0.00	0.02	0.02
Na+	0.03	0.02	0.06	0.05	0.03
K+	1.67	0.67	1.83	1.92	1.88
Ca2+	0.00	0.39	0.00	0.00	0.00
Rb+	0.01	0.01	0.01	0.01	0.01
Cs+	0.00	0.00	0.00	0.00	0.00
Ba2+	0.01	0.00	0.00	0.01	0.01
Cr3+					
Total	16.47	15.90	14.54	16.68	16.60
Anion					
F-	0.45	0.30	0.16	1.02	0.83
Cl-	0.02	0.01	0.00	0.02	0.02
OH-	3.53	3.69	3.83	2.96	3.15
Fe/(Fe+Mg)	0.40	0.44	0.24	0.28	0.37
Al/(Fe+Mg+Al	0.33	0.36	0.94	0.36	0.38

Note: Total Fe was reported as Fe2+

Sample	Bu96006	Bu96006	Bu96006	Bu96015	Bu96015	Bu96007	Bu96007
Mineral	Biotite Relict	Biotite HT	Sericite Sericite	Biotite Relict	Biotite HT	Biotite Relict	Biotite HT
	n= 6	n=10	n= 7	n= 16	n=10	n= 7	n= 12
Oxide							
SiO2	37.51	36.61	47.77	37.39	37.93	38.32	37.76
Al2O3	16.69	17.53	32.23	16.26	16.21	19.45	18.05
TiO2	2.33	1.79	0.21	2.70	2.67	2.27	2.28
FeO	16.41	16.19	2.55	13.27	13.02	13.42	14.56
MgO	12.85	13.74	2.23	15.32	15.46	11.20	12.34
MnO	0.47	0.50	0.05	0.19	0.25	0.23	0.30
CaO	0.01	0.01	0.00	0.01	0.00	0.01	0.01
K2O	9.79	9.06	10.80	9.91	9.99	8.91	9.45
Na2O	0.14	0.07	0.27	0.18	0.15	0.10	0.10
Rb2O	0.12	0.10	0.11	0.10	0.10	0.11	0.10
Cs2O	0.01	0.01	0.00	0.01	0.03	0.03	0.01
BaO	0.14	0.02	0.01	0.02	0.00	0.09	0.02
Cr2O3							
H2O	3.50	3.55	4.67	3.16	3.16	3.67	3.60
SUM	99.96	99.18	100.89	98.51	98.98	97.79	98.59
Cation	(calculated per 22 oxygen equivalents for mica and 23 oxygen for hbl)						
Si4+	5.94	5.80	6.67	5.94	5.98	6.02	5.96
Al3+ (T)	2.06	2.20	1.33	2.06	2.02	1.98	2.04
Al3+ (O)	1.05	1.09	3.97	0.98	1.00	1.62	1.32
Ti4+	0.28	0.21	0.02	0.32	0.32	0.27	0.27
Fe2+	2.17	2.15	0.30	1.76	1.72	1.77	1.93
Mg2+	3.03	3.26	0.46	3.62	3.63	2.63	2.91
Mn2+	0.06	0.07	0.01	0.03	0.03	0.03	0.04
Na+	0.04	0.02	0.07	0.05	0.05	0.03	0.03
K+	1.98	1.83	1.92	2.01	2.01	1.79	1.91
Ca2+	0.00	0.00	0.00	0.00	0.00	0.00	0.00
Rb+	0.01	0.01	0.01	0.01	0.01	0.01	0.01
Cs+	0.00	0.00	0.00	0.00	0.00	0.00	0.00
Ba2+	0.01	0.00	0.00	0.00	0.00	0.01	0.00
Cr3+							
Total	16.63	16.63	14.77	16.79	16.77	16.15	16.41
Anion							
F-	0.76	0.70	0.21	1.06	1.07	0.63	0.68
Cl-	0.02	0.02	0.00	0.02	0.02	0.02	0.02
OH-	3.22	3.28	3.78	2.92	2.91	3.35	3.30
Fe/(Fe+Mg)	0.42	0.40	0.39	0.33	0.32	0.40	0.40
Al/(Fe+Mg+Al	0.37	0.38	0.87	0.36	0.36	0.45	0.41

Note: Total Fe was reported as Fe2+

Sample	11171-4911	11171-4911	11135-3481	11135-3481	11135-3586
Mineral	Biotite Relict	Biotite HT	Biotite Relict	Biotite HT	Biotite HT
	n= 12	n= 7	n=10	n= 17	n= 9
Oxide					
SiO2	37.55	38.97	39.22	39.45	36.50
Al2O3	15.03	14.60	15.98	17.09	16.48
TiO2	2.84	2.38	2.49	1.65	1.82
FeO	12.72	8.92	7.53	7.43	13.62
MgO	16.15	19.33	19.08	18.38	15.06
MnO	0.21	0.17	0.11	0.11	0.14
CaO	0.01	0.00	0.00	0.00	0.03
K2O	9.99	10.32	10.15	10.33	8.31
Na2O	0.19	0.18	0.22	0.20	0.15
Rb2O	0.10	0.10	0.10	0.10	0.10
Cs2O	0.01	0.01	0.02	0.01	0.01
BaO	0.08	0.00	0.18	0.00	0.01
Cr2O3					
H2O	3.05	2.79	2.83	2.91	3.09
SUM	97.92	97.76	97.90	97.66	95.31
Cation	(calculated per 22 oxygen equivalents for mica and 23 oxygen for hbl)				
Si4+	5.86	5.95	5.67	5.70	5.56
Al3+ (T)	2.14	2.05	2.33	2.30	2.44
Al3+ (O)	0.62	0.59	0.40	0.61	0.52
Ti4+	0.33	0.27	0.27	0.18	0.21
Fe2+	1.66	1.14	0.91	0.90	1.74
Mg2+	3.75	4.40	4.11	3.97	3.43
Mn2+	0.03	0.02	0.01	0.01	0.02
Na+	0.06	0.05	0.06	0.06	0.04
K+	1.99	2.01	1.87	1.91	1.61
Ca2+	0.00	0.00	0.00	0.00	0.00
Rb+	0.01	0.01	0.01	0.01	0.01
Cs+	0.00	0.00	0.00	0.00	0.00
Ba2+	0.01	0.00	0.01	0.00	0.00
Cr3+					
Total	16.47	16.50	15.66	15.65	15.58
Anion					
F-	1.14	1.42	1.42	1.35	1.04
Cl-	0.02	0.02	0.01	0.01	0.02
OH-	2.84	2.56	2.57	2.64	2.94
Fe/(Fe+Mg)	0.31	0.21	0.18	0.18	0.34
Al/(Fe+Mg+Al	0.34	0.32	0.35	0.37	0.36

Note: Total Fe was reported as Fe2+

Appendix B-b: Average Microprobe Analyses of Sericite from QSP Alteration

Sample	10969-2627	10969-2627	10969-5452	10969-5452	10969-5452
Mineral	PU ser*	HT ser*	PU ser	HT ser	Vn HT ser*
	n=16	n=18	n=12	n=14	n=4
Oxide					
SiO2	48.58	47.47	49.06	48.32	47.94
Al2O3	33.97	35.12	31.99	32.61	33.18
TiO2	0.44	0.11	0.57	0.18	0.11
FeO	0.72	1.06	0.46	0.46	0.21
MgO	1.09	1.15	2.04	1.98	1.62
MnO	0.01	0.01	0.02	0.01	0.01
CaO	0.02	0.01	0.01	0.01	0.03
K2O	9.34	9.81	9.92	10.01	10.03
Na2O	0.11	0.17	0.09	0.09	0.10
Rb2O	0.09	0.09	0.10	0.09	0.09
Cs2O	0.01	0.01	0.01	0.01	0.00
BaO	0.05	0.13	0.07	0.09	0.10
H2O	4.50	4.45	4.13	4.13	4.18
SUM	98.93	99.58	98.46	98.01	97.59
F (wt%)	0.82	0.90	1.41	1.36	1.23
Cl (wt%)	0.01	0.01	0.00	0.01	0.01
Cation	(calculated based on 22 oxygen equivalent)				
Si4+	6.72	6.57	6.82	6.76	6.73
Al3+ (T)	1.28	1.43	1.18	1.24	1.27
Al3+	5.54	5.73	5.24	5.38	5.49
Al3+ (O)	4.26	4.30	4.06	4.14	4.22
Ti4+	0.05	0.01	0.06	0.02	0.01
Fe2+	0.09	0.12	0.05	0.05	0.02
Mg2+	0.22	0.24	0.42	0.41	0.34
Mn2+	0.00	0.00	0.00	0.00	0.00
Na+	0.03	0.05	0.02	0.03	0.03
K+	1.65	1.73	1.76	1.79	1.80
Ca2+	0.00	0.00	0.00	0.00	0.00
Rb+	0.01	0.01	0.01	0.01	0.01
Cs+	0.00	0.00	0.00	0.00	0.00
Ba2+	0.00	0.01	0.00	0.01	0.01
Total	14.31	14.46	14.40	14.46	14.44
Anion					
F-	0.36	0.39	0.62	0.60	0.55
Cl-	0.00	0.00	0.00	0.00	0.00
OH-	3.64	3.60	3.38	3.40	3.45
Fe/(Fe+Mg)	0.27	0.34	0.11	0.12	0.07
Al/(Fe+Mg+Al)	0.95	0.94	0.92	0.92	0.94
Al/Si	0.82	0.87	0.77	0.80	0.82

Notes:

1. PU ser: pseudomophycing igneous biotite grains
2. HT ser: fine-grained hydrothermal sericite
3. *Vein HT Ser (or next to veinlet)

Sample	10969-5618	10969-5618	10969-6448	10969-6448	11052-2851
Mineral	PU Ser	HT Ser	PU ser	HT Ser	PU Ser
	n=11	n=8	n=7	n=20	n=10
Oxide					
SiO2	52.50	50.10	52.36	48.28	47.89
Al2O3	35.11	36.71	31.14	33.30	32.34
TiO2	0.26	0.20	0.19	0.16	0.66
FeO	0.38	1.58	0.41	1.09	1.16
MgO	1.40	1.29	1.45	1.97	1.42
MnO	0.01	0.01	0.00	0.02	0.01
CaO	0.02	0.00	0.01	0.00	0.00
K2O	6.91	7.85	8.92	10.40	10.46
Na2O	0.07	0.12	0.07	0.12	0.09
Rb2O	0.10	0.10	0.00	0.00	0.11
Cs2O	0.02	0.01	0.01	0.01	0.01
BaO	0.10	0.05	0.05	0.06	0.04
H2O	4.51	4.66	4.37	4.19	4.34
SUM	101.38	102.71	98.99	99.61	98.52
F (wt%)	1.21	0.93	1.14	1.34	0.97
Cl (wt%)	0.00	0.00	0.01	0.01	0.00
Cation	(calculated based on 22 oxygen equivalent)				
Si4+	6.92	6.63	7.13	6.68	6.72
Al3+ (T)	1.08	1.37	0.87	1.32	1.28
Al3+	5.46	5.72	5.05	5.43	5.35
Al3+ (O)	4.38	4.35	4.17	4.11	4.07
Ti4+	0.03	0.02	0.02	0.02	0.07
Fe2+	0.04	0.18	0.05	0.13	0.14
Mg2+	0.27	0.25	0.30	0.41	0.30
Mn2+	0.00	0.00	0.00	0.00	0.00
Na+	0.02	0.03	0.02	0.03	0.02
K+	1.16	1.33	1.56	1.84	1.88
Ca2+	0.00	0.00	0.00	0.00	0.00
Rb+	0.01	0.01	0.00	0.00	0.01
Cs+	0.00	0.00	0.00	0.00	0.00
Ba2+	0.01	0.00	0.00	0.00	0.00
Total	13.92	14.17	14.12	14.53	14.49
Anion					
F-	0.51	0.39	0.49	0.59	0.43
Cl-	0.00	0.00	0.00	0.00	0.00
OH-	3.49	3.61	3.51	3.41	3.57
Fe/(Fe+Mg)	0.13	0.41	0.14	0.24	0.31
Al/(Fe+Mg+Al)	0.95	0.93	0.94	0.91	0.92
Al/Si	0.79	0.86	0.71	0.81	0.80

Sample	11052-2851	11052-5532	11052-5532	11052-6639	11052-6639
Mineral	HT Ser	PU Ser	HT Ser	PU ser	HT ser
	n=11	n=15	n=12	n=6	n=10
Oxide					
SiO2	46.79	48.34	48.97	46.02	47.16
Al2O3	33.05	32.54	34.06	32.80	33.45
TiO2	0.07	0.31	0.09	1.40	0.12
FeO	1.71	0.61	1.23	0.99	0.56
MgO	1.42	1.62	1.72	1.82	1.95
MnO	0.00	0.01	0.02	0.00	0.01
CaO	0.00	0.01	0.01	0.01	0.00
K2O	11.02	9.53	10.21	10.65	10.53
Na2O	0.10	0.09	0.10	0.14	0.15
Rb2O	0.12	0.00	0.00	0.11	0.11
Cs2O	0.01	0.01	0.01	0.00	0.01
BaO	0.05	0.04	0.22	0.12	0.04
H2O	4.30	4.14	4.24	4.09	4.04
SUM	98.65	97.25	100.86	98.15	98.12
F (wt%)	0.98	1.30	1.38	1.33	1.49
Cl (wt%)	0.00	0.01	0.01	0.01	0.01
Cation	(calculated based on 22 oxygen equivalent)				
Si4+	6.61	6.79	6.68	6.51	6.62
Al3+ (T)	1.39	1.21	1.32	1.49	1.38
Al3+	5.50	5.39	5.48	5.47	5.53
Al3+ (O)	4.11	4.17	4.16	3.98	4.15
Ti4+	0.01	0.03	0.01	0.15	0.01
Fe2+	0.20	0.07	0.14	0.12	0.07
Mg2+	0.30	0.34	0.35	0.38	0.41
Mn2+	0.00	0.00	0.00	0.00	0.00
Na+	0.03	0.02	0.03	0.04	0.04
K+	1.99	1.71	1.78	1.92	1.89
Ca2+	0.00	0.00	0.00	0.00	0.00
Rb+	0.01	0.00	0.00	0.01	0.01
Cs+	0.00	0.00	0.00	0.00	0.00
Ba2+	0.00	0.00	0.01	0.01	0.00
Total	14.65	14.36	14.48	14.61	14.58
Anion					
F-	0.44	0.58	0.60	0.59	0.66
Cl-	0.00	0.00	0.00	0.00	0.00
OH-	3.56	3.42	3.40	3.40	3.34
Fe/(Fe+Mg)	0.40	0.17	0.29	0.23	0.14
Al/(Fe+Mg+Al)	0.92	0.93	0.92	0.92	0.92
Al/Si	0.83	0.79	0.82	0.84	0.84

Sample	11052-7037	11052-7037	11052-7285	11052-7285	11052-7369
Mineral	PU Ser	HT Ser	PU ser(?)	HT ser	PU Ser
	n=7	n=10	n=7	n=14	n=8
Oxide					
SiO2	48.26	47.84	47.14	46.44	48.49
Al2O3	34.28	33.73	33.40	33.67	32.36
TiO2	0.35	0.22	0.91	0.34	0.35
FeO	0.44	0.77	0.70	0.94	0.64
MgO	1.61	1.78	1.64	1.54	2.08
MnO	0.01	0.01	0.02	0.00	0.01
CaO	0.00	0.00	0.00	0.00	0.00
K2O	10.75	10.77	10.31	10.55	10.61
Na2O	0.16	0.21	0.19	0.19	0.18
Rb2O	0.08	0.09	0.09	0.10	0.08
Cs2O	0.03	0.02	0.01	0.00	0.02
BaO	0.05	0.10	0.08	0.10	0.07
H2O	4.18	4.08	4.15	4.13	3.94
SUM	100.19	99.63	98.63	98.00	98.83
F (wt%)	1.42	1.51	1.33	1.27	1.72
Cl (wt%)	0.02	0.02	0.00	0.00	0.02
Cation	(calculated based on 22 oxygen equivalent)				
Si4+	6.63	6.63	6.59	6.56	6.75
Al3+ (T)	1.37	1.37	1.41	1.44	1.25
Al3+	5.55	5.51	5.50	5.60	5.31
Al3+ (O)	4.18	4.13	4.10	4.16	4.05
Ti4+	0.04	0.02	0.10	0.04	0.04
Fe2+	0.05	0.09	0.08	0.11	0.07
Mg2+	0.33	0.37	0.34	0.32	0.43
Mn2+	0.00	0.00	0.00	0.00	0.00
Na+	0.04	0.06	0.05	0.05	0.05
K+	1.88	1.90	1.84	1.90	1.88
Ca2+	0.00	0.00	0.00	0.00	0.00
Rb+	0.01	0.01	0.01	0.01	0.01
Cs+	0.00	0.00	0.00	0.00	0.00
Ba2+	0.00	0.01	0.00	0.01	0.00
Total	14.54	14.59	14.52	14.60	14.54
Anion					
F-	0.62	0.66	0.59	0.57	0.75
Cl-	0.00	0.01	0.00	0.00	0.00
OH-	3.38	3.33	3.41	3.43	3.24
Fe/(Fe+Mg)	0.13	0.20	0.19	0.26	0.15
Al/(Fe+Mg+Al)	0.94	0.92	0.93	0.93	0.91
Al/Si	0.84	0.83	0.84	0.85	0.79

Sample	11052-7369	11052-7522	11148-888	11148-888	11148-1140
Mineral	HT ser	HT ser	PU ser	HT ser	PU ser
	n=21	n= 20	n=12	n=12	n=6
Oxide					
SiO2	47.95	46.81	48.68	49.45	46.97
Al2O3	32.83	34.70	33.24	33.14	30.79
TiO2	0.21	0.22	0.50	0.12	0.36
FeO	1.03	1.02	0.66	0.72	1.25
MgO	2.02	1.30	1.52	1.91	1.72
MnO	0.01	0.01	0.01	0.02	0.01
CaO	0.00	0.00	0.02	0.04	0.02
K2O	10.62	10.36	9.71	9.70	9.54
Na2O	0.20	0.21	0.16	0.16	0.14
Rb2O	0.09	0.09	0.11	0.11	0.10
Cs2O	0.01	0.01	0.00	0.00	0.00
BaO	0.06	0.06	0.08	0.17	0.09
H2O	3.96	4.07	4.78	4.77	4.52
SUM	98.99	98.85	99.47	100.31	95.53
F (wt%)	1.68	1.48	0.33	0.43	0.40
Cl (wt%)	0.02	0.01	0.01	0.01	0.01
Cation	(calculated based on 22 oxygen equivalent)				
Si4+	6.68	6.53	6.74	6.79	6.80
Al3+ (T)	1.32	1.47	1.26	1.21	1.20
Al3+	5.39	5.70	5.43	5.36	5.26
Al3+ (O)	4.07	4.23	4.17	4.15	4.06
Ti4+	0.02	0.02	0.05	0.01	0.04
Fe2+	0.12	0.12	0.08	0.08	0.15
Mg2+	0.42	0.27	0.31	0.39	0.37
Mn2+	0.00	0.00	0.00	0.00	0.00
Na+	0.06	0.06	0.04	0.04	0.04
K+	1.89	1.84	1.72	1.70	1.76
Ca2+	0.00	0.00	0.00	0.01	0.00
Rb+	0.01	0.01	0.01	0.01	0.01
Cs+	0.00	0.00	0.00	0.00	0.00
Ba2+	0.00	0.00	0.00	0.01	0.01
Total	14.59	14.56	14.39	14.41	14.45
Anion					
F-	0.74	0.65	0.14	0.19	0.18
Cl-	0.01	0.00	0.00	0.00	0.00
OH-	3.26	3.35	3.86	3.81	3.82
Fe/(Fe+Mg)	0.22	0.31	0.20	0.18	0.29
Al/(Fe+Mg+Al)	0.91	0.94	0.93	0.92	0.91
Al/Si	0.81	0.87	0.80	0.79	0.77

Sample	11148-1140	11170-864.5	11170-864.5	11170-4871.	11170-4871.
Mineral	HT ser	PU Ser	HT Ser	PU Ser	HT ser
	n=8	n= 14	n= 14	n=10	n=20
Oxide					
SiO2	48.62	49.60	48.28	48.16	47.27
Al2O3	33.02	34.20	33.42	34.70	35.17
TiO2	0.12	0.26	0.08	0.45	0.36
FeO	1.24	0.30	0.87	0.61	0.99
MgO	1.73	1.22	2.14	1.46	1.20
MnO	0.02	0.01	0.01	0.02	0.01
CaO	0.03	0.02	0.01	0.01	0.02
K2O	9.61	9.42	10.33	10.61	10.62
Na2O	0.13	0.11	0.14	0.18	0.22
Rb2O	0.11	0.11	0.10	0.10	0.10
Cs2O	0.00	0.02	0.02	0.02	0.03
BaO	0.12	0.06	0.25	0.14	0.11
H2O	4.69	4.61	4.46	4.23	4.28
SUM	99.44	99.93	100.11	100.69	100.40
F (wt%)	0.46	0.73	0.90	1.36	1.21
Cl (wt%)	0.01	0.02	0.02	0.01	0.01
Cation	(calculated based on 22 oxygen equivalent)				
Si4+	6.75	6.78	6.67	6.59	6.51
Al3+ (T)	1.25	1.22	1.33	1.41	1.49
Al3+	5.40	5.51	5.44	5.60	5.71
Al3+ (O)	4.15	4.28	4.11	4.19	4.22
Ti4+	0.01	0.03	0.01	0.05	0.04
Fe2+	0.14	0.03	0.10	0.07	0.11
Mg2+	0.36	0.25	0.44	0.30	0.25
Mn2+	0.00	0.00	0.00	0.00	0.00
Na+	0.03	0.03	0.04	0.05	0.06
K+	1.70	1.64	1.82	1.85	1.87
Ca2+	0.00	0.00	0.00	0.00	0.00
Rb+	0.01	0.01	0.01	0.01	0.01
Cs+	0.00	0.00	0.00	0.00	0.00
Ba2+	0.01	0.00	0.01	0.01	0.01
Total	14.43	14.28	14.54	14.52	14.57
Anion					
F-	0.20	0.31	0.39	0.59	0.53
Cl-	0.00	0.00	0.00	0.00	0.00
OH-	3.80	3.68	3.60	3.41	3.47
Fe/(Fe+Mg)	0.29	0.12	0.19	0.19	0.32
Al/(Fe+Mg+Al)	0.91	0.95	0.91	0.94	0.94
Al/Si	0.80	0.81	0.82	0.85	0.88

Sample	11170-4936	11170-4936	11170-5333	11170-5333
Mineral	PU Ser	HT Ser	PU Ser	HT ser
	n=7	n=14	n=3	n=19
Oxide				
SiO2	48.40	49.43	48.99	48.87
Al2O3	34.78	33.49	33.94	34.77
TiO2	0.53	0.54	0.55	0.24
FeO	0.39	0.90	1.08	0.90
MgO	1.21	1.42	1.96	1.57
MnO	0.01	0.01	0.01	0.01
CaO	0.00	0.00	0.01	0.00
K2O	10.04	9.94	10.27	10.38
Na2O	0.17	0.18	0.13	0.16
Rb2O	0.12	0.12	0.10	0.11
Cs2O	0.04	0.04	0.04	0.04
BaO	0.05	0.13	0.11	0.15
H2O	4.45	4.44	4.31	4.38
SUM	100.20	100.62	101.48	101.58
F (wt%)	0.98	1.02	1.29	1.18
Cl (wt%)	0.01	0.01	0.01	0.01
Cation	(calculated based on 22 oxygen equivalent)			
Si4+	6.63	6.75	6.65	6.63
Al3+ (T)	1.37	1.25	1.35	1.37
Al3+	5.62	5.40	5.43	5.56
Al3+ (O)	4.25	4.15	4.08	4.19
Ti4+	0.05	0.05	0.06	0.02
Fe2+	0.05	0.10	0.12	0.10
Mg2+	0.25	0.29	0.40	0.32
Mn2+	0.00	0.00	0.00	0.00
Na+	0.05	0.05	0.03	0.04
K+	1.76	1.73	1.78	1.80
Ca2+	0.00	0.00	0.00	0.00
Rb+	0.01	0.01	0.01	0.01
Cs+	0.00	0.00	0.00	0.00
Ba2+	0.00	0.01	0.01	0.01
Total	14.41	14.40	14.49	14.49
Anion				
F-	0.43	0.44	0.56	0.50
Cl-	0.00	0.00	0.00	0.00
OH-	3.57	3.56	3.44	3.49
Fe/(Fe+Mg)	0.15	0.26	0.24	0.24
Al/(Fe+Mg+Al)	0.95	0.93	0.91	0.93
Al/Si	0.85	0.80	0.82	0.84

Appendix C: Sample Descriptions

The mineralogy of Butte Quartz Monzonite (BQM) consists of 38.5-42% plagioclase (plg), 18.7-22.6% K-feldspar (ksp), 21.4-23.7% quartz (qtz), 7.6-9.4% biotite (biot), 5% hornblende (hbl), and 1% magnetite. Primary quartz was a stable phase in all alteration processes. Alteration of hornblende, biotite, plagioclase, and K-feldspar are recorded below; If a mineral is not mentioned, it is present and fresh. The percentages below are visual estimates based on petrographic examination and represent the volume percentage.

Abbreviations: sericite: ser; pyrite: py; chlorite: chl; hydrothermal: HT; carb: carbonate; disseminated: diss'd; anhydrite: anhy; chalcopyrite:ccp; molybdenite: mo; quartz: qtz.

Samples with nine digits numbers were from GRL collection. The first five digits represent the drill core number (such as: 11135: DDH 2; 11148: DDH3; 11166: DDH 5; 11171: DDH 8; 11172: DDH 10) and the last four digits indicate the depth (in feet) from surface where the sample was collected. Other samples were from surface collected in 1996.

Bu96001: BQM: py-qtz vein with alteration envelops of Pale Green Sericite (PGS-inner selvage) and Early Dark Micaceous (EDM-outer selvage), cutting weakly biot-altered BQM. (1) PGS: mafic sites were replaced by 40-60 % HT ser (5% secondary biot near EDM selvage), 10-20 % qtz, 20% sulfide(s), 1-20 % ksp, and <5% calcite (or clay ?); feldspars were replaced by fine to coarse grained ser (70-75%), qtz (20%), and 5-10% diss'd sulfide(s); 1% ksp is present (most is around sulfide grains); BQM rock texture is destroyed. (2) the EDM alteration assemblage: mafic minerals were replaced by secondary green and brown biot (60%), ser (5%), and chl (5-10%), 10% ksp, 10% qtz, 10% sulfide(s), and trace rutile. However, some igneous biot grains are intact. Feldspars were replaced by 50% HT ser, 1% biot, <1% chl, 20-40% qtz, <5% diss'd sulfide(s), ~10% secondary ksp, and minor calcite; (3) In BQM, hbl is present with 1-5% HT biot; igneous biot partly (~ 5%, in general) altered to chl, secondary biot, oxide(s) and calcite; plg near EDM alteration zone is partly (5-10%) replaced by HT ser and/or biot, and secondary ksp. Primary ksp remains intact or slightly altered to ser (< 1%). There are numerous chl, and ksp veinlets in the sample.
Isotope compositions (O, H) are obtained from fresh BQM biot and hbl.

Bu96014: BQM: igneous hbl weakly altered 5-10% to calcite, 1-5% to diss'd sulfide(s); Biot is weakly altered and contains up to 5% chl, 2% sulfide(s), minor calcite, and/or epidote, also around the rims of some biot grains have altered to secondary biot, ksp and qtz. Plg is altered to <1% ser.

Bu211: BQM: hbl is partly replaced by 5-40% calcite and 10% sulfides. Biot is replaced by 3-5 % chl. Plg and ksp are weakly altered to biot and ser near hbl. Tiny calcite-chl veinlets cut through the sample. Along the veinlets, hbl is partly (50%) replaced by calcite and sulfide; biot is partly (5-10%) replaced by chl; plg and ksp are partly altered to biot and ser.

Bu214: BQM: hbl is replaced by 5-10% sulfides. Biot contains 1% chl. Plg and ksp are weakly altered to biot near hbl. A vuggy veinlet may have contained anhy?

11172-1865: BQM: 1 cm wide EDM (biot90(%)-ccp5(%)-py-mt-vug5(%)) veinlet with an inner 2 cm wide ksp selvage and outer pervasive biot alteration background. (1) The inner selvage consists of up to 90% pink ksp with ~5% biot, 3% of cavities, and 1-2% calcite. (2) In the pervasive biot alteration: hbl is altered to biot (50%), qtz (40%), ccp and py (5%), calcite (5%), and minor secondary ksp; igneous biot is rimmed (20%) and replaced by secondary biot and calcite. Plg is ~5-10 % altered to clay.

11172-2200: BQM: numerous (<1 mm wide) EDM (biot-ccp-py-mt-anhy) veinlets occur within pervasive biot alteration: hbl is altered to biot (60-70%), qtz (20-30%), ccp and py (5-10%), anhy (1%), and secondary ksp (<2%). Biot rims are partly (2-5%) replaced by secondary biot, ksp, qtz, anhy, and sulfide(s). Plg is slightly altered to HT biot near hbl sites and biot; ksp looks fresh, but exhibits a "dirty cloud" of very fine-grained biot?

11172-2934: BQM: numerous EDM veinlets and 1-3 mm anhy-qtz veinlets occur within pervasive biot alteration zone: Hbl is altered to biot (70%), qtz (10-20%), anhy (1%), ccp and py (5-10%), and minor chl. HT alteration minerals (2-5%) of secondary biot, qtz, and chl formed outer fringe around relict primary biot grains. Plg is weakly altered to biot and ser near hbl sites and biot; ksp is ~1% altered to secondary ksp and anhy(?) near veinlets of qtz-anhy-ccp-biot and anhy-ksp.

11172-3920: BQM: 1.5-2 cm wide qtz-ccp-mo-anhy-ksp-biot veinlets and numerous EDM veinlets with EDM selvage and pervasive biot alteration background: (1) EDM: mafic minerals are replaced by secondary biot (40%), secondary ksp (40%), qtz (10%), chl (1%), and anhy (5-10%); plg is slightly altered to biot, and minor amount of secondary ksp and anhy. (2) Pervasive biot alteration: hbl is replaced by 50-70% biot, 10-30% qtz, 10-20% anhy, and 1% sulfide(s). Biot rims are 1-5% altered to secondary biot ± chl, qtz, oxide(s), and sulfide(s). Plg is locally altered to biot.

11172-4005: BQM: many 1 mm wide biot-ccp-mo-anhy veinlets with EDM alteration selvages. The sample contains 70% of ksp, 10-15% qtz, 10% mafics, <5% anhy, <2% ccp; mafic minerals are replaced by 80% secondary biot, <5% chl, qtz, <5% oxide(s), ± secondary ksp, and anhy. A few relict igneous biot grains are present. Plg (rare-only about 5 grains in the entire sample) is mostly altered to secondary ksp, qtz, and possible very fine-grained biot, and/or calcite. Both primary and secondary ksp are weakly altered to biot.

11172-4166: BQM: 0.5 cm wide biot-ccp-py-anhy veinlets with narrow EDM selvage occur within the pervasive biot alteration zone. (1) EDM selvage is 2-3 mm wide. Both mafic minerals and feldspars are replaced by secondary biot (20%), secondary ksp (40%), qtz (25%), calcite (10%), and sulfides (5%). Rock texture was destroyed. (2) Pervasive biot: hbl was replaced by biot (50%), qtz (30%), and minor secondary ksp, sulfide(s), and calcite. Biot is rimmed by secondary biot and qtz. 10-20% of the plg and 5% of the ksp are replaced by calcite and minor biot.

Bu96017: BQM: 0.3 cm and 0.6 cm wide EDM veinlets (ksp-qtz-biot-sulfides-vug) occur in pervasive biot alteration. Hbl is replaced by 50-70% biot, 30% ksp, 5-10% qtz, 5-10% sulfide(s), and minor rutile. Igneous biot rims are partly (5-10%) replaced by secondary biot, ksp, qtz, and sulfide(s). Plg is slightly altered to biot or ser. ksp was replaced by 55% qtz, 30% secondary ksp and 10% biot, and 5% diss'd sulfide(s) near the veinlets, elsewhere ksp is unaltered. About 5% cavities (anhy?) are present in mafic sites and veinlets.

Bu96018: Biot Breccia: the sample consists of 2% crystals (~1-2 mm) of biot, qtz, ksp, and sulfides sat in a (<0.1 mm) matrix, consisting of about 30% ksp, 50% qtz, 10% fine-grained biot ± chl, 10% diss'd sulfides, and minor oxide(s).

11171-3367: BQM: small EDM veinlets (qtz-ksp-ccp-calcite(5%)-vug(1%)-biot+ser+chl) with EDM alteration selvage and ~2% pore space: mafic minerals are replaced by 60% biot, 20% ksp, 20% qtz, 1% sulfide(s), and 1% rutile. Plg is replaced by 70% biot and ser, 20% ksp, and 10% qtz. Primary ksp is partly replaced by biot, ser, and secondary ksp.

Bu96004: BQM: 0.2 cm wide qtz-ccp-vug(5%)-ser veinlet with a PGS selvage cross-cutting qtz-mo veinlets and EDM (>1mm qtz-ksp, and anhy?? (vug??-sulfides) veinlets with EDM selvages with younger green argillic alteration. (1) PGS: 1-2 mm wide, texture destructive zone contains 70% ser, 5% secondary biot, 20% qtz, 5% sulfide(s), and trace secondary ksp and calcite. (2) EDM selvage with argillic alteration: mafic minerals are replaced by 70-80% secondary biot, 10-20% ksp, 5-20 % qtz, 2% sulfide(s), and <1% rutile. No igneous biot remains. Plg is replaced by 20-30% biot and ser, 30% mont (± kao), 20% ksp, 10% qtz, 2% sulfide(s), and 5-10% oxide(s). Igneous ksp is partly (5-10%) altered to biot. About 5% cavities occur in the veinlets, and a few in mineral sites.
Isotope compositions (O, H) have been obtained from the EDM alteration selvage with argillic alteration.

Bu96006: BQM: two 0.2 cm wide qtz-py veinlets with 0.5 cm wide Pale Green Sericite alteration selvage, and an EDM veinlet with 0.5 cm wide EDM selvage occur within pervasive biot alteration with a later chl-ser-epidote alteration event. (1) PGS mineral assemblage: mafic minerals and feldspar sites are altered to texture-destructive ser, qtz, sulfide(s), oxide(s), and minor clay (?), and trace HT biot, chl, and ksp. (2) EDM selvage: mafic minerals are replaced by green and brown biot, ser, chl (±), qtz, sulfide(s), and rutile. Feldspars are replaced by ser, biot, chl (±), qtz, and diss'd sulfide(s). Very little, if any, ksp is present. (3) pervasive biot zone: hbl is replaced by 70% green and brown biot, 5% chl, minor ser, 10% qtz, 5-10% sulfide(s), 5-10% rutile, and <1% epidote. Igneous biot is partly (up to 15%) replaced by 10% chl, 1-2% secondary biot and ser, and 1% epidote. Plg and ksp are partly (10-50%) replaced by biot and ser, qtz, secondary ksp, sulfide(s), and minor epidote; Igneous ksp is present in the outer zone.
Isotope compositions (O, H) have been obtained from the pervasive biot alteration.

Bu96007: BQM: 0.3 cm vuggy qtz-ccp-py veinlet with 1 cm wide PGS alteration selvage, and EDM/pervasive biot halos with late (**green or white??**) argillic alteration: (1) PGS: mafic sites are replaced by >80% ser, <1% biot, 10% qtz, 5% sulfide(s), and minor rutile; feldspars are replaced by med-grained ser (60%), biot (2%), qtz (30%, sulfide(s) or oxide (<1%); no ksp is present and rock texture was destroyed. (2) EDM with argillic alteration: hbl is replaced by secondary green and brown biot, ser, qtz, sulfide(s), and rutile. Igneous biot rims are about 10% replaced by secondary biot, ser, qtz, minor sulfide(s) and rutile. Feldspars are replaced by ser, biot, qtz, secondary ksp, 5-10% clay, and ± diss'd sulfide(s). (3) In the outer pervasive biot zone, plg is replaced by 70-90% clay(**?**), 10-30% biot and ser, minor ksp. Primary ksp is present in the outer zone. (Numerous vuggy qtz veinlets are present in the sample.)

Isotope compositions (O, H) have been obtained from the pervasive biot zone with late argillic alteration.

Bu96009: Biot Breccia /BQM: 0.3 cm wide qtz-mo veinlets with PGS selvages, and 0.1 cm wide EDM veinlet with EDM selvages, within pervasive biot with weak argillic alteration. (1) Biot Breccia-PGS: primary mafic minerals and feldspar are replaced by ser, secondary biot, chl, qtz, 20% sulfide, secondary ksp, and rutile; The BQM texture is destroyed; (2) EDM selvage with weak argillic alteration: hbl is replaced by 60-70% green and brown biot, minor ser and chl, 5-10% ksp, 10% qtz, and 20% sulfide(s). Igneous biot is partly (10%) rimmed by secondary biot and chl, minor ksp, 1% sulfide(s), and 1% oxide(s). Feldspars are replaced by med-grained ser (40%), secondary ksp (40%), qtz (10-20%), and minor sulfide(s) and oxide(s). <3% clay is present in plg sites. (3) pervasive biotitization with argillic alteration: mafic minerals alteration are similar to those in EDM selvage, but plg is partly (~50%) replaced by kao (%?), ser, biot, and ksp.
Isotope compositions (O, H) have been obtained from the pervasive biot zone with argillic alteration.

Bu960015: BQM: two 0.8 cm wide qtz-ccp-mt veinlets cross cut a qtz-mo veinlet. Numerous EDM veinlets are also present. Pervasive biot alteration is overprinted by late green argillic alteration: hbl is replaced by 60-70% biot, 20-30% qtz, 5-10% ksp, 1% sulfide(s) and rutile, and minor calcite. Primary biot is rimmed and partly replaced by secondary biot, qtz, ksp, minor sulfide(s), rutile, and calcite. Plg is 90% replaced by 60% mont (± kao), 10-20% calcite, 5% ksp, 10% biot and ser, and qtz. About 10% cavities occur in plg and some in hbl sites.

Bu960016: BQM: numerous EDM veinlets with EDM and pervasive biot alteration zone and strong late green and white argillic alteration: hbl is replaced by 50% biot, 10-20% chl, 30% qtz, 5% sulfide(s), minor rutile and calcite. Biot is partly (~20%) replaced by chl (~10%), secondary biot and ser (~10%), sulfide (~2 %), qtz and rutile at grain edges. Feldspars in EDM selvage are replaced by 60% ser, <5% chl and biot, 5-10% calcite, 20-40% qtz, minor secondary ksp, and 0-5% sulfide(s) and oxide(s); in the pervasive biot zone, 10% of primary plg is replaced by clay (indicated by cavities??), and minor biot and ser. Igneous ksp is present in the pervasive biot selvage. In general, near veinlets, there is more chl.
Isotope compositions (O, H) have been obtained from the pervasive biot alteration zone.

11135-3481: BQM: tiny EDM veinlets with EDM alteration selvage: hbl is replaced by 40% biot, 50% qtz and/or ksp, 10% sulfides, and minor oxides. Igneous biot is partly replaced by secondary biot, minor qtz, minor sulfide(s) at grain edges. Near the veinlets, some igneous biot is replaced pseudomorphically by ser. Feldspar is replaced by 50-80 % ser and biot, 20-50% secondary ksp (?) and qtz, and ~1% diss'd sulfide. Minor calcite is present in feldspar sites near the veinlets. About 5% cavities in sample. The BQM texture is destroyed.

11135-3586: Biot Breccia: 0.4 cm wide qtz-ccp-py veinlet and numerous EDM veinlets with EDM alteration selvage: mafics (15%) are replaced by 80% secondary biot and minor chl, 15% qtz, 5% cavities, <2% sulfides and oxides. Feldspar (60%) is replaced by 50-80% HT ser and biot, minor chl, clay minerals (2-10%), 10-50% qtz and/or secondary ksp, and ± sulfide(s). Primary ksp is slightly altered to ser in the outer-selvage. About 3-5% cavities in the sample.

11135-4966: BQM: 0.5 cm wide qtz veinlet and EDM veinlets and calcite veinlets are present in the sample with EDM alteration selvages superimposed by late (**green or white ??**) argillic alteration: (1) EDM selvage: mafic minerals are replaced by 50-80% secondary biot, 20-50% ksp, minor qtz, sulfide(s), and rutile. Feldspar is replaced by secondary ksp, 20% biot, ser, chl (±), minor qtz and calcite. (2) weak EDM alteration selvage with argillic alteration: hbl is replaced by 50% biot, 10-20% ksp, 10% calcite, 5% qtz, 1% sulfide(s), and minor rutile. Biot is partly (10%) replaced by secondary biot, ksp, qtz, and rutile at grain edges; Plg is replaced by 40-60% clay, 20-40% calcite, 15% fine-grained ser, and ~5% ksp. Igneous ksp is replaced by secondary ksp, biot, and calcite along EDM veinlets.
Isotope compositions (O, H) have been obtained from the EDM alteration selvage with argillic alteration.

11171-4911: BQM: numerous 0.1-0.2 cm wide EDM veinlets with inner selvages of EDM and outer pervasive biot with strong late green argillic alteration overprint. (1) EDM: hbl and biot are replaced by 50% secondary biot, 30% ksp, 15% qtz, 10% sulfides, 2% oxide(s), and 3% calcite. Igneous biot in outer zone is 10-20% altered on rims to secondary biot, chl, ser, ksp, minor sulfide(s), and rutile. Feldspars are replaced by 30% biot, ser, chl, 60% secondary ksp, 5% qtz, 5% calcite, and ± sulfide(s). Mont (± kao) is present in the feldspar sites near the outer zone. BQM rock texture is destroyed. (2) Pervasive biot with strong green argillic alteration overprint: mafic minerals alteration is same as the outer zone in EDM, but all plg sites are cavities-indicating that plg is completely replaced by mont and ished out. Igneous ksp is present but slightly altered to sericite.
Isotope compositions (O, H) have been obtained from the pervasive biot zone with strong green argillic alteration.

11148-4219.5: Biot breccia/BQM: several ~0.1 cm wide EDM veinlets with EDM alteration selvage and superimposed strong late green and white argillic alteration. (1) Biot breccia: 40% biot, minor chl, ser (replacing plg and some biot crystals), 40% ksp, 10% qtz, 10% sulfide(s), and about 3-5% of cavities. (2) EDM selvage with argillic alteration: hbl and biot (inner zone) are replaced by 70% qtz, 10-15% secondary biot, minor chl and ser, 10% sulfide(s), minor rutile, and 5% open space. Primary biot (outer zone) is 10% replaced on rims by chl ± ser, qtz, ksp, sulfide(s), and rutile. Plg is replaced by biot and ser (70% -inner zone; 30%-outer zone), 5-10% qtz, ksp (10-20%-inner zone, 50%-outer zone), and 10-20% mont + kao. Igneous ksp is intact or slightly altered to biot or ser.
Isotope compositions (O, H) have been obtained from the EDM alteration selvage with argillic alteration.

11148-4790.5: BQM: ~0.1 cm wide EDM veinlets with cavities and biot crackles occur in pervasive biot alteration with strong white argillic alteration: hbl is replaced by 70% biot, minor ser, 10% ksp, 5% chl, 5% qtz, 5-10% sulfide(s), minor rutile and calcite. Primary biot is partly (10-20%) replaced by secondary biot, chl, qtz, oxide(s), and $CO_3^{=}$ at grain edges and along cleavages. Plg is replaced by kao ± mont (up to 90%), and ser (~10%), but near the veinlets, plg is mainly replaced by ser, chl, ksp, and qtz. Igneous ksp is intact in the outer zone, but it was replaced by ser, biot, and secondary ksp along the veinlets. BQM rock texture is destroyed.

11166-3449: Biot Breccia: EDM veinlets and qtz-mo veinlets are present with EDM alteration which is overprinted by green argillic alteration.

11166-4369: BQM: near qtz-mo veinlet with pervasive biot alteration which is overprinted by late white argillic alteration.

10772-31: BQM: qtz-py-ccp veinlet with pale green sericite selvage: hbl is replaced by fine-grained ser, qtz, ccp, and py. Biot is altered to pseudomorphic ser, carb, ccp and py, and minor qtz. Plg and Kspar are altered to fine to coarse-grained ser, qtz, minor py and ccp, maybe some clay. Texture destroyed. Sample was from Kelly 3400 level, the cross-cut: Kelly 3402XN.

10778-4: BQM: 4 mm qtz±ser±py±ccp veinlet with pale green sericite selvage: hbl is replaced by fine to coarse-grained ser, qtz, ccp, and py. Biot is altered to pseudomorphic ser, carb, rutile, ccp, and py. Plg and Kspar are altered to fine to coarse-grained ser, qtz, ± rutile, minor py and ccp, and abundant clay. Texture destroyed. Sample was from Staward 3400 level, the cross-cut: F3494XNW.

10759-336: BQM: qtz-py-ccp veinlet with dark green sericite selvage: hbl and biot is altered to chl, ccp and py, and minor qtz and ser. Plg and Kspar are altered to fine to coarse-grained ser, shreddy chl, qtz, and some clay. Texture destroyed. Sample was collected from Kelly mine 2000 level, DDH: F2033.

10854-643: BQM: 3 mm qtz-py±ser±chl veinlet with dark green sericite selvage: hbl and biot is altered to chl, qtz, py, rutile, and minor ser. Plg and Kspar are altered to fine to coarse-grained ser, shreddy chl, qtz, and some clay. Texture destroyed. Sample was collected from Kelly mine 2000 level, DDH: F2043.